Auxin-transport-independent control of vein patterning in *Arabidopsis thaliana* leaves

by

Brindhi Hyacinth Amalraj

A thesis submitted in partial fulfilment of the requirements for the degree of

Master of Science

in

Plant Biology

Department of Biological Sciences
University of Alberta

Abstract

Most multicellular organisms solve the problem of long-distance transport of water, signals and nutrients by means of networks of cells and tissues such as the vascular systems of plants and animals. What controls the formation of vascular systems is thus a key question in biology. In animals, where this question has been addressed extensively, the formation of the vascular system requires direct cell-cell interaction and, at least in part, cell migration. Both cell migration and direct cell-cell interaction are precluded in plants by a cell wall that holds cells apart and in place. Therefore, plants form vascular systems differently from animals.

The mechanism by which plants form their vascular systems is poorly understood, but available evidence places the plant signal auxin and its polar transport through plant tissues at the core of such mechanism. How auxin and its polar transport induce vein formation is unclear, but the prevailing hypothesis has long been that the GNOM (GN) guanine-nucleotide exchange factor for ADP-ribosylation-factor GTPases, which regulates vesicle formation in membrane trafficking, coordinates the cellular localization of auxin transporters of the PIN-FORMED (PIN) family between cells. The resulting cell-to-cell, polar transport of auxin would coordinate the polar localization of PIN proteins between auxin-transporting cells and control polar developmental processes such as vein formation. Contrary to predictions of the hypothesis, however, vein formation occurs in the absence of PIN proteins or any known intercellular auxin transporter; instead, auxin-transport-independent vein patterning relies, at least in part, on auxin signal transduction and *GN* controls both auxin transport and signalling to induce vein formation.

Whereas mechanisms by which GN may control PIN polarity and derived polar auxin transport have been suggested, it is unclear how GN could control auxin signalling, which takes place in the nucleus and is inherently non-polar. The most parsimonious account is that auxin

signalling leads to the production of proteins which control vein patterning redundantly with auxin transport and whose localization is controlled by GN. Here we tested predictions of this hypothesis by a combination of gene expression screening and molecular genetic analysis and identified a family of putative candidates for such proteins.

The current hypothesis of vein formation proposes that *GN* controls both auxin transport and auxin signalling to induce vein formation. However, plants in which both auxin transport and signalling are compromised phenocopy only weak alleles of *gn* such as *fewer roots* (*fwr*), suggesting the presence of additional, yet-to-be-identified *GN*-dependent pathways that act redundantly to auxin signalling and transport to induce vein formation. To identify such pathways, we screened for mutations that rescued the fragmented vein-pattern phenotype of gn^{fwr} and identified and characterized seven genetic suppressors of *gn*.

Finally, for the future characterization of the auxin signalling targets that control vein patterning redundantly with auxin transport and of the genes whose mutation suppresses the phenotype of *gn*, we identified and characterized GAL4/GFP enhancer-trap lines for the targeted misexpression of genes of interest in specific cells and tissues of developing leaves.

My results identify *GN*-dependent auxin-transport-independent pathways of vein formation in plants, a process whose logic is thus far unprecedented in multicellular organisms.

Preface

A part of this thesis has been published.

Chapter 4 of this thesis has been published as Amalraj, B., Govindaraju, P., Krishna, A., Lavania, D., Linh, N.M., Ravichandran, S. J. and Scarpella, E. (2020). GAL4/GFP enhancer-trap lines for identification and manipulation of cells and tissues in developing Arabidopsis leaves. *Dev Dyn* 279, 1127-1146. P. Govindaraju, A. Krishna, D. Lavania, N.M. Linh and I contributed equally to this work.

All the authors and the publisher have given their permission for the inclusion of this publication in this thesis.

Acknowledgements

I would like to thank all those who have played an integral part in my graduate school journey; your continuous support and faith have helped me complete the program.

First of all, I thank my supervisor, Dr. Enrico Scarpella for his continuous support and guidance throughout these years. I am grateful for all that I have learned from you on both professional and personal front. You have taught me that dedication, patience and perseverance will always bear fruits.

I would like to thank Dr. Michael Deyholos for agreeing to be on my supervisory committee and for his technical support in chapter 2 of my thesis. Your expertise has been pivotal in identifying critical results of that chapter. I would also like to thank Dr. R. Glen Uhrig for agreeing to be my arm's-length examiner.

I extend my gratitude to the Arabidopsis Biological Resource Centre (ABRC), Keiko Torii, Christian Hardtke and Hidehiro Fukaki for sharing seed material.

I am fortunate to have had supporting colleagues who have taught me techniques and helped me during these years. I thank Linh, Anmol, Dhruv, Priyanka, Sree and Carla for building a cheerful lab environment.

Finally, I would like to thank my dad Amalraj, mom Cecilia, sisters Candy and Sowby for your care, trust and relentless support for pursuing my goals. I would also like to thank my friends for cheering me up whenever I had dull moments. Without you all, I would not have made it this far.

Table of Contents

List of Figures

Chapter 1

Chapter 2

Chapter 3

Chapter 4

Chapter 5

List of tables

Chapter 2

Chapter 4

List of abbreviations

Ab	Abaxial
Ad	Adaxial
Ap	Apical
ADP	Adenosine diphosphate
ARF	AUXIN RESPONSE FACTOR
AUX/IAA	AUXIN/INDOLE-3-ACETIC ACID
AuxRE	Auxin responsive element
Ba	Basal
Col-0	Columbia-0
DAG	Days after germination
Dex	Dexamethasone
DNA	Deoxyribonucleic acid
EAR	ETHYLENE-RESPONSIVE-ELEMENT-BINDING FACTOR-associated amphiphilic repression
e.g.	For example
EMS	Ethyl methylsulfate
erGFP	Endoplasmic-reticulum-localized GREEN FLUORESCENT PROTEIN
Fig	Figure
fwr	fewer roots
GAL4	GALACTOSE-4
GFP	GREEN FLUORESCENT PROTEIN
GR	GLUCOCORTICOID RECEPTOR PROTEIN
HD-ZIP III	HOMEODOMAIN-LEUCINE ZIPPER Class III

He/Ne	Helium/Neon
Hv	Minor vein
Hy	Hydathode
IAA	Indole-3-acetic acid
La	Lateral
Lm	Lamina
LUT	Look-up table
L1,L2,L3	Loop 1, Loop 2, Loop 3
Md	Median
Me	Marginal
MES	2-(N-morpholino) ethanesulfonic acid
mm	Millimeter
MP	MONOPTEROS
Mv	Midvein
nm	Nanometer
NPA	1-N-Naphthylphtalamic acid
nYFP	Nuclear YELLOW FLUORESCENT PROTEIN
ORF	Open reading frame
PBA	Phenyl boronic acid
PD	Plasmodesmata
Pe	Petiole
pH	Power of hydrogen
PIN	PIN-FORMED

PIN1	PIN-FORMED1
PB1	PHAGOCYTIC OXIDASE/BUD EMERGENCE1
PED	PIN1 expression domain
RNA	Ribonucleic acid
rpm	Rotations per minute
RPS5A	RIBOSOMAL PROTEIN S5A
$SCF^{TIR1/AFB}$	S-PHASE KINASE ASSOCIATED PROTEIN1 – CULLIN – F-BOX TRANSPORT INHIBITOR RESISTANT1/AUXIN SIGNALLING F-BOX
SHR	SHORT-ROOT
St	Stoma
tir1;afb2	transport inhibitor response1; auxin signalling f-box2
TPL	Topless
TPR	Topless-related
Tr	Trichome
WT	Wild type
YFP	YELLOW FLUORESCENT PROTEIN
U	Units
UAS	Upstream activating sequence
µm	Micrometer
VP16	VIRAL PROTEIN 16

Notations

WT gene	Uppercase, italics (e.g., *PXY*)
Mutant gene	Lowercase, italics (e.g., *pxy*)
WT protein	Uppercase (e.g., PXY)
Fusions between promoter *A* and gene *B*	A::A (e.g., MP::PXY)
Fusions between gene A and gene B	A:B (e.g., PXY:YFP)

Gene coordinates

All gene coordinates are relative to the adenine (position +1) of the start codon.

Chapter 1: General introduction

1.1 The plant vascular system

In many multicellular organisms, transport of water, nutrients and signals happens through tissue networks such as the vascular system of plants (Taiz et al, 2015). The vascular system of plants consists of vascular strands that interconnect the different parts of an organ and the different organs of a plant (Esau, 1965). Vascular strands are bundles of continuous files of vascular cells arranged next to one another. In different organs, vascular strands are named differently: vascular cylinder or stele in roots; vascular bundles in stems; and veins in flat organs like cotyledons, leaves, petals and sepals.

Mature vascular strands are cylinders composed of two types of vascular tissues: xylem and phloem (Esau, 1965). In roots, xylem is found at the centre of the vascular cylinder; from this central xylem core, xylem "spokes" extend to the periphery of the vascular cylinder and phloem is found between the xylem spokes. In stems, xylem is found at the inner side of the vascular bundle and phloem at the outer side of the bundle. In flat organs, xylem is found at the adaxial (i.e. dorsal) side and phloem at the abaxial (i.e. ventral) side of the veins (Esau, 1965).

Xylem — composed of tracheary elements, parenchyma cells and fibres — mainly transports water and minerals, whereas phloem — composed of sieve elements, companion cells, fibres and sclereids — mainly transports photosynthates (Esau, 1965; Taiz et al, 2015)

1.2. Formation of the first vascular cells

In Arabidopsis, the first vascular cells form during the transition from the dermatogen to the globular stage of embryogenesis (Scheres et al, 1994).

The Arabidopsis dermatogen-stage embryo consists of eight outer cells, which are the precursors of the epidermis and eight inner cells, which are the precursors of all other tissue types. These eight inner cells divide longitudinally, resulting in four innermost cells, which in the basal half of the embryo will elongate to form procambial cells, the precursors of all vascular cells (Esau, 1965; Scheres et al., 1994). Even though the first vascular cells are anatomically recognizable in globular-stage embryos, vascular markers are already expressed in dermatogen-stage embryos, suggesting that the identity of those first vascular cells had been specified earlier (Smit et al., 2020).

1.3. Auxin signalling and the formation of the first vascular cells

Formation of the first vascular cells requires signal transduction of the plant hormone auxin: dermatogen-stage embryos of mutants in auxin signalling components express vascular-specific markers abnormally — if at all — and the eight inner cells of these embryos fail to divide longitudinally and to form procambial cells in early-globular-stage embryos (Berleth & Jurgens, 1993; Hamann et al., 1999; Hobbie et al., 2000; Dharmasiri et al., 2005; Yoshida et al., 2014; Smit et al., 2020).

Auxin signal transduction is the result of the interaction between two families of proteins: the AUXIN RESPONSE FACTOR (ARF) family of transcription factors and the AUXIN/INDOLE-3-ACETIC-ACID-INDUCIBLE (AUX/IAA) family of transcriptional repressors (recently reviewed in Powers & Strader, 2020).

The Arabidopsis genome codes for 29 AUX/IAA proteins, which contain three conserved domains (Powers & Strader, 2020). Domain I contains an EAR (ETHYLENE-RESPONSIVE ELEMENT-BINDING FACTOR-associated amphiphilic repression) motif that binds members of the TOPLESS (TPL)/TPL-RELATED (TPR) family of transcriptional co-repressors. Domain

II is the auxin-binding domain and the PHAGOCYTIC OXIDASE/BUD EMERGENCE1 (PB1) domain (previously referred to as domains III/IV) binds ARF proteins.

The Arabidopsis genome encodes 23 ARF proteins, which contain three conserved domains (Powers & Strader, 2020). The DNA-binding domain binds to auxin responsive elements (AuxREs) — specific sequences of DNA found within the promoters of auxin inducible genes. The middle domain confers transcriptional-activation- or transcriptional-repression-specificity and the PB1 domain binds other ARF or AUX/IAA proteins.

At low levels of intracellular auxin, AUX/IAA proteins bind ARF proteins and prevent them from activating gene expression (Powers & Strader, 2020). At high levels of intracellular auxin, auxin binds both the F-box subunit of the $SCF^{TIR1/AFB}$ (S-PHASE-KINASE-ASSOCIATED PROTEIN1 – CULLIN – F-$BOX^{TRANSPORT\ INHIBITOR\ RESISTANT1\ /\ AUXIN\ SIGNALLING\ F\text{-}BOX}$) E3 ubiquitin ligase complex and domain II of an AUX/IAA protein. Binding of auxin to the $SCF^{TIR1/AFB}$ complex and an AUX/IAA protein leads to the transfer of ubiquitin from the $SCF^{TIR1/AFB}$ complex to the AUX/IAA protein. The ubiquitinated AUX/IAA protein is targeted for degradation, thereby relieving ARF proteins from repression and allowing them to activate expression of their targets.

Though this model explains the mode of action of activating ARF proteins, it does not explain how repressor ARF proteins act. One possibility is that repressor ARF proteins repress transcription by directly binding to TPL/TPR proteins (Causier et al., 2012). One other possibility is that repressor ARF proteins bind to AuxRE sites and thus compete with activating ARF proteins (Chandler, 2016).

1.4. Auxin transport and the formation of vascular strands

Though auxin signalling is required for the formation of vascular cells, auxin transport seems to play a role in their organization into vascular strands (Berleth et al., 2000; Sachs, 1981). This role of auxin transport is suggested by experiments in which auxin is applied to mature plant tissues. Indeed, auxin application causes the differentiation of continuous files of vascular cells into vascular strands that connect the applied auxin to the pre-existing vascular strands.

The auxin-induced vascular-strand formation is characterized by the following properties: (1) the response is local, as it is initiated at the site of auxin application; (2) it is polar, as it is oriented toward the pre-existing vascular strands basal to the site of auxin application; (3) it is continuous, as it generates uninterrupted files of vascular cells; (4) it is constrained laterally, as only narrow strips of cells, rather than all the cells near the site of auxin application, differentiate into vascular cells (Berleth et al., 2000; Sachs, 1981). These properties suggest that the auxin-induced vascular-differentiation response recruits polar signals that already exist in plant tissues and that probably correspond to the polar transport of auxin.

Auxin is indeed synthesized in apical, immature regions of the plant and transported to the root tip through vascular strands (Michniewicz et al., 2007; Normanly, 2010; Zhao, 2010). The apical-basal transport of auxin has been suggested to be the result of the polar localization of auxin efflux proteins to the basal plasma membrane of auxin-transporting cells (Raven, 1975; Rubery & Sheldrake, 1974). Indeed, the weak acid indole-3-acetic acid (IAA), which is the most abundant auxin in plants, is non-charged in the acidic extracellular space and can freely diffuse into the cells through the plasma membrane. By contrast, in the more alkaline intracellular space, IAA becomes negatively charged and therefore can no longer diffuse freely through the plasma

membrane. As such, specialized auxin efflux proteins, which are encoded by members of the *PIN-FORMED* (*PIN*) family, transport auxin out of the cell (Petrasek et al., 2006).

These observations form the basis of the "auxin canalization hypothesis", which postulates that the more a cell transports auxin, the better it becomes at transporting auxin (Sachs 1981, 1991, 2000). This hypothesis proposes that positive feedback exists between auxin movement through a cell and localization of auxin efflux proteins to the site where auxin leaves the cell. The hypothesis predicts that the pre-existing vascular strands will gradually restrict dispersed auxin flow to preferential auxin transport through files of cells. These cell files will eventually differentiate into vascular strands that connect the applied auxin to the pre-existing vascular strands.

Consistent with predictions of the auxin canalization hypothesis, local application of auxin results in broad PIN1 expression domains between the site of auxin application and the pre-existing vascular strands (Mazur et al., 2016; Sauer et al., 2006). Broad domains of PIN1 expression become restricted to sites of auxin-induced vascular-strand formation in which PIN1 is localized to the side of the plasma membrane opposite to the source of auxin application and toward the pre-existing vascular strands.

1.5. The pattern of veins in the leaf

In the leaves of eudicots such as Arabidopsis, the vein network is composed of a central I-shaped midvein; lateral veins, which branch from the midvein and connect to distal veins to form loops; and minor veins, which branch from the midvein and loops and either end freely or connect to other veins (Telfer & Poethig, 1994; Nelson & Dengler, 1997; Kinsman & Pyke, 1998; Candela et al., 1999; Mattsson et al., 1999; Sieburth, 1999; Steynen & Schultz, 2003; Sawchuk et al.,

2013; Verna et al., 2015). Minor veins and loops curve near the leaf margin to give rise to a scalloped vein network outline.

1.6. Vein patterning, vein formation, auxin transport and auxin signalling

The vein pattern of Arabidopsis leaves is, at least in part, the combined result of auxin transport and auxin signalling (Verna et al., 2019).

Expression and polar localization of PIN1 to the plasma membrane suggest that veins are formed by two different mechanisms: one by which the midvein and lateral veins are formed; the other by which minor veins are formed (Scarpella et al., 2006; Wenzel et al., 2007).

Midvein and lateral veins form from broad PIN1 expression domains (PEDs) in the leaf inner tissue and PIN1 is localized isotropically, or nearly so, in the plasma membrane of the cells in those broad PEDs (Benkova et al., 2003; Reinhardt et al., 2003; Scarpella et al., 2006; Wenzel et al., 2007; Bayer et al., 2009; Hay et al., 2006; Heisler et al., 2005). Over time, broad PEDs become restricted to sites of formation of midvein and lateral veins and in the cells of midvein and lateral veins, PIN1 becomes localized to the side of the plasma membrane facing the pre-existing veins the PEDs connect to. Broad PEDs are associated with convergence points of PIN1 polarity in the epidermis of the shoot apical meristem and developing leaves, but convergence points of epidermal PIN1 polarity and positioning of midvein and lateral veins are not causally related to one another (Govindaraju et al., 2020).

In contrast to midvein and lateral veins, minor veins form from PEDs that are not associated with epidermal convergence points of PIN1 polarity and instead branch from pre-existing veins (Scarpella et al., 2006; Wenzel et al., 2007; Marcos & Berleth, 2014). Over time, a

few of those PEDs will weaken and disappear, but most of them will become restricted to narrow sites of minor vein formation (Marcos & Berleth, 2014). PEDs associated with minor vein formation can remain connected to pre-existing veins on one side only, in which case PIN1 is localized to the side of the plasma membrane facing the pre-existing veins the PEDs connect to (Scarpella et al., 2006; Wenzel et al., 2007; Marcos & Berleth, 2014). However, PEDs can, over time, connect to pre-existing veins on both sides and at the ends of these PEDs, PIN1 is localized to the sides of the plasma membrane facing the pre-existing veins the PEDs connect to. The two resulting opposite polarities are connected by a "bipolar cell", a cell where PIN1 is localized to two opposite sides of the plasma membrane.

Vein loops have a composite origin: minor-vein-associated PEDs branch from lateral-vein-associated PEDs and connect to the midvein or other lateral veins to form continuous loops (Scarpella et al., 2006; Wenzel et al., 2007). At the ends of each loop-associated PED, PIN1 is localized to the sides of the plasma membrane facing the pre-existing veins the PED connects to and the opposite PIN1 polarities are connected by a bipolar cell.

If vascular strand formation only depended on the polarity of auxin transport, which in turn depends on PIN protein localization (Wisniewska et al., 2006), the most severe *pin* mutants should form no vascular strands. Instead, mutants in all the *PIN* genes with vein patterning function (*pin1;3;4;6;7;8*) form veins in a reproducible, albeit abnormal, pattern, suggesting that there is residual vein patterning activity in these mutants (Verna et al., 2019). Because *pin1,3,6;4;7;8* leaves respond to auxin application by forming new veins, the residual vein-patterning activity in these mutants must be provided, at least in part, by auxin signalling.

Auxin signalling had never been associated with vein patterning because auxin signalling mutants have a normal vein pattern, albeit with fewer veins (Przemeck et al., 1996; Hardtke &

Berleth, 1998; Candela et al., 1999; Alonso-Peral et al., 2006; Strader et al., 2008; Esteve-Bruna et al., 2013; Verna et al., 2019). Instead, plants in which both auxin transport and auxin signalling are compromised have vein pattern defects that are more severe than those of plants in which only auxin transport is compromised (Verna et al., 2019). In the most severe cases, vascular cells are no longer aligned along the length of the vein but are arranged in seemingly random orientations. These findings support the conclusion that the residual vein patterning activity of auxin transport mutants is provided by auxin signalling; it furthermore suggests that the relationship between auxin transport and auxin signalling in vein patterning is asymmetrical. Plants with compromised auxin transport have an abnormal vein pattern (Sawchuk et al., 2013, Verna et al., 2015, Verna et al., 2019; Mattsson 1999; Sieburth 1999), suggesting that auxin transport is essential for vein patterning even in the presence of a normal auxin signalling pathway. By contrast, plants with compromised auxin signalling have a normal vein pattern (Przemeck et al., 1996; Hardtke & Berleth, 1998; Candela et al., 1999; Alonso-Peral et al., 2006; Strader et al., 2008; Esteve-Bruna et al., 2013; Verna et al., 2019), suggesting that auxin signalling is not required for vein patterning in the presence of a normal auxin transport pathway. In conclusion, auxin transport can compensate for the absence of auxin-signalling-dependent vein patterning activity, but auxin signalling cannot compensate for the absence of auxin-transport-dependent vein patterning activity (Verna et al., 2019).

1.7. Scope and outline of the thesis

The evidence discussed above suggests that auxin induces the polar formation of veins and that such inductive and orienting property of auxin depends on the function of *PIN* genes. How auxin precisely controls *PIN* gene function and derived polar formation of veins is unclear, but the prevailing hypothesis has long been that the GNOM (GN) guanine-nucleotide exchange factor

for ADP-ribosylation-factor GTPases, which regulates vesicle formation in membrane trafficking, coordinates the cellular localization of PIN proteins between cells; the resulting cell-to-cell, polar transport of auxin would coordinate the polar localization of PIN proteins between auxin-transporting cells and control polar developmental processes such as vein formation (reviewed in, e.g., (Berleth et al., 2000; Richter et al., 2010; Nakamura et al., 2012; Linh et al., 2018)). Contrary to predictions of the hypothesis, however, auxin-induced polar vein-formation occurs in the absence of PIN proteins or any known intercellular auxin transporter (Verna et al., 2019), suggesting the presence of auxin-transport-independent vein-patterning pathways. The goal of my M.Sc. research was to identify such pathways in Arabidopsis leaves.

The auxin-transport-independent vein-patterning activity relies, at least in part, on auxin signalling and *GN* turns out to be controlling both auxin transport and signalling to induce vein formation (Verna et al., 2019) (Figure 1.1). Whereas mechanisms by which GN may control PIN polarity and derived polar auxin transport have been suggested (reviewed in (Richter et al., 2010; Luschnig and Vert, 2014); see also (Naramoto et al., 2014) and references therein), it is unclear how *GN* could control auxin signalling, which takes place in the nucleus and is inherently non-polar (reviewed in (Leyser, 2018)). The most parsimonious account is that auxin signalling leads to the production of proteins which control vein patterning and whose localization is controlled by GN. In Chapter 2, we tested this hypothesis and identified a family of putative candidates for such proteins that includes the receptor-like kinase PHLOEM INTERCALATED WITH XYLEM (PXY) (Fisher & Turner, 2007).

The current hypothesis of vein formation proposes that GN controls both auxin transport and auxin signalling to induce vein formation (Verna et al., 2019). However, plants in which both auxin transport and signalling are compromised phenocopy only weak alleles of *gn*,

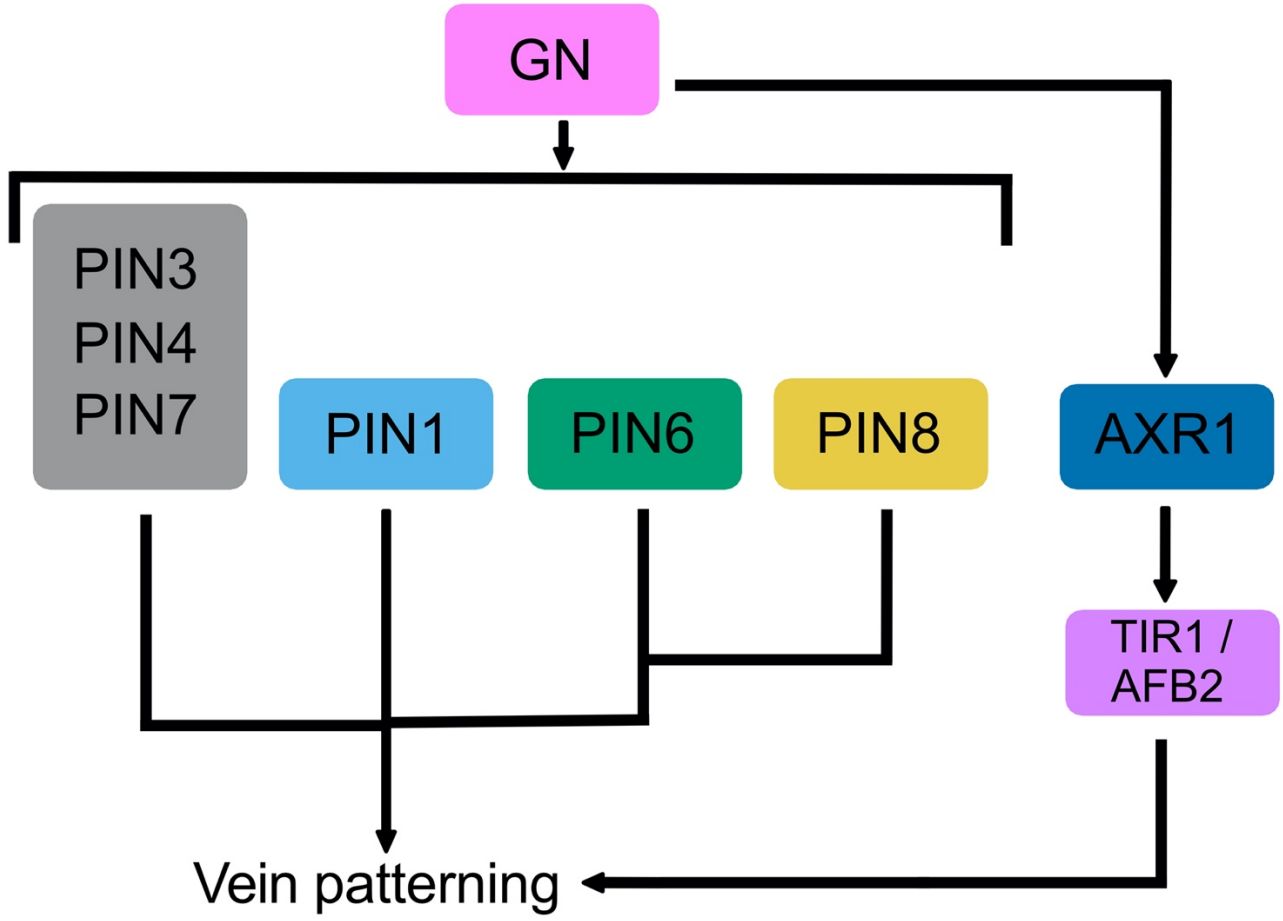

Figure 1.1. Control of auxin-transport- and auxin-signalling-dependent vein patterning by GNOM

Genetic interaction network controlling vein patterning. Arrows indicate positive effects.

suggesting the presence of additional, yet-to-be-identified *GN*-dependent pathways that act redundantly to auxin signalling and transport to induce vein formation. To identify such pathways, in Chapter 3 we identified and characterized six genetic suppressors of the fragmented vein-pattern phenotype of the *fewer roots* allele of *gn*.

The identification of putative candidate proteins which are targets of auxin signalling, which control vein patterning and whose localization is controlled by GN required gene misexpression by different promoters. This imposed the burden of generating different constructs for different gene and promoter combinations. This approach could have been simplified if GAL4/GFP enhancer-trap lines existed in Columbia-0 — the genotype of reference in Arabidopsis (Koornneef and Meinke, 2010) — with which to drive expression of genes of interest in desired cells and tissues of developing leaves. Unfortunately, such lines were not available when I started my M.Sc.. In Chapter 4, we addressed this limitation and provided GAL4/GFP enhancer-trap lines in the Col-0 background of Arabidopsis for the identification and manipulation of cells and tissues in developing leaves (Amalraj et al., 2020).

Finally, in Chapter 5 we propose and discuss a hypothesis to account for how the auxin signalling target *PXY* — identified in Chapter 2 — could control vein formation redundantly with auxin transport.

Chapter 2: Identification and characterization of new GNOM-dependent regulators of vein patterning

2.1. Introduction

Most multicellular organisms solve the problem of long-distance transport of signals and nutrients by means of tissue networks such as the vascular system of vertebrate embryos and the vein network of plant leaves. How vascular networks are formed is thus a key question in biology. In vertebrates, the formation of the embryonic vascular system relies on direct cell-cell interaction and, at least in part, on cell migration (e.g., (Noden, 1988; Xue et al., 1999)). By contrast, both direct cell-cell interaction and cell migration are precluded in plants by a cell wall that keeps cells apart and in place. Therefore, vascular networks form differently in plants.

How plants form vein networks in their leaves is unclear; however, auxin is so far the only known molecule that can induce vascular strand formation in plant tissues (reviewed in (Sachs, 1981; Berleth et al., 2000; Sawchuk and Scarpella, 2013; Ravichandran et al., 2020)). This unique property of auxin seems to depend on its polar transport through plant tissues (Thompson, 1966). Indeed, auxin is primarily synthesized in immature apical organs, such as leaf and flower primordia and is transported basally to the roots through vascular strands (Went, 1928; Thimann and Skoog, 1934; Avery, 1935; Wangermann, 1974). The resulting apical-basal transport of auxin seems to depend on the polar localization of auxin transporters of the PIN-FORMED (PIN) family to the basal plasma-membrane of auxin-transporting cells (Petrasek et al., 2006; Wisniewska et al., 2006).

How plants coordinate PIN polar localization between auxin-transporting cells is unclear, but for the past 20 years the prevailing hypothesis has been that GNOM (GN) — a guanine-

nucleotide exchange factor for ADP-ribosylation factors that regulates vesicle formation in membrane trafficking — controls the cellular localization of PIN proteins; the resulting cell-to-cell, polar transport of auxin would coordinate PIN polarity between auxin-transporting cells and control polar developmental processes such as vein formation (reviewed in, e.g., (Berleth et al., 2000; Richter et al., 2010; Nakamura et al., 2012; Linh et al., 2018)). Contrary to predictions of this hypothesis, however, vein formation occurs in the absence of PIN proteins or any known intercellular auxin transporter; it turns out that auxin-transport-independent vein patterning relies, at least in part, on auxin signalling and that GN controls both auxin transport and signalling to induce vein formation (Verna et al., 2019).

Whereas mechanisms by which GN may control PIN polarity and derived polar auxin transport have been suggested (reviewed in (Richter et al., 2010; Luschnig and Vert, 2014); see also (Naramoto et al., 2014) and references therein), it is unclear how GN could control auxin signalling, which takes place in the nucleus and is inherently nonpolar (reviewed in (Leyser, 2018)). The most parsimonious account is that auxin signalling leads to the production of proteins which control vein patterning and whose localization is controlled by GN (Verna et al., 2019). These proteins, if existing, would be expressed at lower levels in plants in which both auxin transport and auxin signalling are inhibited than in plants in which only auxin transport is inhibited. By leveraging this expectation, here we combined gene expression screening and molecular genetic analysis to test the hypothesis that auxin signalling leads to the production of proteins which control vein patterning synergistically with auxin transport and whose localization is controlled by GN.

2.2. Results & discussion

2.2.1. A gene expression screen for auxin signalling targets that control vein patterning synergistically with auxin transport

To test the hypothesis that auxin signalling leads to the production of proteins which control vein patterning synergistically with auxin transport and whose localization is controlled by GN, we screened for genes whose expression is lower in plants in which both auxin transport and auxin signalling are inhibited than in plants in which only auxin transport is inhibited.

To identify such genes, we first sequenced mRNA from (1) 4-day-old leaves of WT grown in the presence of 100 μM N-1-naphthylphthalamic acid (NPA), which inhibits auxin transport (Morgan and Söding, 1958) and of the double mutant *transport inhibitor response1* ; *auxin signalling f-box2* (*tir1*;*afb2*), which lacks the two auxin receptors that most contribute to auxin signalling (Dharmasiri et al., 2005), grown in the presence of 100 μM NPA; and (2) 4-day-old leaves of WT grown in the presence of 25 μM NPA and of WT grown in the presence of 25 μM NPA and 10 μM phenylboronic acid (PBA), which inhibits auxin signalling (Matthes and Torres-Ruiz, 2016). We found (1) 21,572 genes that were expressed in both NPA-grown WT and NPA-grown *tir1*;*afb2*; and (2) 21,585 genes that were expressed in both NPA-grown WT and PBA and NPA-grown WT (Figure 2.1).

We next asked for which genes expression was (1) ≥1.5-fold higher in NPA-grown WT than in NPA-grown *tir1*;*afb2* and (2) ≥1.5-fold higher in NPA-grown WT than in PBA- and NPA-grown WT. We found (1) 1,877genes whose expression was ≥1.5-fold higher in NPA-grown WT than in NPA-grown *tir1*;*afb2* and (2) 4,066 genes whose expression was ≥1.5-fold higher in NPA-grown WT than in PBA- and NPA-grown WT (Figure 2.1).

Figure 2.1. Flowchart of screen for auxin signalling targets that control vein patterning synergistically with auxin transport

Proportional Venn diagrams of number of genes expressed in the indicated genotypes and treatments.

Finally, we asked for which genes expression was both ≥1.5-fold higher in NPA-grown WT than in NPA-grown *tir1*;*afb2* and ≥1.5-fold higher in NPA-grown WT than in PBA- and NPA-grown WT. We found 887 such genes (Figure 2.1).

Because GN regulates protein trafficking to the plasma membrane (reviewed in (Richter et al., 2010; Luschnig and Vert, 2014); see also (Naramoto et al., 2014) and references therein), we expect genes encoding proteins which control vein patterning synergistically with auxin transport, whose expression is controlled by auxin signalling and whose localization is controlled by GN to encode proteins that are localized to the plasma membrane or secreted to the extracellular space. Therefore, we asked which of the 887 genes whose expression was both ≥1.5-fold higher in NPA-grown WT than in NPA-grown *tir1*;*afb2* and ≥1.5-fold higher in NPA-grown WT than in PBA- and NPA-grown WT encoded proteins that are predicted to be localized to the plasma membrane or secreted to the extracellular space. By means of the SUBA4 tool (Hooper et al., 2017), we found 292 such genes (Figure 2.1).

2.2.2. Contribution of auxin signalling targets to vein network formation

Two hundred ninety-two genes (1) are expressed at lower levels in plants in which both auxin transport and auxin signalling are inhibited than in plants in which only auxin transport is inhibited and (2) encode proteins that are predicted to be localized to the plasma membrane or secreted to the extracellular space (Figure 2.1).

To test whether such auxin signalling targets control vein network formation, we selected 28 of the 292 genes because they belong to families that have been shown to have functions in cell polarization, auxin signalling, auxin transport, or vascular development (Wu et al., 2001; Cheung et al., 2003; Lukowitz et al., 2004; DeYoung et al., 2006; Mouchel et al., 2006; Fisher

and Turner, 2007; Lavy et al., 2007; Ceserani et al., 2009; Scacchi et al., 2009; Beuchat et al., 2010; Hazak et al., 2010; Agusti et al., 2011; Lin et al., 2012; Chen et al., 2013; Nibau et al., 2013; Uchida and Tasaka, 2013; Wang et al., 2013; Choi et al., 2014; Smékalová et al., 2014; Matthes and Torres-Ruiz, 2016; Enders et al., 2017; Ruiz Sola et al., 2017; Li et al., 2019) (Table 2.1). We identified mutants in those 28 genes and, for 18 of them, in their 25 most-closely related genes (Table 2.1). Should those 53 genes mediate auxin signalling functions in vein network formation, their mutants would have vein network defects similar to those of auxin signalling mutants; we asked whether that were so.

WT Arabidopsis grown under normal conditions forms separate leaves whose vein networks are defined by at least four reproducible features : (1) a narrow I-shaped midvein that runs the length of the leaf; (2) lateral veins that branch from the midvein and join distal veins to form closed loops; (3) minor veins that branch from midvein and loops and either end freely or join other veins; (4) minor veins and loops that curve near the leaf margin, giving a scalloped outline to the vein network (Telfer and Poethig, 1994; Nelson and Dengler, 1997; Kinsman and Pyke, 1998; Candela et al., 1999; Mattsson et al., 1999; Sieburth, 1999; Steynen and Schultz, 2003; Sawchuk et al., 2013; Verna et al., 2015; Verna et al., 2019) (Fig. 2.2A,B,E).

Vein networks of *tir1*;*afb2* and PBA-grown WT deviate from those of WT grown under normal conditions in two respects: (1) closed loops were often replaced by open loops, i.e. loops that contact the midvein or other loops at only one of their two ends; (2) veins were often replaced by “vein fragments”, i.e. stretches of vascular elements that fail to contact other stretches of vascular elements at either one of their two ends (Verna et al., 2019) (Fig. 2.2C–D)

Table 2.1. Auxin signalling targets and closely related genes of which we assessed function in vein network formation

Auxin signalling target		**Closely related genes**		**Function**
Locus ID	Gene Name	Locus ID	Gene name	
AT5G51350	*MOL1*			Vascular development (Agusti et al., 2011)
AT3G05140	*RBK2*			Auxin signalling (Enders et al., 2017)
AT5G05160	*RUL1*			Vascular development (Agusti et al., 2011)
AT1G71830	*SERK1*			Vascular development (Li et al., 2019)
AT2G01950	*VH1*/*BRL2*			Vascular development (Cesarani et al., 2008)
AT3G49670	*BAM2*	AT3G23920	*BAM1*	Vascular development (Deyoung et al., 2006)
		AT4G17090	*BAM3*	
AT2G47160	*BOR1*	AT3G62270	*BOR2*	Auxin signalling
AT1G15460	*BOR4*	AT3G06450	*BOR3*	(Matthes and Torres-
		AT1G74810	*BOR5*	Ruiz, 2016)

Auxin signalling target		**Closely related genes**		**Function**
Locus ID	Gene Name	Locus ID	Gene name	
AT1G80760	*NIP6;1*/*NLM7*	AT4G10380	*NIP5;1*/*NLM6*	Auxin signalling (Matthes and Torres-Ruiz, 2016)
AT3G09070	*OPS*	AT2G38070	*OPL*	Cell polarization and vascular development (Ruiz Sola et al., 2017)
AT5G61480	*PXY*/*TDR*	AT1G08590	*PXL1*	Vascular development (Fisher et al., 2007)
		AT4G28650	*PXL2*	
AT2G36570	*PXC1*			Vascular development (Wang et al., 2013)
AT5G01890	*PXC2*			
AT2G41820	*PXC3*			
AT5G16490	*RIC4*	AT1G27380	*RIC2*	Cell polarization (Wu et al., 2001)
AT4G28556	*RIC7*	AT2G20430	*RIC6*	
AT1G17140	*RIP1*/*ICR1*			Auxin signalling, cell polarization and vascular development (Lavy et al., 2007, Hazak et al., 2010)
AT1G78430	*RIP2*/*ICR4*			
AT4G28950	*ROP9*/*RAC7*	AT3G48040	*ROP10*/*RAC8*	Auxin signalling and cell polarization (Nibau et al,

Auxin signalling target		**Closely related genes**		**Function**
Locus ID	Gene Name	Locus ID	Gene name	
				2013, Cheung et al., 2003, Choi et al., 2014)
		AT5G62880	*ROP11*/*RAC10*	
AT1G31880	*BRX*/*NLM9*	AT3G14000	*BRXL2*	Auxin signalling, cell polarization and vascular development (Mouchel at al., 2006, Scacchi et al., 2009, Beuchat et al., 2010)
AT2G35600	*BRXL1*	AT1G54180	*BRXL3*	
AT5G20540	*BRXL4*			
AT2G26330	*ER*/*QRP1*	AT5G62230	*ERL1*	Auxin signalling, cell polarization and vascular development (Uchida et al., 2013, Chen et al., 2013)
AT5G07180	*ERL2*			
AT2G42800	*RLP29*	AT1G34290	*RLP5*	Auxin signalling and cell polarization (Lukowitz et al., 2004, Smekalova et al., 2014)

Auxin signalling target		**Closely related genes**		**Function**
Locus ID	Gene Name	Locus ID	Gene name	
AT5G45770	*RLP55*	AT1G65380	*RLP10*/*CLV2*	
		AT1G80080	*RLP17*/*TMM*	
		AT4G18760	*RLP51/SNC2*	
		AT5G65830	*RLP57*	
		AT1G63700	*YDA*/*EMB71*	
AT1G11130	*SCM*/*SUB*	AT2G20850	*SRF1*	Vascular development (Lin et al., 2012)
		AT4G03390	*SRF3*	
AT3G02640	*TMP*	AT5G16250	*TMPL*	Unknown

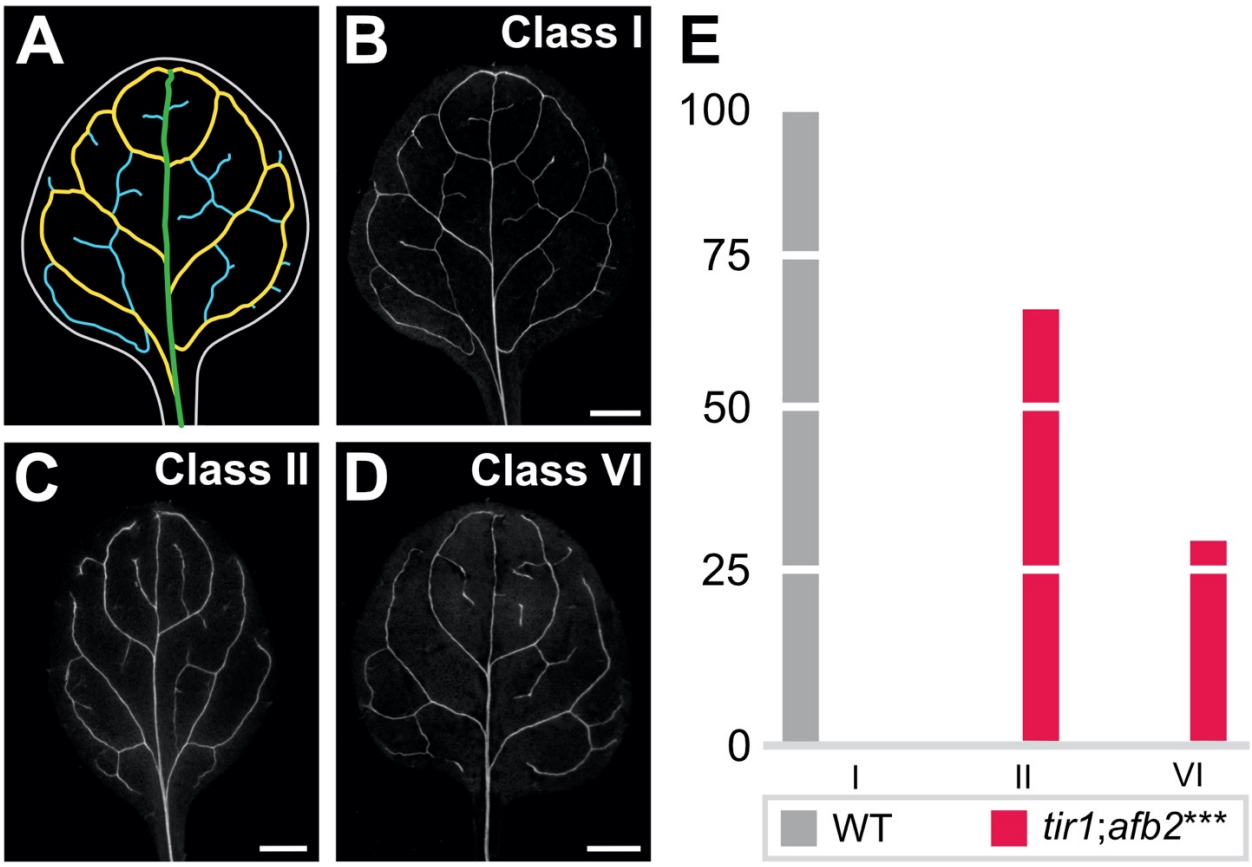

Figure 2.2. Contribution of auxin signalling to vein patterning

(A,B) Vein pattern of WT mature first leaf. In A: green, midvein; yellow, loops; cyan, minor veins. (B–D) Dark-field illumination of mature first leaves illustrating phenotype classes (top right): class I, narrow I-shaped midvein and scalloped vein-network outline (B); class II, open vein-network outline (C); class VI, fragmented vein network and open vein-network outline (D). (E) Percentages of leaves in phenotype classes. Difference between *tir1*;*afb2* and WT was significant at $P<0.001$ (***) by Kruskal- Wallis and Mann-Whitney test with Bonferroni correction. Sample sizes: WT, 43; *tir1;afb2*, 41. Bars: (B–D) 1 mm.

We divided the 28 auxin signalling targets of which we tested the contribution to vein network formation in three groups: (1) genes for which we did not address possible functional redundancy with closely related genes; (2) genes for which we partially addressed possible functional redundancy with closely related genes; (3) genes for which we fully addressed possible functional redundancy with closely related genes.

2.2.2.1. Genes for which we did not address possible functional redundancy with closely related genes

The vein networks of *more lateral growth1* (*mol1), rho-related-protein-from-plants-binding protein kinase2* (*rbk2*), *reduced in lateral growth1* (*rul1*), *somatic embryogenesis receptor-like kinase1* (*serk1*) and *vascular highway1* / *brassinosteroid-insensitive1-like2* (*vh1*/*brl2*; *vh1* hereafter) were no different from those of WT (Figure 2.3), suggesting that the respective WT genes have no function in vein network formation or their function is redundant.

2.2.2.2. Genes for which we partially addressed possible functional redundancy with closely related genes

The vein networks of the *barely any meristem1* (*bam1*), *bam2*, *bam3*, *requires high boron1* (*bor1*), *bor2*, *bor3*, *bor4* and *bor5* single mutants and the *bam1 bam3* (*bam1*;*3* hereafter), *bor1*;*2*, *bor1*;*3* and *bor4*;*5* double mutants were no different from those of WT (Fig. 2.4B,C), suggesting that the respective WT genes have no function in vein network formation or their function is redundant.

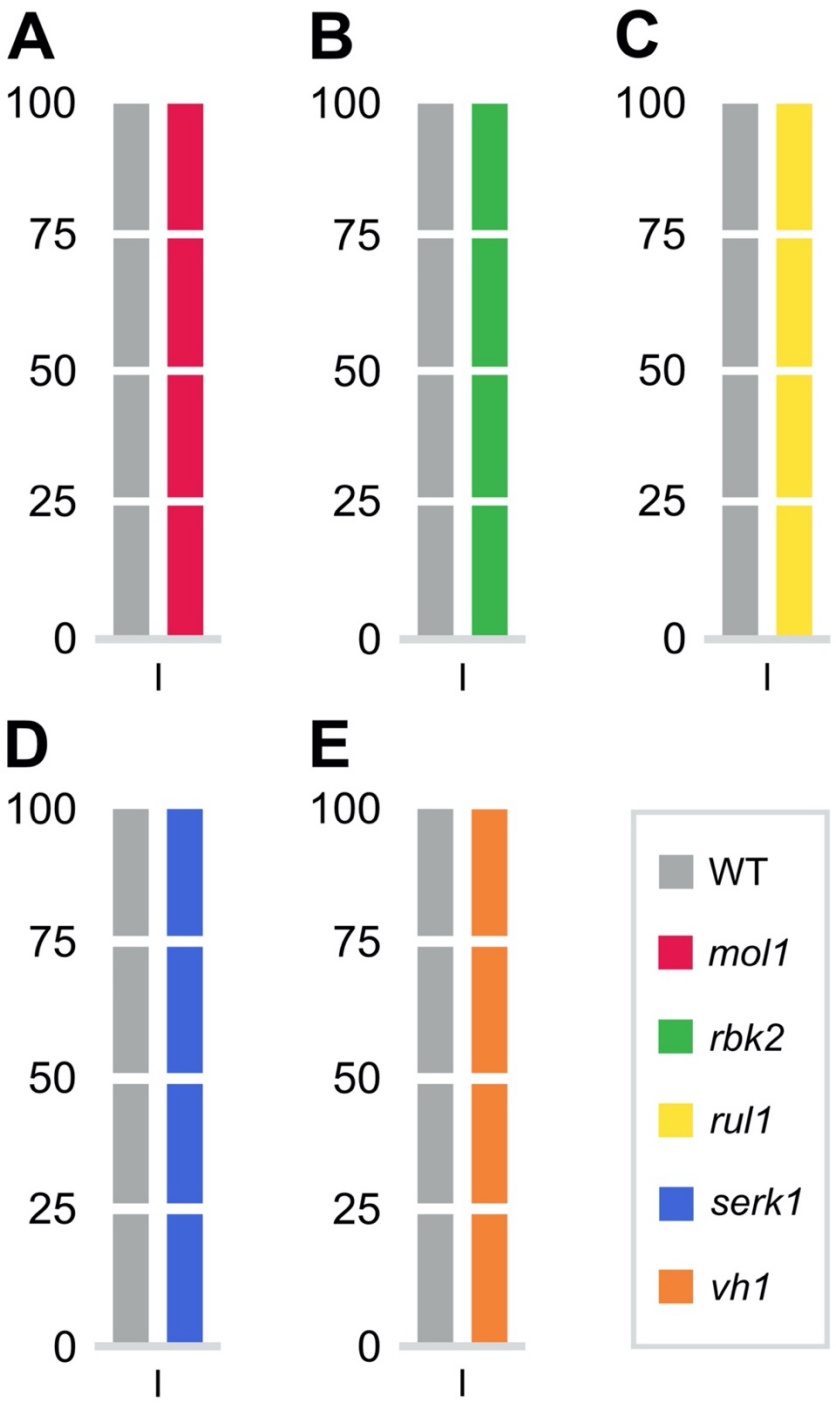

Figure 2.3. Contribution of auxin signalling targets to vein patterning

(A–E) Percentages of leaves in phenotype classes (defined in Figure 2.2). Sample sizes: WT, 41 (A); WT, 39 (B); WT, 40 (C); WT, 42 (D); WT, 40 (E); *mol1*, 40; *rbk2*, 41; *rul1*, 43; *serk1*, 44; *vh1*, 40.

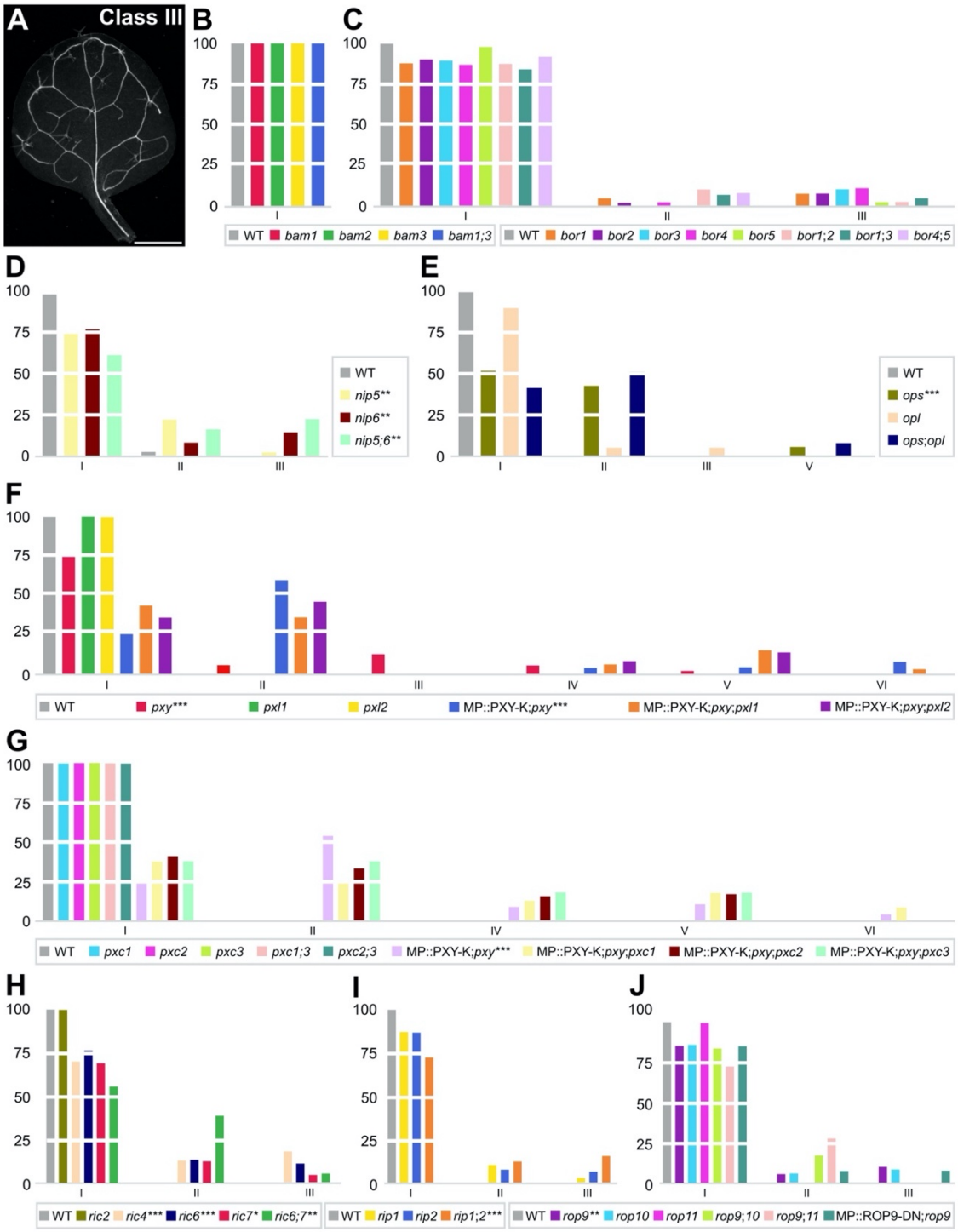

Figure 2.4. Contribution of auxin signalling targets to vein patterning

Dark-field illumination of mature first leaf illustrating phenotype class III (top right): narrow Y-shaped midvein and scalloped vein-network outline; class IV: narrow Y-shaped midvein and

open vein-network outline (not shown); class V: fragmented vein network (not shown). (B–J) Percentages of leaves in phenotype classes (defined above and in Figure 2.2). Difference between *nip5;1* and WT, *nip6;1* and WT, *nip5;1*;*6;1* and *nip5;1*, *ops* and WT, *pxy* and WT, MP::PXYΔK;*pxy* and *pxy, ric4* and WT, *ric6* and WT, *ric7* and WT, *ric6*;*7* and *ric7*, *rip1*;*2* and WT and *rop9* and WT was significant at $P<0.05$ (*), $P<0.01$ (**), or $P<0.001$ (***) by Kruskal-Wallis and Mann-Whitney test with Bonferroni correction. Sample sizes: WT, 41 (B); WT, 46 (C); WT, 51 (D); WT, 42 (E); WT, 39 (F); WT, 41 (G); WT, 42 (H); WT, 47 (I); WT, 47 (J); *bam1*, 42; *bam2*, 42; *bam3*, 39; *bam1*;*3*, 41; *bor1*, 42; *bor2*, 53; *bor3*, 49; *bor4*, 47; *bor5*, 47; *bor1*;*2*, 41; *bor1*;*3*, 43; *bor4*;*5*, 39; *nip5*, 50; *nip6*, 49; *nip5*;*6*, 49; *ops*, 40; *opl*, 42; *ops*;*opl* 41; *pxy*, 56; *pxl1*, 40; *pxl2*, 42; MP::PXYΔK*;pxy, 52;* MP::PXYΔK*;pxy;pxl1*, 36; MP::PXYΔK*;pxy;pxl2*, 37; *pxc1*, 36; *pxc2*, 33; *pxc3*, 39; *pxc1;3*, 37; *pxc2;3*, 38; MP::PXYΔK*;pxy*, 49; MP::PXYΔK*;pxy;pxc1*, 40; MP::PXYΔK*;pxy;pxc2*, 39; MP::PXYΔK*;pxy;pxc3*, 40; *ric2*, 43; *ric4*, 40; *ric6*, 38; *ric7*, 48; *ric6;7*, 41; *rip1*, 40; *rip2*, 39; *rip1*;*2*, 40; *rop9*, 61; *rop10*, 36; *rop11*, 40; *rop9*;*10*, 42; *rop9*;*11*, 44; MP::ROP9^{T20A};*rop9*, 41. Bar: (A) 1 mm.

By contrast, in ~25% of the leaves of *nod26-like intrinsic protein5;1* / *nod26-like major intrinsic protein6* (*nip5;1*/*nlm6*; *nip5;1* hereafter) and *nip6;1*/*nlm7* (*nip6;1* hereafter), loops were open or midveins were Y-shaped (Fig. 2.4A,D), suggesting that *NIP5;1* and *NIP6;1* non-redundantly control vein network formation. Because the vein network defects of *nip5;1*;*6;1* were more severe than those of *nip5;1* but no different from those of *nip6;1* (Fig. 2.4D), we conclude that *NIP6;1* acts upstream of *NIP5;1* in the same vein-network formation pathway.

In ~50% of the leaves of *octopus* (*ops*), loops were open or veins were fragmented (Fig. 2.4E), suggesting that *OPS* non-redundantly controls vein network formation. By contrast, the vein networks of *octopus-like2* (*opl2*) were no different from those of WT (Fig. 2.4E), suggesting that *OPL2* has no nonredundant functions in vein network formation. Moreover, because the vein networks of *ops*;*opl2* were no different from those of *ops* (Fig.2 4E), we conclude that *OPL2* also lacks functions in vein network formation that are redundant to those of *OPS*. Alternatively, *OPL2* functions in *OPS*-dependent vein network formation are masked by redundancy with other *OPL* genes.

In 25% of the leaves of *phloem intercalated with xylem* / *tracheary element differentiation inhibitory factor receptor* (*pxy*/*tdr; pxy* hereafter), loops were open, midveins were Y-shaped, or veins were fragmented (Fig. 2.4F), suggesting that *PXY* non-redundantly controls vein network formation. To test whether *PXY* also controlled vein network formation redundantly, we created — as previously done for other receptor kinases (Amaya et al., 1991; Ueno et al., 1991; Hemmati-Brivanlou and Melton, 1992) — a dominant-negative version of PXY that has the ligand-binding domain but lacks the signal transduction domain (PXYΔK) (Table 2.2) (Fig. 2.5A,B); we overexpressed PXYΔK in the *pxy* background by the

Table 2.2. Origin and nature of lines

Line	Origin/nature
mol1-1	SAIL 384_A06 (ABRC); Agusti et al., 2011
rbk2-K272	SALK_033272 (ABRC); contains a single T-DNA insertion at position +184 of *RBK2* (AT3G05140)
rul1-2	SALK_121868C (ABRC); Agusti et al., 2011
serk1-1	SALK_044330 (ABRC); Albrecht et al., 2005
vh1-K625	SALK_142625C (ABRC); contains a single T-DNA insertion at position +126 of *VH1* (AT2G01950)
bam1-3	CS16304 (ABRC); DeYoung et al., 2006
bam2-T967	GK-791G02-024967(ABRC); contains a single T-DNA insertion at position +64 of *BAM2* (AT3G49670)
bam3-2	CS800012 (ABRC); DeYoung et al., 2006
bor1-3	SALK_037312 (ABRC); Kasai et al., 2011
bor2-K630	SALK_206630C (ABRC); contains a single T-DNA insertion at position +94 of *BOR2* (AT3G62270)
bor3-K011	SALK_016011 (ABRC); contains a single T-DNA insertion at position +164 of *BOR3* (AT3G06450)
bor4-K793	SALK_133793(ABRC); contains a single T-DNA insertion at position +126 of *BOR4* (AT1G15460)
bor5-T946	GK-786D04-024946 (ABRC); contains a single T-DNA insertion at position +75 of *BOR5* (AT1G74810)

Line	Origin/nature
nip5;1-1	SALK_122287C (ABRC); Takano et al., 2006
nip6;1-1	SM 3.15719 (ABRC); Tanaka et al., 2008
ops-2	SALK_139316 (ABRC); Truernit et al., 2012
opl2-1	SALK_004773C (ABRC); Ruiz Sola et al., 2017
pxy-3	CS9872 (ABRC); Fisher et al., 2007
MP::PXYΔK	Transcriptional fusion of *MP* (AT1G18950; -3281 to -1; primers: "MP SalI Fwd" and "MP BamHI Rev") to the sequence encoding PXYΔK (AT5G61480; +1 to +2148; primers "PXY-K BamH1 Fwd" and "PXYK Kpn1 Rev")
pxl1-1	SALK_001782 (ABRC); Etchells et al., 2013
pxl2-1	SALK_114354C (ABRC); Etchells et al., 2013
pxc1-3	WISCDSLOX470G6 (ABRC); Wang et al., 2013
pxc2-K351	SALK_055351C (ABRC); contains a single T-DNA insertion at position +89 of *PXC2* (AT5G01890)
pxc3-K805	SALK_092805C (ABRC); contains a single T-DNA insertion at position +189 of *PXC3* (AT2G41820)
ric4-K799	SALK_015799C (ABRC); contains a single T-DNA insertion at position +136 of *RIC4* (AT5G16490)
ric2-K885	SALK_070885 (ABRC); contains a single T-DNA insertion at position +128 of *RIC2* (AT1G27380)
ric6-K237	SALK_066237 (ABRC); contains a single T-DNA insertion at position +198 of *RIC6* (AT2G20430)

Line	Origin/nature
ric7-K781	CS923572 (ABRC); contains a single T-DNA insertion at position +137 of *RIC7* (AT4G28556)
rip1-LG05	SAIL_265_G05 (ABRC); contains a single T-DNA insertion at position +141 of *RIP1* (AT1G17140)
rip2-LG04	SAIL_1234_G04 (ABRC); contains a single T-DNA insertion at position +105 of *RIP2* (AT1G78430)
rop9-LG06	SAIL_222_C06 (ABRC); contains a single T-DNA insertion at position +154 of *ROP9* (AT4G28950)
rop10-K190	SALK_030190 (ABRC); contains a single T-DNA insertion at position +94 of *ROP10* (AT3G48040)
rop11-K681	SALK_039681 (ABRC); contains a single T-DNA insertion at position +112 of *ROP11* (AT5G62880)
MP::ROP9^{T20A}	Transcriptional fusion of *MP* (AT1G18950; -3281 to -1; primers: "MP SalI Fwd" and "MP BamHI Rev") to ROP9^{T20A} (AT4G28950; +1 to +1417; primers: "ROP9-DN Fwd" and "ROP9-DN Rev" and "ROP9-BamH1 Fwd" and "ROP9-Kpn1 Rev")
brxl4-K411	SALK_022411C (ABRC); contains a single T-DNA insertion at position +163 of *BRXL4* (AT5G20540)
brx(Uk-1);*brxl1-1*;*brxl2-1*;*brxl3-1*	Briggs et al., 2006
er-105	CS89504 (ABRC); Torii et al., 1996
erl2-1	CS6588 (ABRC); Shpak et al., 2004

Line	Origin/nature
er-105;*erl2-1*	Shpak et al., 2004
er-105;*erl1-2*;*erl2-1*	Shpak et al., 2004
rlp5-1	SALK_112291 (ABRC); Wang et al., 2008
rlp10-1	GABI_686A09 (ABRC); Wang et al., 2008
rlp17-1	CS6140 (ABRC); Wang et al., 2008
rlp29-1	SALK_022220 (ABRC); Wang et al., 2008
rlp55-1	SAIL_633_E08 (ABRC); Wang et al., 2008
rlp51-1	SALK_143038 (ABRC); Wang et al., 2008
rlp57-1	SALK_077716 (ABRC); Wang et al., 2008
yda-1	CS6392 (ABRC); Lukowitz et al., 2004
yda-2	CS6393 (ABRC); Lukowitz et al., 2004
scm-2	SALK_086357 (ABRC); (Kwak et al., 2005)
srf1-2	SALK_081679 (ABRC); Eyuboglu et al., 2007
srf3-1	SALK_204435 (ABRC); Eyuboglu et al., 2007
MP::SCMΔK	Transcriptional fusion of *MP* (AT1G18950; -3281 to -1; primers: "MP SalI Fwd" and "MP BamHI Rev") to the sequence encoding SCMΔK (AT1G11130; +1 to +2654; primers "SCM-K BamH1 Fwd"and "SCM-K Kpn1 Rev")
RPS5A::SCMΔK	Transcriptional fusion of *RPS5A* (AT3G11940; -2236 to –1; primers: "RPS5A SmaI For" and "RPS5A SmaI Rev") to the sequence encoding SCMΔK (AT41G11130; +1 to +2654; primers "SCM-K Kpn1 Fwd" and "SCM-K Kpn1 Rev")

Line	Origin/nature
tmp-K336	SALK_060336 (ABRC); contains a single T-DNA insertion at position +102 of *TMP* (AT3G02640)
tmpl-K814	SALK_031814C (ABRC); contains a single T-DNA insertion at position +73 of *TMPL* (AT5G16250)

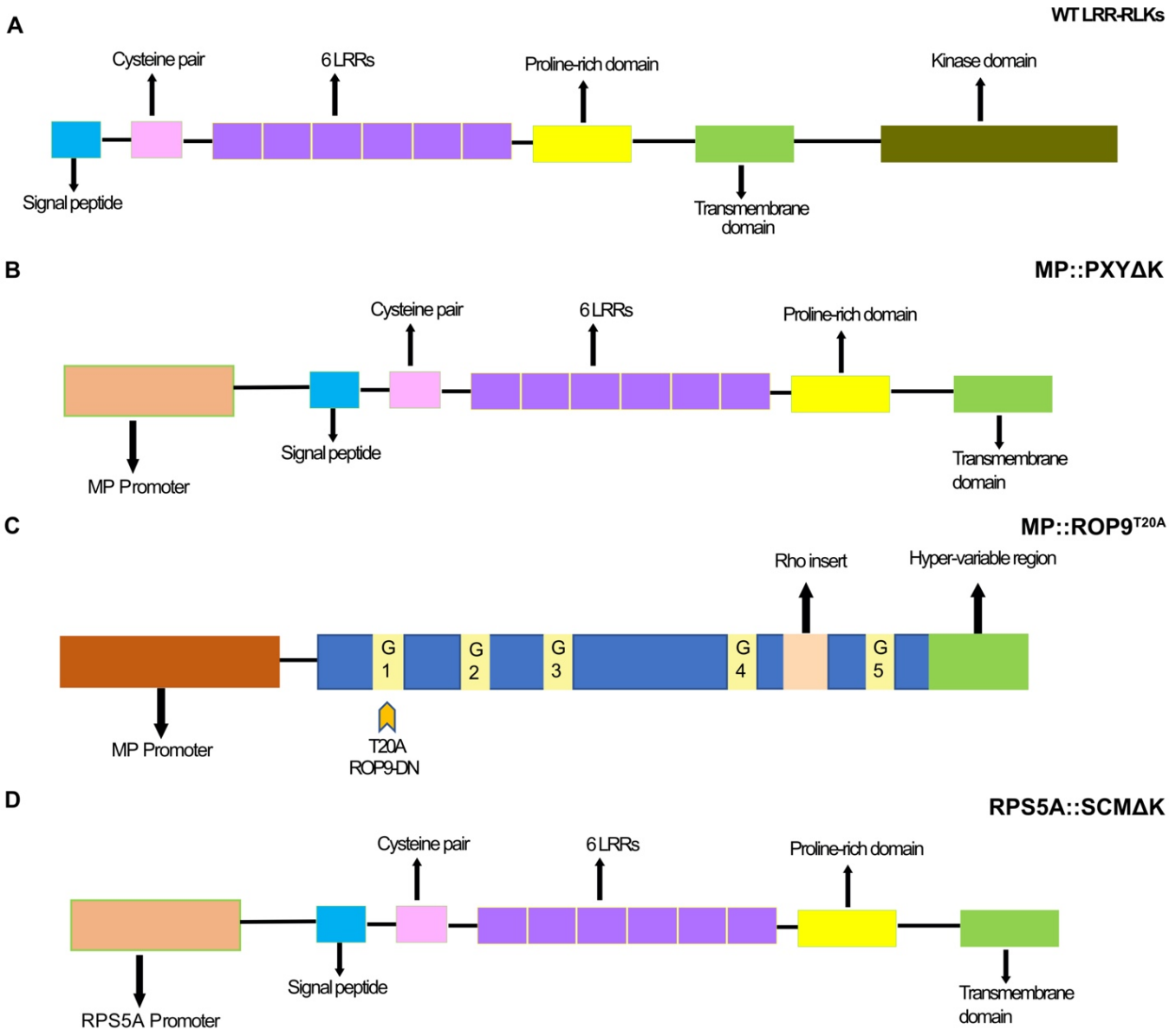

Figure 2.5. Structure of dominant-negative variant constructs

(A) Domain structure of WT LRR-RLK proteins. (B) Domain structure of MP::PXYΔK. (C) Domain structure of MP::ROP9^{T20A}. (D) Domain structure of RPS5A::SCMΔK.

MONOPTEROS (*MP*) promoter, which is active in developing veins (Sawchuk et al., 2013); and we analyzed the vein networks of the resulting MP::PXYΔK;*pxy*. Because the vein networks defects of MP::PXYΔK;*pxy* were more severe than those of *pxy* (Fig. 2.4F), we conclude that *PXY* also controls vein network formation redundantly. We next asked whether such redundant functions were provided by *PXY-LIKE1* (*PXL1*) and *PXL2*, mutation of which leads to normal vein networks (Fig. 2.4F). To address this question, we analyzed vein networks of MP::PXYΔK;*pxy*;*pxl1* and MP::PXYΔK;*pxy*;*pxl2*. Because the vein networks defects of MP::PXYΔK*;pxy;pxl1* and MP::PXYΔK*;pxy;pxl2* were no different from those of MP::PXYΔK;*pxy* (Fig. 2.4F), we conclude that *PXL1* and *PXL2* have no function in *PXY*-dependent vein network formation or their functions are redundant with each another's.

The vein networks of *pxy/tdr-correlated1* (*pxc1*), *pxc2*, *pxc3*, *pxc1*;*3* and *pxc2*;*3* were no different from those of WT (Fig. 2.4G), suggesting that *PXC* genes have no nonredundant functions in vein network formation. Because of the similarity between *PXC* genes and *PXY*/*PXL* genes (Wang et al., 2013), we asked whether *PXC* genes functioned redundantly with *PXY*/*PXL* genes in vein network formation. To address this question, we analyzed vein networks of MP::PXYΔK;*pxy*;*pxc1*, MP::PXYΔK*;pxy;pxc2 and* MP::PXYΔK*;pxy;pxc3*. Because the vein networks defects of MP::PXYΔK*;pxy;pxc1*, MP::PXYΔK*;pxy;pxc2* and MP::PXYΔK*;pxy;pxc3* were more severe than those of MP::PXYΔK;*pxy* (Fig. 2.4G), we conclude that *PXC* genes have no function in *PXY*-dependent vein network formation or their functions are redundant with one another's.

The vein networks of *rho-related-protein-from-plants-interactive cdc42 rac-interactive-binding motif-containing protein2* (*ric2*) were no different from those of WT (Fig. 2.4H), suggesting that *RIC2* has no nonredundant functions in vein network formation. By contrast, in

~15–30% of the leaves of *ric4*, *ric6* and *ric7*, loops were open or midveins were Y-shaped (Fig. 2.4H), suggesting that *RIC4*, *RIC6* and *RIC7* non-redundantly controls vein network formation. Because the vein network defects of *ric6*;*7* double mutant were more severe than those of *ric7* but no different from those of *ric6* (Fig. 2.4H), we conclude that *RIC6* acts upstream of *RIC7* in the same vein-network formation pathway.

The vein networks of *rho-related-protein-from-plants-interactive partner1* / *interactor of constitutively active rho-related-protein-from-plants1* (*rip1*/*icr1*; *rip1* hereafter) and *rip2*/*icr4* (*rip2* hereafter) were no different from those of WT (Fig. 2.4I), suggesting that RIP1 and RIP2 have no nonredundant function in vein network formation. Because in ~25% of the leaves of *rip1;2* loops were open or midveins were Y-shaped (Fig. 2.4I), we conclude that RIP1 and RIP2 function redundantly with each other in vein network formation.

In ~15% of the leaves of *rho-related protein from plants9* / *rat-sarcoma-related-c3-botulinum-toxin-substrate-like7* (*rop9*/*rac7*; *rop9* hereafter), loops were open or midveins were Y-shaped (Fig. 2.4J), suggesting that *ROP9* non-redundantly controls vein network formation. By contrast, the vein networks of *rop10*/*rac8* (*rop10* hereafter) and *rop11/rac10* (*rop11* hereafter) were no different from those of WT (Fig. 2.4J), suggesting that *ROP10* and *ROP11* have no nonredundant functions in vein network formation. To test whether *ROP10* and *ROP11* functioned redundantly with *ROP9* in vein network formation, we analyzed the vein networks of *rop9*;*10* and *rop9*;*11*. Because the vein network defects of the *rop9*;*10* and *rop9*;*11* were no different from those of *rop9* (Fig. 2.4J), we conclude that *ROP10* and *ROP11* have no function in *ROP9*-dependent vein network formation or their functions are redundant with each other's. To test whether *ROP9* has any redundant functions in vein network formation, we created — as previously done (Feiguelman et al., 2018) — a dominant-negative version of ROP9 ($ROP9^{T20A}$)

(Table 2.2) (Fig. 2.5C); we overexpressed ROP9^{T20A} by the *MP* promoter in the *rop9* background; and we analyzed the vein networks of the resulting MP::ROP9^{T20A};*rop9*. Because the vein network defects of MP::ROP9^{T20A};*rop9* were no different from those of *rop9* (Fig. 2.4J), we conclude that *ROP9* has no redundant functions in vein network formation.

2.2.2.3. Genes for which we fully addressed possible functional redundancy with closely related genes

The vein networks of the *brevix-radis-like4* (*brxl4*) single mutant were no different from those of WT, but in ~40% of the leaves of *brx*;*brxl1*;*2*;*3*, loops were open or midvein were Y-shaped (Fig. 2.6A). Because the vein networks of *brx*;*brxl1*;*2*;*3*;*4* were no different from those of *brx*;*brxl1*;*2*;*3* (Fig. 2.6A), we conclude that *BRXL4* has no function in vein network formation. By contrast, *BRX* and *BRXL1–3* control vein network formation, but their relative contribution remains undetermined.

The vein networks of *erecta* / *quantitative resistance to plectosphaerella1* (*er*/*qrp1*; *er* hereafter) were no different from those of WT, but in ~20% of the leaves of *er-like2* (*erl2*), loops were open, midveins were Y-shaped, or veins were fragmented (Fig. 2.6B). Because the vein network defects of *er*;*erl2* were more severe than those of *erl2* (Fig. 2.6B), we conclude that *ER* controls vein network formation redundantly with *ERL2*. By contrast, the vein network defects of *er*;*erl1*;*2* were no different from those of *er*;*erl2* (Fig. 2.6B); therefore, *ERL1* has no function in vein network formation.

The vein networks of *receptor-like protein5* (*rlp5*), *rlp10*/*clavata2* (*rlp10*/*clv2*; *rlp10* hereafter*), rlp17* / *too many mouths* (*rlp17*/*tmm*; *rlp17* hereafter), *rlp29*, *rlp17*;*29* and *rlp55* were

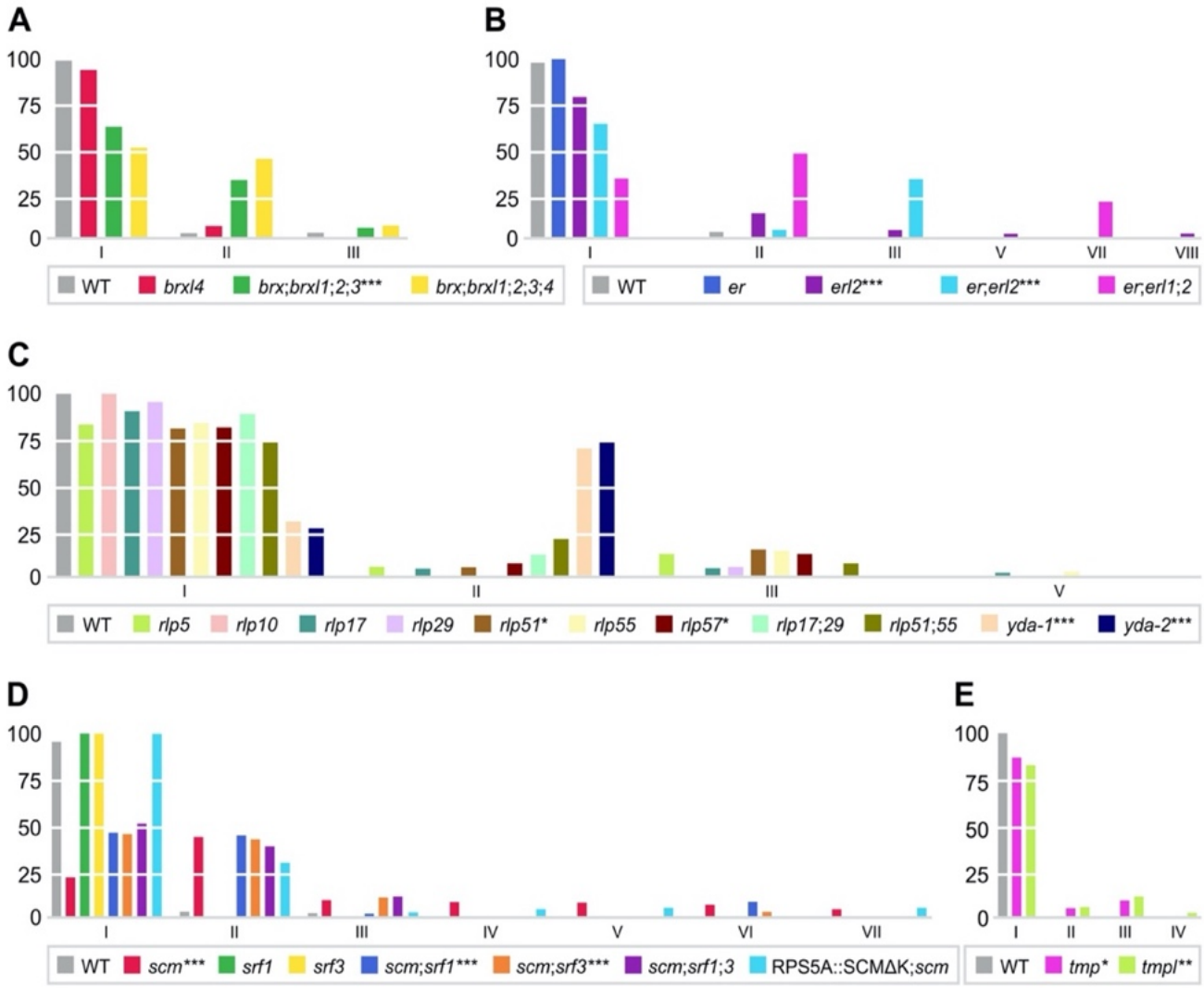

Figure 2.6. Contribution of auxin signalling targets to vein patterning

(A–E) Percentages of leaves in phenotype classes. Class I–VI defined in Figures 2.2 and 2.4; class VII: Y-shaped midvein and fragmented vein network (not shown); class VIII: Y-shaped midvein, open vein-network outline and fragmented vein network (not shown). Difference between *brx*;*brxl1*;*2*;*3* and WT, *erl2* and WT, *er*;*erl2* and *erl2*, *rlp51* and WT, *rlp57* and WT, *yda-1* and *rlp51*, *yda-1* and *rlp57*, *yda-2* and *rlp51*, *yda-2* and *rlp57*, *scm* and WT, *scm*;*srf1* and *scm*, *scm*;*srf3* and *scm*, *tmp* and WT and *tmpl* and WT was significant at $P<0.05$ (*), $P<0.01$ (**), or $P<0.001$ (***) by Kruskal- Wallis and Mann-Whitney test with Bonferroni correction.

Sample sizes: WT, 49 (A); WT, 40 (B); WT, 43 (C); WT, 44 (D); WT, 45 (E); *brxl4*, 50; *brx*;*brxl1*;*2*;*3*, 47; *brx*;*brxl1*;*2*;*3*;*4*, 48; *er*, 75; *erl2*, 106; *er*;*erl2*, 74; *er*;*erl1*;*2*, 55; *rlp5*, 41; *rlp10*, 43; *rlp17*, 54; *rlp29*, 42; *rlp51*, 42; *rlp55*, 51; *rlp57* 43; *rlp17*;*29*, 45; *rlp51*;*55*, 46; *yda-1*, 23; *yda-2*, 27; *scm*, 106; *srf1*, 41; *srf3*, 39; *scm;srf1*, 70; *scm*;*srf3*, 76; *scm*;*srf1*;*3*, 71; MP::SCMΔK;*scm*, 44; *tmp*, 46; *tmpl*, 57.

no different from those of WT (Fig. 2.6C), suggesting that the respective WT genes have no function in vein network formation or their function is redundant. By contrast, in ~20% of the leaves of *rlp51* / *suppressor of nonexpresser-of-pathogen-related-genes1-1 constitutive2* (*rlp51*/*snc2*; *rlp51* hereafter) and *rlp57*, loops were open and midveins were Y-shaped (Fig. 2.6C), suggesting that *RLP51* and *RLP57* non-redundantly control vein network formation. Because the vein network defects of the *rlp51*;*55* double mutant were no different from those of *rlp51* (Fig. 2.6C), we conclude that *RLP55* has no function in vein network formation or its function is redundant.

RLP-dependent signalling in development is mainly mediated by *YODA* / *EMBRYO-DEFECTIVE71* (*YDA*/*EMB71*; *YDA* hereafter) (reviewed in (He et al., 2018; Zhang et al., 2018)). Therefore, to test whether the *RLP* family has functions in vein network formation beyond those provided by *RLP51* and *RLP57*, we compared the vein networks of *yda* with those of *rlp51* and *rlp57*. Because the vein network defects of *yda* are more severe than those of *rlp51* and *rlp57* (Fig. 2.6C), we conclude that the *RLP* family has functions in vein network formation beyond those provided by *RLP51* and *RLP57*.

In ~80% of the leaves of *scrambled*/*strubbelig* (*scm*/*sub*; *scm* hereafter), loops were open, midveins were Y-shaped, or veins were fragmented (Fig. 2.6D), suggesting that *SCM* non-redundantly controls vein network formation. To test whether *SCM* also controlled vein network formation redundantly, we analyzed the vein networks of double and triple mutants between *scm* and mutations in *SUB-RECEPTOR FAMILY1* (*SRF1*) and *SRF3*, which have no nonredundant function in vein network formation (Fig. 2.6D). Furthermore, we created — as previously done (Kwak et al., 2014) — a dominant-negative version of SCM that has the ligand-binding domain

but lacks the signal transduction domain (SCMΔK) (Table 2.2) (Fig. 2.5D); we overexpressed SCMΔK in the *scm* background by the broadly active *RIBOSOMAL PROTEIN S5A* (*RPS5A*) promoter (Weijers et al., 2001); and we analyzed the vein networks of the resulting RPS5A::SCMΔK;*scm*.

The vein network defects of *scm*;*srf1* and *scm*;*srf3* were milder than those of *scm*; the vein network defects of *scm*;*srf1*;*3* were no different from those of *scm*;*srf1* and *scm*;*srf3*; and the vein network defects of RPS5A::SCMΔK;*scm* were no different from those of *scm*;*srf1*;*3* (Fig. 2.6D). Therefore, we conclude that *SCM* promotes vein network formation and that, at least in part, it does so by repressing the inhibitory function of *SRF1* and *SRF3*. Furthermore, we conclude that *SCM* has no redundant functions in vein network formation.

Finally, in ~15% of the leaves of *transmembrane protein* (*tmp*) and *tmp-like* (*tmpl*), loops were open, midveins were Y-shaped, or veins were fragmented (Fig. 2.6E), suggesting that *TMP* and *TMPL* non-redundantly control vein network formation. We were unable to identify plants that are *tmp* homozygous and *tmpl* heterozygous, *tmp* heterozygous and *tmpl* homozygous, or *tmp* homozygous and *tmpl* homozygous among 48 plants progeny of selfed *TMP*/*tmp*;*TMPL*/*tmpl* plants (Table 2.3), suggesting that the double mutant is gametophytic lethal and that *TMP* and *TMPL* redundantly control a fundamental cellular function.

In conclusion, our results suggest that vein network formation is controlled by the auxin signalling targets *BRX* and *BRXL1–3*; *ERL2* and, redundantly with *ERL2*, *ER*; *NIP5* and *NIP6*; *OPS*; *PXY*, non-redundantly and redundantly with *PXY*-related genes; *RIC4*, *RIC6* and *RIC7*; *RIP1* and *RIP2*, redundantly with each other; *RLP51* and *RLP57*, through *YDA*; *ROP9*; *SCM*; and *TMP* and *TMPL*.

Table 2.3. Genotype distribution in progeny of selfed *TMP*/*tmp*;*TMPL*/*tmpl* plants

Genotype	Expected frequency	Observed frequency (Proportion)
TMP/*TMP*;*TMPL*/*TMPL*	0.0625	0.0930 (4/43)
TMP/*TMP*;*TMPL*/*tmpl*	0.1250	0.2330 (10/43)
TMP/*TMP*;*tmpl*/*tmpl*	0.0625	0.2090 (9/43)
TMP/*tmp*;*TMPL*/*TMPL*	0.1250	0.1860 (8/43)
TMP/*tmp*;*TMPL*/*tmpl*	0.2500	0.1160 (5/43)
TMP/*tmp*;*tmpl*/*tmpl*	0.1250	0.000 (0/43)
tmp/*tmp*;*TMPL*/*TMPL*	0.0625	0.1630 (7/43)
tmp/*tmp*;*TMPL*/*tmpl*	0.1250	0.000 (0/43)
tmp/*tmp*;*tmpl*/*tmpl*	0.0625	0.000 (0/43)

Difference between observed and theoretical frequency distributions of *TMP*/*tmp*;*tmpl*/*tmpl*, *tmp*/*tmp*;*TMPL*/*tmpl* and *tmp*/*tmp*;*tmpl*/*tmpl* was significant by Pearson's chi-squared ($\chi 2$) goodness-of-fit test ($\alpha=0.05$, dF=1).

2.2.3. Interaction between auxin transport and auxin signalling targets in vein patterning

Eleven groups of auxin signalling targets control, redundantly or non-redundantly, vein network formation (Figures 2.4 and 2.6). Were these genes controlling vein patterning synergistically with auxin transport, the vein network defects of their mutants would be enhanced by growth in the presence of NPA, which phenocopies loss of auxin-transport-dependent vein patterning activity (Verna et al., 2019); we asked whether that were so.

Consistent with previous reports (Mattsson et al., 1999; Sieburth, 1999; Verna et al., 2019), growth in the presence of NPA reproducibly induced characteristic vein-pattern defects in WT: (1) the vein network comprised more lateral veins; (2) lateral veins failed to join midvein but ran parallel to it to form a wide midvein; (3) lateral veins ended in a marginal vein that closely paralleled the leaf margin, giving a smooth outline to the vein network; (4) veins were thicker (Fig. 2.7A,E).

By comparison, leaves of NPA-grown *tir1*;*afb2* and NPA-and PBA-grown WT had a narrower midvein and a denser and more reticulated vein network; furthermore, the vein network outline of NPA-grown *tir1*;*afb2* and NPA-and PBA-grown WT was jagged because of narrow clusters of vascular elements that were oriented perpendicular to the leaf margin and that were laterally connected by veins or that, in the most severe case, were aligned in seemingly random orientations (Verna et al., 2019) (Fig. 2.7B,E).

The vein pattern defects of NPA-grown *brx*;*brxl1*;*2*;*3*, *er*;*erl2*, *nip6;1*, *ops*, *ric4*, *ric6*, *rip1*;*2*, *rlp51*, *rlp57*, *rop9*, *tmp*, *tmpl* and *yda* were no different from those of NPA-grown WT (Fig. 2.7B,E). By contrast, the vein patterns of NPA-grown *scm* were intermediate between those of *scm* and of NPA-grown WT (Fig. 2.7A,E), suggesting that *scm* is, at least partially, insensitive

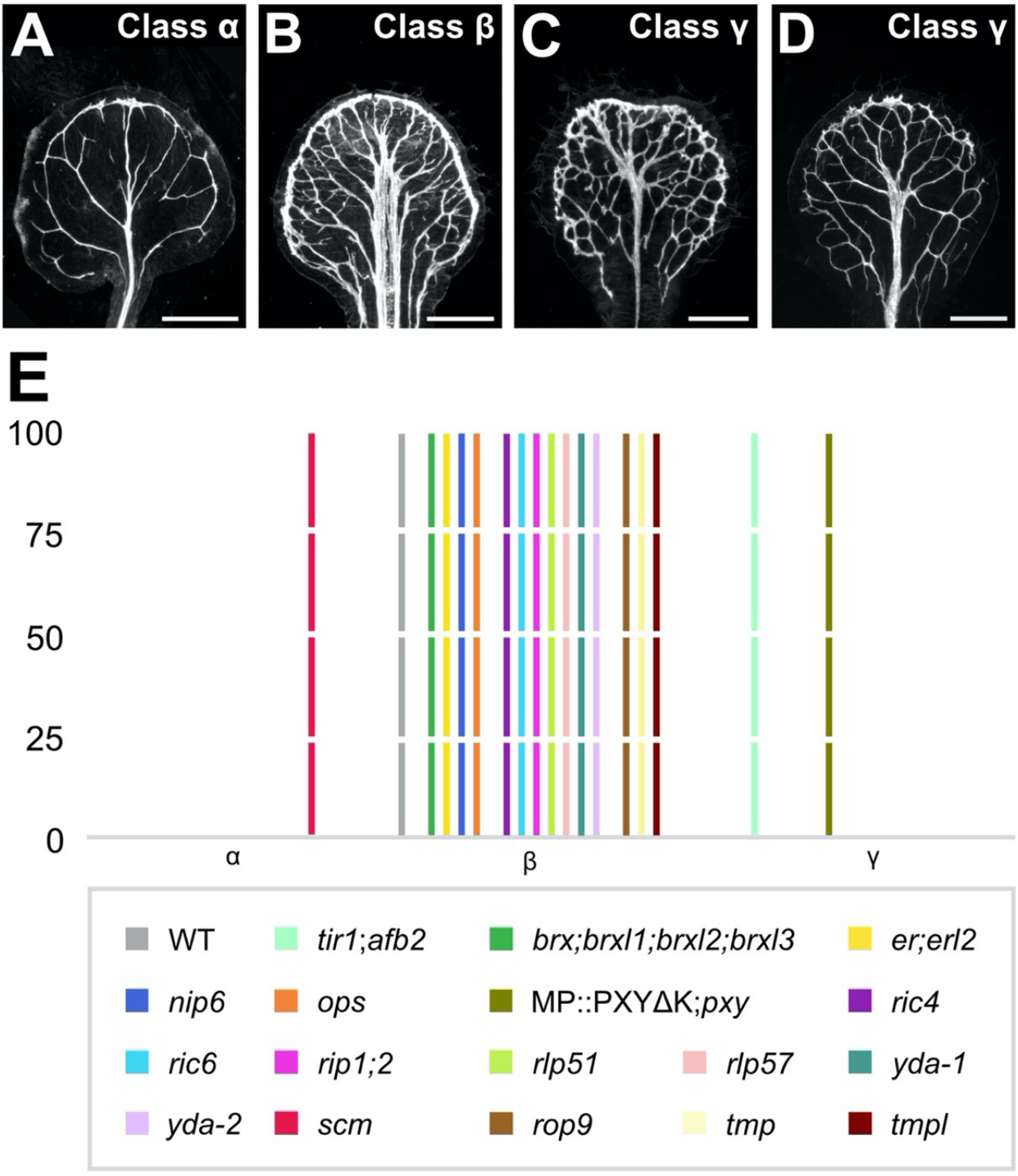

Figure 2.7. Contribution of auxin signalling targets and auxin transport to vein patterning

(A–D) Dark-field illumination of mature first leaves illustrating phenotype classes (top right): class α, narrow midvein and apically thickened vein-network outline (A, NPA-grown *scm*); class

β, wide midvein, more lateral-veins and conspicuous marginal vein (B); class γ, narrow midvein, dense vein network and jagged vein-network outline (C, NPA-grown *tir1*;*afb2*; D, NPA-grown MP::PXYΔK;*pxy*). (E) Percentages of leaves in phenotype classes. Difference between NPA-grown *tir1*;*afb2* and NPA-grown WT, between NPA- and PBA-grown WT and NPA-grown WT, between NPA-grown *scm* and NPA-grown WT and between NPA-grown MP::PXYΔK;*pxy* and NPA-grown WT was significant at $P<0.001$ (***) by Kruskal-Wallis and Mann-Whitney test with Bonferroni correction. Sample sizes: NPA-grown WT, 75; NPA-grown *tir1*;*afb2*, 39; NPA-grown *brx*;*brxl1*;*2*;*3*, 37; NPA-grown *er*;*erl2*, 52; NPA-grown *nip6;1*, 38; NPA-grown *ops*, 39; NPA-grown MP::PXYΔK;*pxy*, 41; NPA-grown *ric4*, 42; NPA-grown *ric6*, 43; NPA-grown *rip1*;*2*, 40; NPA-grown *rlp51*, 40; NPA-grown *rlp57*, 38; NPA-grown *yda-1*, 30; NPA-grown *yda-2*, 28; NPA-grown *rop9*, 41; NPA-grown *scm*, 53; NPA-grown *tmp*, 38; NPA-grown *tmpl*, 39. Bars: (A–D) 1 mm.

to NPA. Nevertheless, because the vein network defects of none of those mutants were enhanced by growth in the presence of NPA, we conclude that the respective WT genes do not control vein patterning synergistically with auxin transport; however, it is possible that such synergistic function is masked by functional redundancy among those genes or with other members of their respective families.

Consistent with available evidence (Schuetz et al., 2008), *er*;*erl1*;*2* formed no leaves in the presence of NPA (Table 2.4), suggesting that auxin-dependent ER/ERL-mediated signalling and auxin transport synergistically control leaf formation.

Finally, the vein pattern defects of NPA-grown MP::PXYΔK;*pxy* were no different from those of NPA-grown *tir1*;*afb2* and NPA- and PBA-grown WT (Fig. 2.7C–E) (Verna et al., 2019), suggesting that auxin-dependent PXY-mediated signalling and auxin transport synergistically control vein patterning.

2.3. Conclusions

To understand how plants uniquely control the formation of their vascular networks, we sought to identify targets of auxin signalling which control vein patterning synergistically with auxin transport and whose localization is controlled by GN.

We found 11 groups of auxin signalling targets that encode proteins that (1) are predicted to be localized to the plasma membrane or secreted to the extracellular space and (2) redundantly or non-redundantly control vein network formation: *BRX* and *BRXL1–3*; *ERL2* and, redundantly with *ERL2*, *ER*; *NIP5* and *NIP6*; *OPS*; *PXY*, non-redundantly and redundantly with *PXY*-related genes; *RIC4*, *RIC6* and *RIC7*; *RIP1* and *RIP2*, redundantly with each other; *RLP51* and *RLP57*, through *YDA*; *ROP9*; *SCM*; and *TMP* and *TMPL*.

Table 2.4. Phenotype distribution in NPA-grown progeny of selfed *er*/*er*;*ERL1*/*erl1*;*erl2*/*erl2* plants

Phenotype	Observed frequency (Proportion)	Expected frequency[1]
Leafed Seedlings	0.7705 (47/61)	0.75
Leafless Seedlings	0.2295 (14/61)	0.25

Difference between observed and theoretical frequency distributions of leafed and leafless seedlings was not significant by Pearson's chi-squared ($\chi 2$) goodness-of-fit test ($\alpha=0.05$, dF=1).

[1] Based on the hypothesis that leafless seedlings are *er*/*er*;*erl1*/*erl1*;*erl2*/*erl2*.

Of these 11 groups, we found that the group composed of *ER*, *ERL1* and *ERL2* controls leaf formation synergistically with auxin transport and that composed of *PXY* and related genes controls vein patterning redundantly with auxin transport. Because the *ER/ERL* and the *PXY*/*PXL* families redundantly control vascular tissue patterning in stem and hypocotyl (Wang et al., 2019), it will be interesting to test whether such functional redundancy extends to vein patterning.

Members of the ER/ERL and PXY/PXL families are predicted to localize to the plasma membrane, but clear evidence of such localization is only available for TDR/PXY (Hirakawa et al., 2008). In the future, it will be interesting to test whether the members of those families indeed localize to the plasma membrane and whether their localization depends on GN.

Finally, it is of course possible that other groups of auxin signalling targets control vein patterning synergistically with auxin transport but that their function is masked by lethality — as for *TMP* and *TMPL*, for example — or functional redundancy with members of the same or other families. In the future, it will be interesting to test also these possibilities. Already now, however, we have identified at least one auxin-signalling-dependent pathway — that in which *PXY* and related genes function — which controls vein patterning synergistically with auxin transport. This finding is consistent with the hypothesis that GN induces vein formation by controlling, in addition to auxin transport, the localization of proteins produced in response to auxin signalling (Verna et al., 2019).

2.4. Materials & methods

2.4.1. Plants

Origin and nature of lines, genotyping strategies and oligonucleotide sequences are Tables 2.2, 2.5 and 2.6, respectively. Seeds were sterilized and sown as in (Sawchuk et al., 2008). NPA were dissolved in dimethyl sulfoxide and dissolved chemicals were added (25 μM final NPA concentration, unless otherwise noted) to growth medium just before sowing. Stratified seeds were germinated and seedlings and plants were grown under continuous light (~100 μmol m^{-2} s^{-1}) as described previously (Verna et al., 2019). Plants were transformed and representative lines were selected as in (Sawchuk et al., 2008).

2.4.2. Imaging

Mature leaves were fixed in 6 : 1 ethanol : acetic acid, rehydrated in 70% ethanol and water and mounted in 8 : 2 : 1 chloral hydrate : glycerol : water. Mounted leaves were imaged as in (Odat et al., 2014). Image brightness and contrast were adjusted by linear stretching of the histogram in the Fiji distribution (Schindelin et al., 2012) of ImageJ (Schneider et al., 2012; Schindelin et al., 2015; Rueden et al., 2017).

2.4.3. RNA Isolation and sequencing

Total RNA was extracted as in (Chomczynski and Sacchi, 1987) from 4-day-old leaves of seedlings grown in half-strength Murashige and Skoog salts, 15 g l^{-1} sucrose, 0.5 g l^{-1} MES, pH 5.7, at 23°C under continuous light (~80 μmol m^{-2} s^{-1}) on a rotary shaker at 50 rpm. DNA was

Table 2.5. Genotyping strategies

Line	Strategy
mol1-1	*MOL1:* "MOL1-SAIL_384_A06-LP" and "MOL1-SAIL_384_A06-RP"; *mol1-1*: "LBb1.3" and "MOL1-SAIL_384_A06-RP"
rbk2-K272	*RBK2:* "RBK2-SALK_033272-LP" and "RBK2-SALK_033272-RP"; *rbk2-K272*: "LBb1.3" and "RBK2-SALK_033272-RP"
rul1-2	*RUL1*: "RUL1-SALK_121868-LP" and "RUL1-SALK_121868-RP"; *rul1-2*: "LBb1.3" and "RUL1-SALK_121868-RP"
serk1-1	*SERK1*: "SERK1-SALK_044330-LP" and "SERK1-SALK_044330-RP"; *serk1-1*: "LBb1.3" and "SERK1-SALK_044330-RP"
vh1-K625	*VH1*: "VH1/BRL2-SALK_142625-LP" and "VH1/BRL2-SALK_142625-RP"; *vh1-K625*: "LBb1.3" and "VH1/BRL2-SALK_142625-RP"
bam1-3	*BAM1*: "BAM1-SALK_015302-LP" and "BAM1-SALK_015302-RP"; *bam1-3*: "LBb1.3" and "BAM1-SALK_015302-RP"
bam2-T967	*BAM2*: "GABI_791G02 LP" and "GABI_791G02 RP"; *bam2-T967*: "8404" and "GABI_791G02 RP"
bam3-2	*BAM3*: "BAM3-SALK_044433-LP" and "BAM3-SALK_044433-RP"; *bam3-2*: "LBb1.3" and "BAM3-SALK_044433-RP"

Line	Strategy
bor2-K630	*BOR2*: "BOR2_SALK_206630_LP" and "BOR2_SALK_206630_RP"; *bor2-K630*: "LBb1.3" and "BOR2_SALK_206630_RP"
bor3-K011	*BOR3*: "BOR3_SALK_016011_LP" and "BOR3_SALK_016011_RP"; *bor3*: "LBb1.3" and "BOR3_SALK_016011_RP"
bor4-K793	*BOR4:* "BOR4_SALK_133793_LP" and "BOR4_SALK_133793_RP"; *bor4*: "LBb1.3" and "BOR4_SALK_133793_RP"
bor5-T946	*BOR5*: "BOR5_CS475450_LP" and "BOR5_CS475450_RP"; *bor5-T946*: "8474" and "BOR5_CS475450_RP"
nip5;1-1	*NIP5;1*: "nip5;1-1_SALK_122287_LP" and "nip5;1-1_SALK_122287_RP"; *nip5;1-1*: "LBb1.3" and "nip5;1-1_SALK_122287_RP"
nip6;1-1	*NIP6;1*: "nip6;1-1_CS106354_LP" and "nip6;1-1_CS106354_RP"; *nip6;1-1*: "Spm32" and "nip6;1-1_CS106354_RP"
ops-2	*OPS*: "ops-2_SALK_139316_LP" and "ops-2_SALK_139316_RP"; *ops-2*: "LBb1.3" and "ops-2_SALK_139316_RP"

Line	Strategy
opl2-1	*OPL2*: "opl2-1_SALK_004773_LP" and "opl2-1_SALK_004773_RP"; *opl2-1*: "LBb1.3" and "opl2-1_SALK_004773_RP"
pxy-3	*PXY*: "SEQ. P_ SALK_026128 LP" and "SEQ. P_ SALK_026128 RP"; *pxy-3*: "LBb1.3" and "SEQ. P_ SALK_026128 RP"
pxl1-1	*PXL1*: "PXL1-SALK_001782-LP" and "PXL1-SALK_001782-RP"; *pxl1-1*: "LBb1.3" and "PXL1-SALK_001782-RP"
pxl2-1	*PXL2*: "PXL2-SALK_114354-LP" and "PXL2-SALK_114354-RP"; *pxl2-1*: "LBb1.3" and "PXL2-SALK_114354-RP"
pxc1-3	*PXC1*: "PXC1-WiscDsLox470G6 -LP" and "PXC1-WiscDsLox470G6-RP"; *pxc1-3*: "p745" and "PXC1-WiscDsLox470G6-RP"
pxc2-K351	*PXC2*: "PXC2-SALK_055351-LP" and "PXC2-SALK_055351-RP"; *pxc2-K351*: "LBb1.3" and "PXC2-SALK_055351-RP"
pxc3-K805	*PXC3*: "PXC3-SALK_092805-LP" and "PXC3-SALK_092805-RP"; *pxc3-805*: "LBb1.3" and "PXC3-SALK_092805-RP"
ric4-K799	*RIC4*: "RIC4_SALK_015799_LP" and "RIC4_SALK_015799_RP"; *ric4-K799*: "LBb1.3" and "RIC4_SALK_015799_LP"
ric2-K885	*RIC2*: "RIC2-SALK_070885-LP" and "RIC2-SALK_070885-LP"; *ric2-K885*: "LBb1.3" and "RIC2-SALK_070885-RP"

Line	Strategy
ric6-K237	*RIC6*: "RIC6_SALK_066237_LP" and "RIC6_SALK_066237_RP"; *ric6-K237*: "LBb1.3" and "RIC6_SALK_066237_RP"
ric7-K781	*RIC7*: "RIC7_CS923572_LP" and "RIC7_CS923572_RP"; *ric7-K781*: "LBb1.3" and "RIC7_CS923572_RP"
rip1-LG05	*RIP1*: "RIP1/ICR1_CS812315_LP" and "RIP1/ICR1_CS812315_RP"; *rip1_LG05*: "LB3" and "RIP1/ICR1_CS812315_RP"
rip2-LG04	*RIP2*: "RIP2_CS878725_LP" and "RIP2_CS878725_RP"; *rip2-LG04*: "LBb1.3" and "RIP2_CS878725_RP"
rop9-LG06	*ROP9*: "ROP9_CS872231_LP" and "ROP9_CS872231_RP"; *rop9-LC06*: "LB3" and "ROP9_CS872231_RP"
rop10-K190	*ROP10*: "ROP10_SALK_030190_LP" and "ROP10_SALK_030190_RP"; *rop10-K190*: "p745" and "ROP10_SALK_030190_RP"
rop11-K681	*ROP11*: "ROP11/ROP10-1-SALK_039681-LP" and "ROP11/ROP10-1-SALK_039681-RP"; *rop11-K681*: "LBb1.3" and "ROP11/ROP10-1-SALK_039681-RP"

Line	Strategy
brx(Uk-1);*brxl1-1*;*brxl2-1*;*brxl3-1*	*BRX*/*brx*(*Uk-1*): "brx (Uk-1) FP" and "brx (Uk-1) HinF1 RP"; HinfI *BRXL1*: "BRXL1_SALK_038885_LP" and "BRXL1_SALK_038885_RP"; *brxl1-1*: "LBb1.3" and "BRXL1_SALK_038885_RP" *BRXL2*: "BRXL2_SALK_032250_LP" and "BRXL2_SALK_032250_RP"; *brxl2-1*: "LBb1.3" and "BRXL2_SALK_032250_RP" *BRXL3*: "BRXL3_SALK_017909_LP" and "BRXL3_SALK_017909_RP"; *brxl3-1*: "LBb1.3" and "BRXL3_SALK_017909_RP"
er-105	*ER*: "ERg2248" and "ERg3016rc": *er-105*: "ERg2248" and "er-105rc"
erl1-2	*ERL1*: "erl1- 2 ERL1g4411" and "ERL1g2846; *erl1-2*: "JL202" and "erl1- 2 ERL1g4411"
erl2-1	*ERL2*: "erl 2- 1 erl2g2166" and "erl 2-1 ertj3182"; *erl2-1*: "erl 1-2 JL202" and "erl2-1 ertj3182"
rlp10-1	*RLP10:* "RLP10-GABI_686A09_LP" and "RLP10-GABI_686A09_RP"; *rlp10-1*: "8404" and "RLP10-GABI_686A09_RP"

Line	Strategy
rlp17-1	*RLP17*: "RLP17- FLAG014F03_LP" and "RLP17-FLAG014F03_RP"; *rlp17-1*: "Ws-LP" and "RLP17-FLAG014F03_RP"
rlp29-1	*RLP29*: "SALK_02220_ATRLP29_LP" and SALK_02220_ATRLP29_RP"; *rlp29-1*: "LBb1.3" and "SALK_02220_ATRLP29_RP"
rlp5-1	*RLP5*: "SALK_112291_ATRLP5_LP" and "SALK_112291_ATRLP5_RP"; *rlp5-1*: "LBb1.3" and "SALK_112291_ATRLP5_RP"
rlp51-1	*RLP51*: "SALK_143038_ATRLP51_LP" and "SALK_143038_ATRLP51_RP"; *rlp51-1*: "LBb1.3" and "SALK_143038_ATRLP51_RP"
rlp55-1	*RLP55*: "SAIL_633_E08_ATRLP55_LP" and "SAIL_633_E08_ATRLP55_RP"; *rlp55-1*: LB3 and "SAIL_633_E08_ATRLP55_RP"
rlp57-1	*RLP57*: "SALK_077716_ATRLP57_LP" and "SALK_077716_ATRLP57_RP"; *rlp57-1*: "LBb1.3" and "SALK_077716_ATRLP57_RP"
yda-1	*YDA:* "YDA-1 LP" and "YDA-1 RP"; *yda-1*: PCR followed by digestion with Tru1I enzyme at 65°C
scm-2	*SCM*: "scm-2 SALK_086357 LP" and "scm-2 SALK_086357 RP"; *scm-2*: "LBb1.3" and "scm-2 SALK_086357 RP"

srf1-1	*SRF1*: “SALK_081679_LP” and “SALK_081679_RP”; *srf1-1*: “LBb1.3” and “SALK_081679_RP”
srf2-1	*SRF2*: “SALK_204435_LP” and “SALK_204435_RP”; *srf2-1*: “LBb1.3” and “SALK_204435_RP”
tmp-K336	*TMP*: SALK_060336_LP” and SALK_060336_RP”; *tmp-K336*: “LBb1.3” and SALK_060336_RP”
tmpl-K814	*TMPL*: “SALK_031814_LP” and “SALK_031814_RP”; *tmpl-K814*: “LBb1.3” and “SALK_031814_RP”

Table 2.6. Oligonucleotide sequence

Name	Sequence (5’ to 3’)
MOL1-SAIL_384_A06-LP	TTT CAC CTT GGA AAC TGT TGG
MOL1-SAIL_384_A06-RP	TCA ACA CTC CTG AAG TTT CCG
RBK2-SALK_033272-LP	AGA AAC CAT GGA GGA GAG AGC
RBK2-SALK_033272-RP	ACT TTC CCT GAA TTT TCA CCG
RUL1-SALK_121868-LP	GTA ACA TTC CTT CCG GTC TCC
RUL1-SALK_121868-RP	GAG TTA AAG GTG TCT TCC CGG
SERK1-SALK_044330-LP	ATA CAC AAA AGT GAA ACG GCG
SERK1-SALK_044330-RP	TAA TGA CAC AGA GAG GCC ACC
VH1/BRL2-SALK_142625-LP	GTC CGA TTC CTC AGA GAG GTC
VH1/BRL2-SALK_142625-RP	GTT GGT CTT TTC CCG CTT AAG
BAM1-SALK_015302-LP	GGA GCT AAT TGC GGA TTA ACC
BAM1-SALK_015302-RP	GGA ACT AAA CCG GAG AGG TTG
GABI_791G02 RP	GTT AGC TCG TTA CCG GAA ACC
BAM3-SALK_044433-LP	CTG CAA CTT CTT CTC CGT TTG
BAM3-SALK_044433-RP	GAT TCC TTC GAA ACT CGG ATC
bor1-3_SALK_037312_LP	ATG CTT GAT GTT CCA ATC GTC
bor1-3_SALK_037312_RP	ATC CAT GTG AGA CCA AAG CAG
BOR2_SALK_206630_LP	AAA TCG AGA CGC AAC AAA CAC
BOR2_SALK_206630_RP	TTAC TTT GCC TTC ATG GCA ATC
BOR3_SALK_016011_LP	TTA GCT GTA TTA GGC GCT TGC
BOR3_SALK_016011_RP	TTG TTG CAT TGT TTC TGA TGC

Name	Sequence (5’ to 3’)
BOR4_SALK_133793_LP	TTT AAA ATG GAA AAT TGG CCC
BOR4_SALK_133793_RP	AAA CGT ATC ACG GAT CAC GAG
BOR5_CS475450_LP	CCA GGG ATC TCC TCA TAC TCC
BOR5_CS475450_RP	TCT GTT TCT TCC TCT GCA AGC
nip5; 1-1_SALK_122287_LP	TCC TAG CTC CAT TTT CGT TTT C
nip5; 1-1_SALK_122287_RP	CTC CAA GTG TGA CGT AAA CCC
nip6; 1-1_CS106354_LP	TCA TCG TTG GTT CAA ACA CTG
nip6; 1-1_CS106354_RP	TTG CTC CAT CTC AAA AGC TTC
ops-2_SALK_139316_LP	CAC ACC GTT GGT TTG GTT AAC
ops-2_SALK_139316_RP	TCT TCC TCT AAA AAG CCT CCG
opl2-1_SALK_004773_LP	AAA CAA ATG GCT TGT CCC TTC
opl2-1_SALK_004773_RP	TTC GTC GAT TAC ACT TCT GGG
SEQ. P_ SALK_026128 LP	CCC CAC ACA AAA ACC ATA ATG
SEQ. P_ SALK_026128 RP	AAA AAT CGA GAA GCT TGA GGG
PXL1-SALK_001782-LP	AAT CGA TGG TCT ATC CTT CGG
PXL1-SALK_001782-RP	TAT GCG GTG GAG TTC TAC CAC
PXL2-SALK_114354-LP	ACC TCT ATG CCA CAC ACC AAG
PXL2-SALK_114354-RP	CAA GCT CTG ACG GAA TCT CAC
PXC1-WiscDsLox470G6 -LP	CAC ACT CTT CCG TCT CCA AAC
PXC1-WiscDsLox470G6 -RP	TCT AAC ACC GCC TTG TAC ACC
PXC2-SALK_055351-LP	CAA TCT CTC GGG AAG TCT TCC
PXC2-SALK_055351-RP	CCT TCT CTC ACC GTC TCA CAC

Name	Sequence (5’ to 3’)
PXC3-SALK_092805-LP	TTC ATC ACT TGC ACT GTC TCG
PXC3-SALK_092805-RP	GAC TGC TCA GAT TCC CTA CCC
RIC4_SALK_015799_LP	CCA GAA GTT CTA CTC CCC GAG
RIC4_SALK_015799_RP	CAA AAC ATT TGG TGG GTT GTC
RIC2-SALK_070885-LP	TTT GGG GAC AAG GTC AGT ATG
RIC2-SALK_070885-RP	GAA TCT TTC GTA ACC CTT CCG
RIC6_SALK_066237_LP	ACG ACA CGT ATT CGA ATC CTG
RIC6_SALK_066237_RP	GGC TAC AAC TTG TAA CCG CAC
RIC7_CS923572_LP	CTG GAC TCT GCT CGT GAA ATC
RIC7_CS923572_RP	AAA TAG GAA ATC CAA CGG ACG
RIP1/ICR1_CS812315_LP	ACA AAA GAA TGA AAC ATG CGG
RIP1/ICR1_CS812315_RP	GAT CAG ACG GTT GGA ATG
RIP2_CS878725_LP	TGT CAG ACC GAT TGA TAA GGG
RIP2_CS878725_RP	GCG CCA CTA AGT GAG AGT GAG
ROP9_CS872231_LP	TGT CAT TTA AAA TTG GCC CAC
ROP9_CS872231_RP	TTT GAA TTT ACC GGC AGT GTC
ROP10_SALK_030190_LP	CTC GCC GTT ACT AAG GGA ATC
ROP10_SALK_030190_RP	TGA TGC CCT TAG ATG TTC TGG
ROP11/ROP10-1-SALK_039681-LP	ATT GAC AGT GGT GCC TTC AAC
ROP11/ROP10-1-SALK_039681-RP	CGA TTC GTA ACG CCA TAC TTG
BRXL4_SALK_022411_LP	TTG AGC AAA GGA GAC AAC ATC
BRXL4_SALK_022411_RP	GGG TTT TTG ATT AGC CGA GAC

Name	Sequence (5’ to 3’)
brx (Uk-1) FP	CCA TAC CCT TTC ATG GGT GGA AGT
brx (Uk-1) Hinf1 RP	GAT ATG AAC ACC AGG TTC TAC TTG AGC GAT
BRXL1_SALK_038885_LP	CGA CTG AGC AGA GAT GGA TTC
BRXL1_SALK_038885_RP	CAG ACA GAG GTG AGG AGG ATG
BRXL2_SALK_032250_LP	TCA AAA GTT GAC AAA ATG CGG
BRXL3_SALK_017909_LP	TTC TGG GTT TTG CTT GAA ATG
BRXL3_SALK_017909_RP	GCC AAA ATA CCC ATC CTT GAC
BRXL4_SALK_022411_LP	TTG AGC AAA GGA GAC AAC ATC
BRXL4_SALK_022411_RP	GGG TTT TTG ATT AGC CGA GAC
ERg2248	AAG AAG TCA TCT AAA GAT GTG A
er-105rc	AGC TGA CTA TAC CCG ATA CTG A
ERg3016rc	AGA ATT TTC AGG TTT GGA ATC TGT
erl 2-1 ertj3182	ACA AAT CTG AGA GAG TTA ATG CAA AGC AG
erl1g4411	CCG GAG AGA TTG TTG AAG G
JL202	CAT TTT ATA ATA ACG CTG CGG ACA TCT AC
erl2g2166	GCC TAT TCC ACC AAT ACT TG
ertj3182.rc	ACA AAT CTG AGA GAG TTA ATG CAA AGC AG
RLP17- FLAG014F03_LP	GTT CAC GAA GCG GTC GGA

Name	Sequence (5’ to 3’)
RLP17- FLAG014F03_RP	CAA CGA TCC ACA GCT TGT GAG
Ws-2	CGG CTA TTG GTA ATA GGA CAC TGG
SALK_112291_AtRLP5_LP	TCA CAG TTT TGC CCT CGT ATC
SALK_112291_AtRLP5_RP	TGC GTG TTT GAC TCT ACA TGC
SALK_022220_AtRLP29_LP	CCA CAC GTG TCA CTT TCA GTC
SALK_022220_AtRLP29_LP	CTA CAC CTT CCG GGA TTC TTC
SALK_143038_ATRLP51_LP	ACC AGA CCG GTT TAA GAT TGG
SALK_143038_ATRLP51_RP	TGA GTG GGA ACC AAC TAA ACG
SAIL_633_E08_ATRLP55_LP	CTC TTA ACC ACC GTC TCC TCC
SAIL_633_E08_ATRLP55_RP	CAA ACG ACA CCT TTT AGC GAG
SALK_077716_ATRLP57_LP	AAT GAA CCC TCC CTA TTG CTG
SALK_077716_ATRLP57_RP	ATG AAA GCT CTA TAA TGC GCG
YDA-1 LP	GGT GGA TCC TCA TGG ACG AG
scm-2 SALK_086357 LP	GTT CCT GTG AGC TTG TTG TCC
scm-2 SALK_086357 RP	TAT CAC TTT GGG AGC ACC ATC
SALK_081679_LP	GTC CTTG AGG GGA AGA TCT TG
SALK_081679_RP	TCT TAC CAA TCC TGA CGA TGG
SALK_204435_LP	TGG CAG AAT TCG AGA ATG AAC
SALK_204435_RP	TGA GTA GCG TTA GGA GGC AAG
SALK_060336_LP	GAT TAC AAC ACA GAG CCC ACC
SALK_060336_RP	GAT CGT GTT CTT CGA GCT CTG
SALK_031814_LP	TTT CTG CAC CTC TAT TTG TTG C

Name	Sequence (5’ to 3’)
SALK_031814_RP	TGG GCC CAC CTT ATT AAA ATC
LBb1.3	ATT TTG CCG ATT TCG GAA C
Spm32	TAC GAA TAA GAG CGT CCA TTT TAG AGT GA
LB3	TAG CAT CTG AAT TTC ATA ACC AAT CTC GAT ACA C
P745	AAC GTC CGC AAT GTG TTA TTA AGT TGT C

removed with Invitrogen's TURBO DNA-free TM kit and RNA quality was evaluated with an RNA 6000 Nano chip on an Agilent 2100 Bioanalyzer. RNA was delivered to the service provider BGI (Shenzen, China), where it was sequenced using a BGISEQ instrument, with a single-end, 50-bp protocol.

2.4.4. Gene expression analysis

Clean reads, from which primers and low-quality bases had been trimmed, were delivered by the service provider as fastq files. Analysis was done by Dr. M.K. Deyholos (University of British Columbia). The fastq files were uploaded to NCBI SRA and were mapped to the Arabidopsis reference genome ((Lamesch et al., 2012), TAIR10 Release, https://phytozome.jgi.doe.gov/) using HISAT2 (Kim et al., 2015) with default parameters. The resulting SAM files were sorted using samtools (view -Su, sort) ((Li et al., 2009) and the sorted output, along with the current Arabidopsis genome annotation (TAIR10 Release downloaded from https://phytozome.jgi.doe.gov in .gff3 format) were used as input for the StringTie assembler (Pertea et al., 2016) and differential gene expression was calculated using cuffdiff (Trapnell et al., 2012).

Chapter 3: Identification and characterization of genetic suppressors of the *gnom*$^{fewer\ roots}$ phenotype

3.1. Introduction

Multicellular organisms transport water, nutrients and signals through tissue systems such as the vascular systems of plants and animals. Therefore, how vascular systems are formed is a key question in biology. In animals, formation of the vascular system relies on direct cell-to-cell communication and at least in part on cell migration (e.g., (Noden, 1988; Xue et al., 1999)) — two processes that are precluded in plants because of a cell wall that keeps cells apart and in place. Therefore, vascular systems form differently in plants.

How vascular systems form in plants is unclear, but the current hypothesis proposes that EMB30/GNOM (GN hereafter) — a guanine-nucleotide exchange factor for ADP-ribosylation factors that regulates vesicle formation in membrane trafficking (Shevell et al., 1994; Busch et al., 1996; Steinmann et al., 1999) — controls both polar transport and signal transduction of the plant hormone auxin to induce vein formation (Verna et al., 2019). However, plants in which both auxin transport and signalling are compromised phenocopy only weak *gn* alleles (Verna et al., 2019), suggesting the presence of additional, yet-to-be-identified *GN*-dependent pathways that act redundantly to auxin signalling and transport to induce vein formation.

To identify auxin-transport and auxin-signalling-independent vein-patterning pathways controlled by *GN*, it would be highly informative to identify suppressors of the *gn* phenotype. However, strong and intermediate *gn* alleles are seedling lethal (Franzmann et al., 1989; Mayer et al., 1993; Koizumi et al., 2000; Geldner et al., 2004; Okumura et al., 2013; Moriwaki et al., 2014; Verna et al., 2019) and it is thus impossible to obtain a homozygous seed stock of those

alleles to be used for mutagenesis. Fortunately, the *fewer root* weak allele of *gn* (*gn*^{fwr}), which is characterized by fragmented vein networks in its leaves (Verna et al., 2019), can instead be maintained as homozygous (Okumura et al., 2013). Here we report the identification and initial characterization of suppressors of the fragmented vein-pattern phenotype of *gn*^{fwr}.

3.2. Results & discussion

3.2.1. Identification of genetic suppressors of the *gnom*$^{fewer\ roots}$ phenotype

To identify vein patterning pathways controlled by *GN*, we screened for mutations that suppress the fragmented vein networks of *gnom*$^{fewer\ roots}$ (*gn*^{fwr}) leaves (Verna et al., 2019). To facilitate visualization of vein networks, we introduced in the *gn*^{fwr} background a cytoplasmic YFP expressed by the *SHORT-ROOT* promoter (SHR::4xYFP), which is active in vascular tissues (Gardiner et al., 2011).

The vein pattern of first leaves is complete no earlier than 8 days after germination (DAG) (Scarpella et al., 2004), but that of cotyledons is already complete by 4 DAG (Sieburth, 1999). We reasoned that if *gn*^{fwr} cotyledons had the same vein pattern defects as *gn*^{fwr} leaves and if such defects correlated with defects in SHR::4xYFP expression pattern, mutations that suppress the fragmented vein pattern of *gn*^{fwr} could be identified in cotyledons of live 4-DAG seedlings by fluorescence stereomicroscopy; we tested whether that were so.

Cotyledons of 7-DAG *gn*^{fwr} seedlings have fragmented vein networks and such a defect correlates with a defective SHR::4xYFP expression pattern in 4-DAG cotyledons (Figure 3.1). Therefore, to identify mutations that suppress the fragmented vein pattern of *gn*^{fwr}, we screened for mutations that suppress the fragmented pattern of SHR::4xYFP expression in cotyledons of live 4-DAG *gn*^{fwr} seedlings by fluorescence stereomicroscopy.

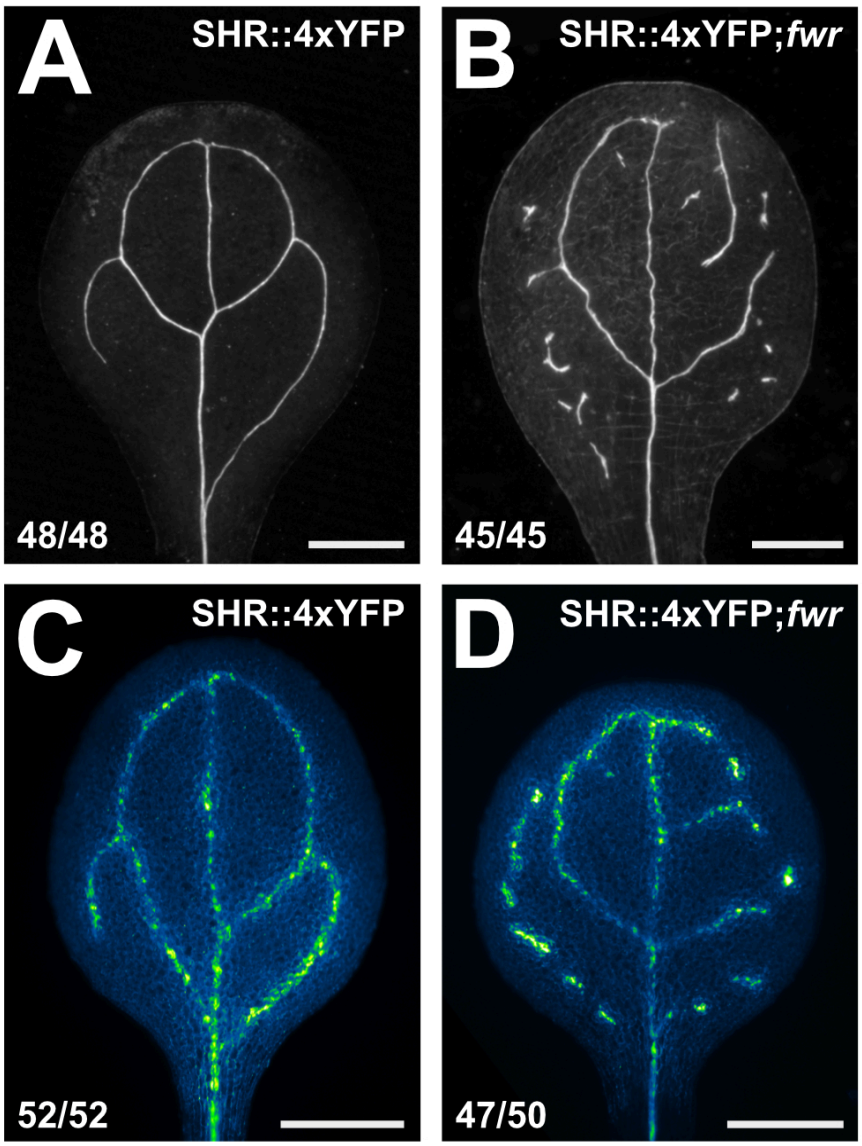

Figure 3.1. Vein Networks and *SHR* expression in gn^{fwr} cotyledons

(A–D) Top right: genotype. Bottom left: reproducibility index, i.e. number of cotyledons with the displayed features / number of cotyledons analyzed. (A,B) Dark-field illumination of cleared mature cotyledons 7 days after germination (DAG). (C,D) Epifluorescence microscopy of 4-DAG cotyledons. Look-up table (ramp in C) visualizes global background (black), autofluorescence (blue) and levels of YFP expression (cyan to white through green and yellow). Scale bars: (A,B) 1 mm; (C,D) 0.5 mm.

3.2.1.1. Mutagenesis

We mutagenized ~14,000 seeds of SHR::4xYFP; *gn*^{fwr} with 0.3% ethyl methanesulfonate (EMS) and ~7,000 seeds of SHR::4xYFP; *gn*^{fwr} with 0.5% EMS. Because we expect *gn*^{fwr} suppressors to be fertile, we sowed the mutagenized (M1) seeds in pools. Available evidence suggests up to 50% lethality in the M1 population (Odat, 2015). Therefore, we sowed M1 seeds in pools of ~200 seeds each, which is expected to lead to ≥100 M1 plants / pool.

We sowed 70 pools of M1 seeds for the population generated by mutagenesis with 0.3% EMS ("0.3%-EMS population") and 20 pools of M1 seeds for the 0.5%-EMS population. The average number of M1 plants / pool was 176 ± 8 (*n*=30) for the 0.3%-EMS population and 98 ± 5 (*n*=20) for the 0.5%-EMS population, suggesting ~10% lethality for the 0.3%-EMS population and ~50% lethality for the 0.5%-EMS population.

Efficient mutagenesis is expected to result in albino sectors in 0.1–1% of M1 plants (Lightner and Caspar, 1998). Therefore, to assess mutagenesis efficiency, we counted the number of M1 plants with albino sectors.

We found 65 M1 plants with albino sectors in 30 pools of the 0.3%-EMS population and 39 M1 plants with albino sectors in 10 pools of the 0.5%-EMS population. The M1 plants from the 0.5%-EMS population, in which ~4% of the M1 plants had albino sectors, were sterile, suggesting that each M1 plant in the 0.5%-EMS population contains at least one gametophytic lethal mutation. By contrast, the M1 plants in the 0.3%-EMS population, in which ~1% of the M1 plants had albino sectors, were fertile.

We harvested in pools M2 seeds of the 0.3%-EMS population — derived from the selfing of the respective M1 plants — and to assess the saturation level of mutagenesis in the 0.3%-EMS M1 population, we counted the number of *fusca* (*fus*) mutant seeds in the 0.3%-EMS M2 seed

population. Because there are 14 *FUS* genes in Arabidopsis (Miséra et al., 1994) and because the Poisson formula suggests that at least five mutant alleles per gene are required to infer that a genome has been saturated with mutations (Jürgens et al., 1991), at least 70 M1 plants segregating *fus* mutants in the M2 population have to be recovered to infer that the genome has been saturated with mutations.

Because 12 M2 individuals have to be examined to recover at least one recessive mutant with P=0.80 (Jürgens et al., 1991; Redei and Koncz, 1992), we inspected >12 M2 seeds / M1 plant. Because there were ~176 M1 plants / pool in the 0.3%-EMS population, we weighed >2,112 M2 seeds / M1 pool for 30 0.3%-EMS M1 pools and counted their number of *fus* seeds. Because it is impossible to know whether two *fus* seeds found in the same M2 seed pool derive from the same M1 plant or from two different ones, we conservatively assumed that all the *fus* seeds found in an M2 seed pool derived from the same M1 plant. In other words, we equated the number of M2 seed pools that contain *fus* seeds with the number of M1 plants segregating *fus* mutants in the M2 generation.

We found that 29 of the 30 0.3%-EMS M1 pools contained *fus* seeds, suggesting that there is at least one M1 plant in each of those 29 pools that is segregating the *fus* mutation. Therefore, the average number of mutant alleles per *FUS* gene in the 30 M1 pools is 2.1 and according to the Poisson formula the level of mutagenesis saturation in those ~5,280 M1 plants is 88%. Consequently, the level of mutagenesis saturation in the entire 0.3%-EMS M1 population is >99%. We conclude that the entire Arabidopsis genome has been saturated with mutations in the 0.3%-EMS M1 population.

3.2.1.2. Screening

To identify at least one recessive *gn^{fwr}* suppressor with 80% probability, we sowed >2,112 M2 seeds for each of the 30 M1 pools of the 0.3%-EMS population for which we had calculated the level of mutagenesis saturation and screened with a fluorescence stereomicroscope M2 seedlings 4 and 5 DAG. We screened nearly 65,000 M2 seedlings progeny of ~5,280 M1 plants and transferred to soil ~750 putative *gn^{fwr}* suppressors with WT-looking pattern of SHR::4xYFP expression in their cotyledons.

The vein pattern in the mature first leaves of ~740 of those ~750 putative *gn^{fwr}* suppressors was no different from that of *gn^{fwr}*, suggesting that in those ~740 M2 plants the suppression was specific to the cotyledon vein pattern or to the expression of SHR::4xYFP. By contrast, the vein pattern in the mature first leaves of the remaining 10 putative *gn^{fwr}* suppressors was no different from that of WT, suggesting that in those 10 M2 plants the suppression was not specific to the cotyledon vein pattern or to the expression of SHR::4xYFP.

We genotyped the 10 putative *gn^{fwr}* suppressors with WT-looking pattern of SHR::4xYFP expression in their cotyledons and of veins in their leaves and found that four of them were homozygous or heterozygous *gn^{fwr}*-to-*GN* revertants. By contrast, the six remaining putative *gn^{fwr}* suppressors were *gn^{fwr}* homozygotes, suggesting that they contain second-site mutations that suppress the *gn^{fwr}* phenotype.

3.2.2. Characterization of genetic suppressors of the *gn^{fwr}* phenotype

3.2.2.1. Inheritance

We identified six M2 plants that contain second-site mutations that suppress the *gn^{fwr}* phenotype (Figure 3.2). To determine the pattern of inheritance of those second-site mutations, we crossed

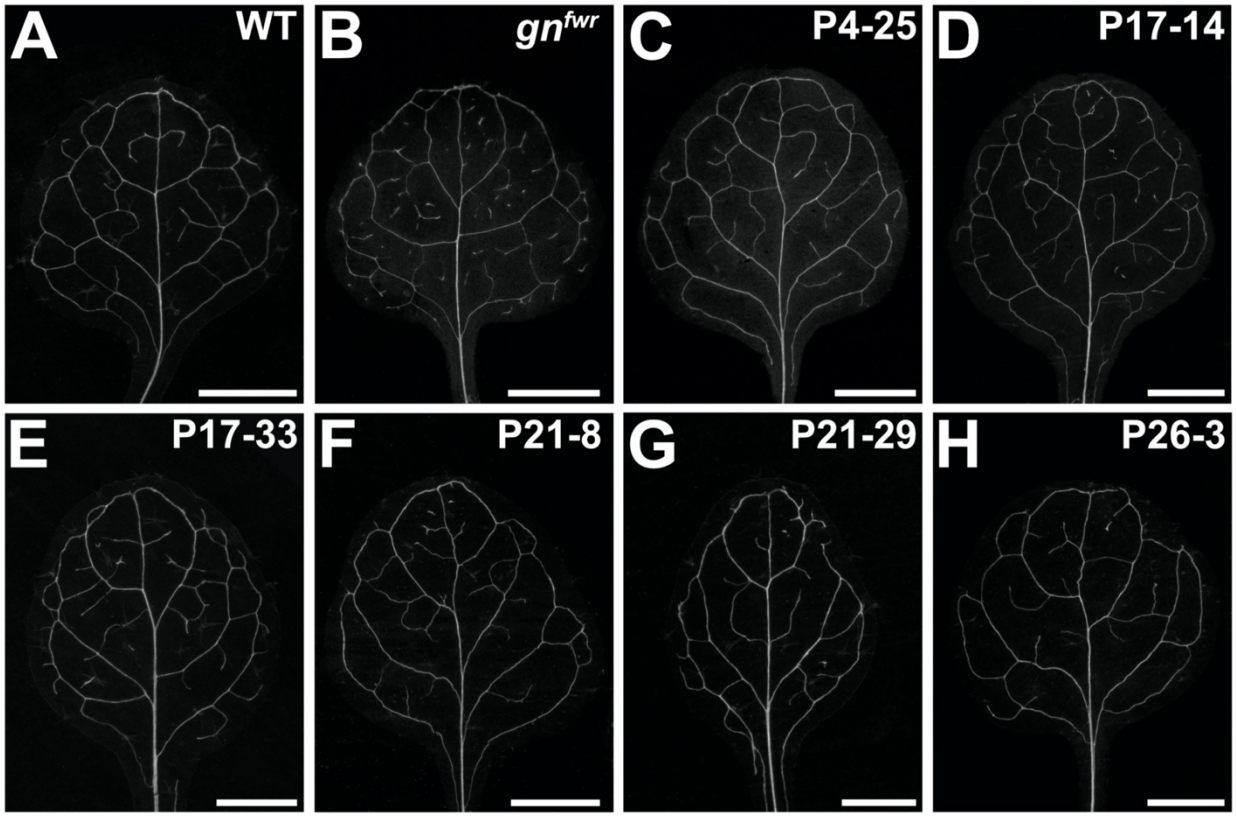

Figure 3.2. Leaf vein networks of suppressors of the *gn*^{fwr} phenotype

(A–H) Dark-field illumination of cleared first leaves 14 DAG; top right: genotype. Scale bars: (A–H) 1 mm.

to *gn*^{fwr} M3 plants that (1) derived from the selfing of those six M2 plants, (2) were homozygous for the *gn*^{fwr} mutation and (3) had a WT-looking vein pattern in their mature first leaves; we then analyzed the vein patterns in the mature first leaves of the resulting F1 plants.

All (*n*=20) the F1 plants resulting from the cross between suppressor line P4-25 and *gn*^{fwr} had fragmented vein networks in their leaves, suggesting that the effects of the respective suppressor mutation are recessive and the mutation is homozygous in the M3 plant that was used for that cross.

All (*n*=17) the F1 plants resulting from the cross between suppressor line P17-14 and *gn*^{fwr} had WT-looking vein patterns in their leaves, suggesting that the effects of the corresponding suppressor mutation are dominant and completely penetrant and the mutation is homozygous in the M3 plant that was used for that cross.

Approximately 90% (16/18) of the F1 plants resulting from the cross between suppressor line P17-33 and *gn*^{fwr}, ~75% (14/19) of the F1 plants resulting from the cross between suppressor line P21-8 and *gn*^{fwr} and ~60% (11/19) of the F1 plants resulting from the cross between suppressor line P26-3 and *gn*^{fwr} had WT-looking vein patterns in their leaves, suggesting that the effects of the respective suppressor mutations are dominant and incompletely penetrant and the mutations are homozygous in the M3 plants that were used for those crosses.

Finally, ~40% (6/16) of the F1 plants resulting from the cross between suppressor line P21-29 and *gn*^{fwr} had WT-looking vein patterns in their leaves, suggesting that the effects of the corresponding suppressor mutation are dominant and completely penetrant and the mutation is heterozygous in the M3 plant that was used for that cross. Consistent with this interpretation, ~75% (28/36) of the M4 plants progeny of the M3 plant that was used for the cross to *gn*^{fwr} had

WT-looking pattern, which is no different from the expected frequency distribution by Pearson's chi-squared ($\chi 2$) goodness-of-fit test (α=0.05, dF=1).

3.2.2.2. Penetrance

To determine the degree of penetrance of the effects of the suppressor mutations on the *gn*^{fwr} phenotype, we analyzed the vein patterns in the mature first leaves of M4 plants that were homozygous for both the *gn*^{fwr} and the suppressor mutations.

All the leaves (*n*=36) of the M4 plants homozygous for the suppressor mutations in lines P4-25 and P17-14 had WT-looking vein patterns, suggesting that the penetrance of the respective suppressor mutations is complete.

By contrast, ~90% of the leaves (*n*=35) of M4 plants homozygous for the suppressor mutation in line P17-33, ~80% of the leaves (*n*=40) of M4 plants homozygous for the suppressor mutation in line P21-8 and ~90% of the leaves (*n*=33) of M4 plants homozygous for the suppressor mutation in line P26-3 had WT-looking vein patterns, suggesting that the penetrance of the respective suppressor mutations is incomplete.

3.2.2.3. Intra- or extragenicity

The penetrance of the suppressor mutations in lines P4-25 and P17-14 is complete. To determine whether the respective suppressor mutations are intragenic or extragenic, we crossed plants homozygous for both the *gn*^{fwr} and the respective suppressor mutations to WT plants and analyzed the vein patterns in the mature first leaves of the resulting F2 plants.

All (*n*=97) the F2 plants derived from the cross between WT and plants homozygous for both the *gn*^{fwr} and the suppressor mutations in line P4-25 had WT-looking vein patterns,

suggesting with $P>0.99$ that the corresponding suppressor mutation is intragenic or closely linked to the *gn*^{fwr} mutation. Sequencing of the *gn*^{fwr} coding sequence in two plants homozygous for both the *gn*^{fwr} and the suppressor mutation in line P4-25 failed to identify mutations in addition to the *gn*^{fwr} mutation, suggesting that the suppressor mutation in line P4-25 is extragenic and closely linked to the *gn*^{fwr} mutation, or is intragenic and outside of the *gn*^{fwr} coding sequence.

Four of the 95 F2 plants derived from the cross between WT and plants homozygous for both the *gn*^{fwr} and the suppressor mutations in line P17-14 had fragmented vein networks, suggesting that the corresponding suppressor mutation is extragenic. However, the difference between observed and expected frequency distributions of F2 plants with fragmented vein networks was significant by Pearson's chi-squared ($\chi 2$) goodness-of-fit test ($\alpha=0.05$, dF=1), suggesting that the suppressor mutation in line P17-14 is linked to the *gn*^{fwr} mutation, which is located at position 4,792,019 on chromosome 1. Because the recombination frequency between two points on a chromosome is $1 - \sqrt{(1 - 2x)}$, where x is the frequency of recombinant phenotypes in an F2 population, the recombination frequency between *gn*^{fwr} and the suppressor mutation in line P17-14 is ~0.088, or ~8.8 cM, which in Arabidopsis corresponds to ~2,200 kb (Lukowitz et al., 2000). Therefore, the suppressor mutation in line P17-14 is located between positions ~4,789,819 and ~4,794,219 on chromosome 1.

3.3. Conclusions

To identify *GN*-dependent pathways that act redundantly to auxin signalling and transport to induce vein formation, we screened for genetic suppressors of the *gn*^{fwr} phenotype. We identified six second-site such mutations that suppress the fragmented vein pattern of *gn*^{fwr} leaves. The effects of one of those six mutations are recessive, whereas the effects of the remaining five mutations are dominant. The effects of the recessive mutation and of one of the five dominant

mutations are completely penetrant; the effects of the other four dominant mutations are incompletely penetrant.

In the future, it will be important to understand whether the completely penetrant, recessive suppressor mutation is intra- or extragenic — for example, by determining whether any mutation exists outside of the *gn*^{fwr} coding sequence in that suppressor line. It will also be important to test whether any of the suppressor mutations is allele-specific, which could be less informative of *GN*-dependent vein-patterning pathways, by assessing the ability of the mutations to rescue the phenotype of other weak alleles of *gn* — for example, *gn-18* (Verna et al., 2019). Finally, it will be interesting to sequence the whole genome of all the extragenic, non-allele-specific *gn* suppressors to identify the corresponding suppressor mutations.

3.4. Materials & methods

3.4.1. Plants

Origin and nature of the SHR::4xYFP and *gn*^{fwr} lines are in (Okumura et al., 2013; Marquès-Bueno et al., 2016). The *GN* and *gn*^{fwr} alleles were genotyped as in (Verna et al., 2019). Approximately 14,000 seeds (~0.28 g or 560 µl) of SHR::4xYFP;*gn*^{fwr} were incubated with 40 ml of 0.3% or 0.5% w/v ethyl methanesulfonate (Sigma-Aldrich M0880) in 50-ml conical tubes on a rocking platform O/N at 22°C. After mutagenesis, seeds were washed 10 times, 30 minutes each, with 50 ml of sterile water; transferred to sterile 0.1% w/v agar at a final density of ~20 seeds/ml; stratified for 4 days at 4°C; and sowed on soil-filled trays (~10 ml, i.e. 200 seeds/pool; 10 pools/tray). M2 seeds were sterilized as in (Lindsey et al., 2017); all other seeds were sterilized as in (Sawchuk et al., 2008). Sterilized seeds were sown and stratified as in (Sawchuk

et al., 2008). Stratified seeds were germinated and seedlings and plants were grown as described previously (Verna et al., 2019).

3.4.2. Imaging

Seedlings and developing cotyledons were mounted and imaged as in (Sawchuk et al., 2008). Mature leaves were fixed in 6 : 1 ethanol : acetic acid, rehydrated in 70% ethanol and water and mounted in 8 : 2 : 1 chloral hydrate : glycerol : water. Mounted leaves were imaged as in (Odat et al., 2014). Image brightness and contrast were adjusted by linear stretching of the histogram in the Fiji distribution (Schindelin et al., 2012) of ImageJ (Schneider et al., 2012; Schindelin et al., 2015; Rueden et al., 2017).

Chapter 4: GAL4/GFP enhancer-trap lines for identification and manipulation of cells and tissues in developing Arabidopsis leaves[2]

4.1. Introduction

The unambiguous identification of cell and tissue types and the selective manipulation of their properties is key to our understanding of developmental processes. Both the unambiguous identification and the selective manipulation can most efficiently be achieved by the GAL4 system (Brand and Perrimon, 1993). In such a system, a minimal promoter in a construct randomly inserted in a genome responds to neighboring regulatory elements and activates the expression of a gene, included in the same construct, encoding a variant of the GAL4 transcription factor of yeast; the same construct also includes a GAL4-responsive, UAS-driven lacZ, GUS, or GFP, which reports GAL4 expression. Independent, phenotypically normal lines, in which the construct is inserted in different genomic locations, are selected because they reproducibly express the GAL4-responsive reporter in cell- or tissue-specific patterns. Lines with cell- or tissue-specific GAL4-driven reporter expression can then be used to characterize the behavior of the labeled cells or tissues (Yang et al., 1995), to identify mutations that interfere with that behavior (Guitton et al., 2004), or to identify genes expressed in the labeled cells or

[2] Adapted from Amalraj, B., Govindaraju, P., Krishna, A., Lavania, D., Linh, N. M., Ravichandran, S. J. and Scarpella, E. (2020). GAL4/GFP enhancer-trap lines for identification and manipulation of cells and tissues in developing Arabidopsis leaves. *Dev Dyn* **279**, 1127-1146.

tissues by cloning the DNA flanking the insertion site of the enhancer-trap construct (Calleja et al., 1996). Furthermore, lines with cell- or tissue-specific GAL4 expression can be crossed with lines with UAS-driven RNAi constructs to trigger cell or tissue-specific gene silencing (Nagel et al., 2002), dominant-negative alleles to interfere with the WT gene function in specific cells or tissues (Elefant and Palter, 1999), toxic genes to induce cell- or tissue-specific ablation (Reddy 1997), or genes of interest to investigate necessary or sufficient functions in specific cells or tissues (Gunthorpe et al., 1999). Though the GAL4 system does not allow to restrict the expression of UAS-driven transgenes to a temporal window that is narrower than that in which GAL4 is expressed, the system allows exquisite spatial control of transgene expression (McGuire et al., 2004).

One of the first implementations of the GAL4 system in Arabidopsis was the Haseloff collection of GAL4/GFP enhancer-trap lines, in which an endoplasmic-reticulum-localized GFP (erGFP) responds to the activity of a fusion between the GAL4 DNA-binding domain and the activating domain of VP16 of *Herpes simplex* (Berger et al., 1998; Haseloff, 1999). The Haseloff collection is the most extensively used GAL4 system in Arabidopsis (e.g., (Sabatini et al., 1999; Weijers et al., 2003; Laplaze et al., 2005; Sawchuk et al., 2007; Gardner et al., 2009; Wenzel et al., 2012)), even though it is in the C24 background. This is problematic because the phenotype of hybrids between C24 and Col-0, generally considered the reference genotype in Arabidopsis (Koornneef and Meinke, 2010), is different from that of either parent (e.g., (Groszmann et al., 2014; Kawanabe et al., 2016; Radoeva et al., 2016; Zhang et al., 2016)). The use of GAL4/GFP enhancer-trap lines in the C24 background to investigate processes in the Col-0 background thus imposes the burden of laborious generation of ad-hoc control backgrounds. Therefore, most desirable is the generation and characterization of GAL4/GFP enhancer-trap collections in the

Col-0 background. Two such collections have been reported: the Berleth collection, which has been used to identify lines that express GAL4/GFP in vascular tissues (Ckurshumova et al., 2009); and the Poethig collection, which has been used to identify lines that express GAL4/GFP in stomata (Garnder et al., 2009).

Here we screened the Poethig collection; we provide a set of lines for the specific labeling of cells and tissues during early leaf development and we show that these lines can be used to address key questions in plant developmental biology.

4.2. Results & discussion

To identify enhancer-trap lines in the Col-0 background of Arabidopsis with reproducible GAL4-driven GFP expression during early leaf development, we screened the collection that Scott Poethig had generated with Jim Haseloff's GAL4/GFP enhancer-trap construct (Fig. 4.1A) and had donated to the Arabidopsis Biological Resource Center. We screened 312 lines for GFP expression in first leaves 4 and 5 DAG by fluorescence stereomicroscopy (see Materials & Methods); 29 lines satisfied this criterion (Table 4.1). In 10 of these 29 lines, we detected GFP in specific cells or tissues in first leaves 4 and 5 DAG by epifluorescence microscopy (see Materials & Methods); nine of these 10 lines were phenotypically normal (Table 4.1). We imaged GFP expression in first leaves of these nine lines from 2 to 5 DAG by confocal laser scanning microscopy.

The development of Arabidopsis leaves has been described previously (Pyke et al., 1991; Larkin et al., 1994; Telfer and Poethig, 1994; Kinsman and Pyke, 1998; Candela et al., 1999; Donnelly et al., 1999; Mattsson et al., 1999; Kang and Dengler., 2002; Kang and Dengler., 2004; Mattsson et al., 2003; Scarpella et al., 2004). Briefly, at 2 DAG the first leaf is recognizable as a cylindrical primordium with a midvein at its center (Fig. 4.1B). By 2.5 DAG, the primordium has

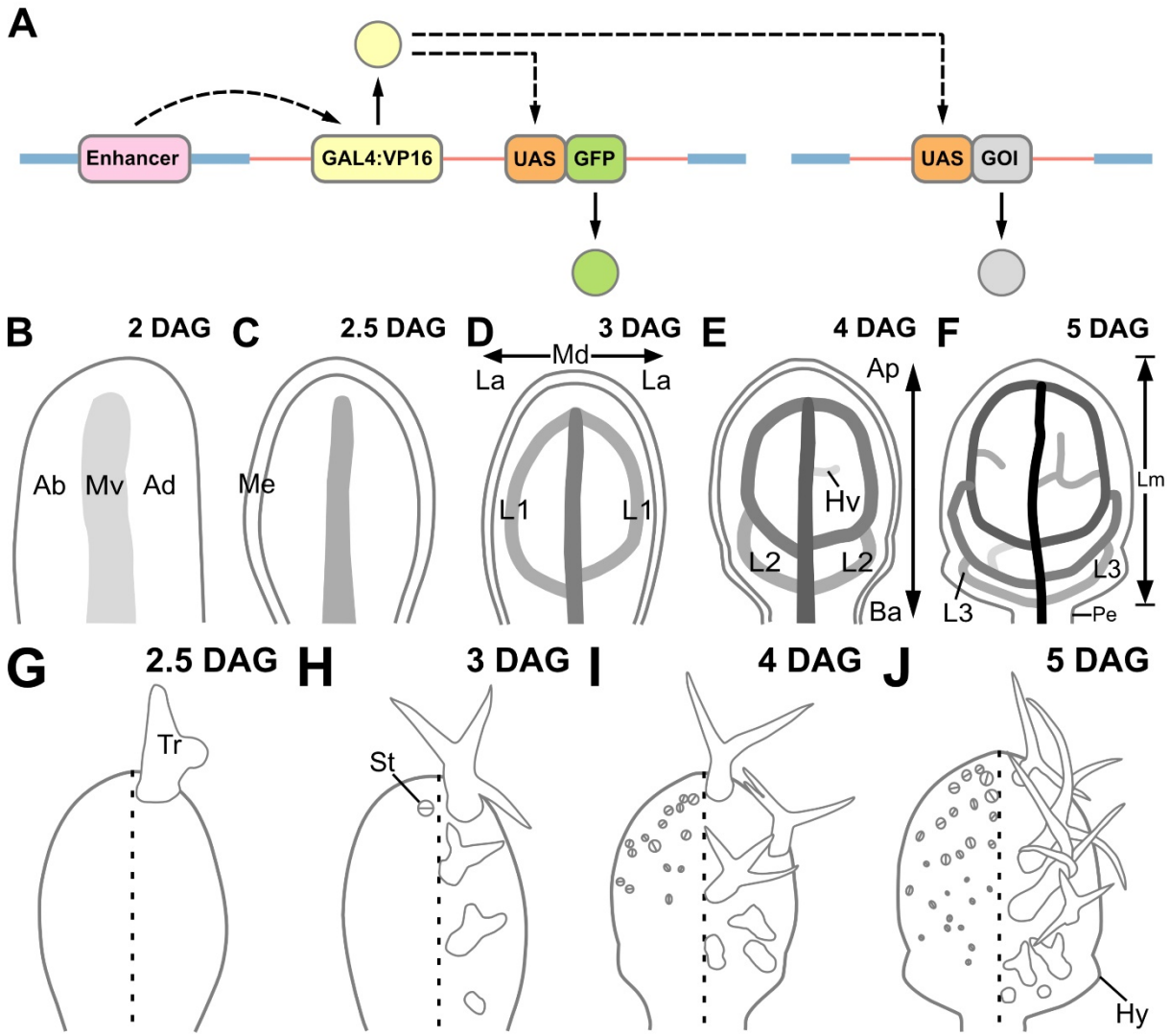

Figure 4.1. Poethig GAL4/GFP enhancer-trap lines and Arabidopsis leaf development

(A) Cell- or tissue-specific enhancers in the Arabidopsis genome (blue line) activate transcription (dashed arrow) of a codon-usage-optimized translational fusion between the sequence encoding the GAL4 DNA-binding domain and the sequence encoding the activating domain of the Viral Protein 16 of *Herpes simplex* (GAL4:VP16) in a T-DNA construct (red line) that is randomly inserted in the Arabidopsis genome. Translation of the GAL4:VP16 fusion gene (solid arrow) leads to cell- or tissue-specific activation of transcription of a UAS-driven, endoplasmic-reticulum-localized, improved GFP gene (mGFP5) (Siemering et al., 1996; Haseloff et al., 1997).

Crosses between lines with cell- or tissue-specific expression of GAL4:VP16 and lines with UAS-driven genes of interest (GOIs) lead to activation of GOI transcription in specific cells or tissues. See text and (Berger et al., 1998; Haseloff, 1999) for details. (B–J) First leaves. Top right: leaf age in days after germination (DAG); see Materials & methods for definition. (B–F) Development of leaf and veins; increasingly darker grays depict progressively later stages of vein development. (B) Side view, median plane. Abaxial (ventral) side to the left; adaxial (dorsal) side to the right. (C–F) Front view, median plane. See text for details. (G–J) Development of stomata and trichomes in abaxial (left) or adaxial (right) epidermis. Front ventral (left) or dorsal (right) view, epidermal plane. See text for details. Ab: abaxial; Ad: adaxial; Ap: apical; Ba: basal; Hv: minor vein; Hy: hydathode; L1, L2 and L3: first, second and third loop; La: lateral; Lm: lamina; Md: median; Me: marginal epidermis; Mv: midvein; Pe: petiole; St: stoma; Tr: trichome.

Table 4.1. Origin and nature of lines

ABRC stock no.	Donor stock no.	Expression in developing leaves	Tissue- and/or stage-specific expression	Phenotypically normal
CS24240	E53	N[a]	…	…
CS24241	E306	N	…	…
CS24242	E337	N	…	…
CS24243	E362	N	…	…
CS24244	E456	N	…	…
CS24245	E513	N	…	…
CS24246	E652	N	…	…
CS24247	E751	N	…	…
CS24248	E788	N	…	…
CS24249	E829	N	…	…
CS24250	E1012	N	…	…
CS24251	E1075	N	…	…
CS24252	E1195	N	…	…
CS24253	E1247	N	…	…
CS24254	E1287	N	…	…
CS24255	E1324	N	…	…
CS24256	E1332	Y[b]	N	…
CS24257	E2042	N	…	…
CS24258	E2065	N	…	…
CS24259	E2072	N	…	…
CS24260	E2119	N	…	…
CS24262	E2168	N	…	…
CS24264	E2242	N	…	…
CS24265	E2263	N	…	…
CS24266	E2271	N	…	…
CS70072	E1092	N	…	…

ABRC stock no.	Donor stock no.	Expression in developing leaves	Tissue- and/or stage-specific expression	Phenotypically normal
CS70073	E1100	N	…	…
CS70074	E1127	N	…	…
CS70075	E1128	N	…	…
CS70076	E1130	N	…	…
CS70077	E1155	N	…	…
CS70078	E1161	N	…	…
CS70079	E1176	N	…	…
CS70080	E1222	N	…	…
CS70081	E1223	N	…	…
CS70082	E1237	N	…	…
CS70083	E1238	N	…	…
CS70084	E1250	N	…	…
CS70085	E1252	N	…	…
CS70086	E1271	N	…	…
CS70087	E1289	Y	N	…
CS70088	E1304	N	…	…
CS70089	E1322	N	…	…
CS70090	E1325	N	…	…
CS70091	E1331	N	…	…
CS70092	E1341	N	…	…
CS70093	E1344	N	…	…
CS70094	E1356	N	…	…
CS70095	E1361	N	…	…
CS70096	E1362	N	…	…
CS70097	E1370	N	…	…
CS70098	E1387	N	…	…
CS70099	E1388	N	…	…
CS70100	E1395	N	…	…

ABRC stock no.	Donor stock no.	Expression in developing leaves	Tissue- and/or stage-specific expression	Phenotypically normal
CS70102	E1405	N	…	…
CS70103	E1416	N	…	…
CS70104	E1439	N	…	…
CS70105	E1439m	N	…	…
CS70106	E1457	N	…	…
CS70107	E1567	N	…	…
CS70108	E1570	N	…	…
CS70109	E1607	N	…	…
CS70110	E1626	N	…	…
CS70111	E1627	N	…	…
CS70112	E1628	N	…	…
CS70113	E1638	N	…	…
CS70114	E1644	N	…	…
CS70115	E1662	N	…	…
CS70116	E1663	Y	N	…
CS70117	E1665	N	…	…
CS70118	E1678	N	…	…
CS70119	E1684	N	…	…
CS70120	E1689	N	…	…
CS70121	E1691	N	…	…
CS70122	E1701	N	…	…
CS70123	E1728	N	…	…
CS70125	E1751	N	…	…
CS70126	E1765	N	…	…
CS70127	E1767	N	…	…
CS70128	E1785	N	…	…
CS70129	E1786	N	…	…
CS70130	E1797	N	…	…

ABRC stock no.	Donor stock no.	Expression in developing leaves	Tissue- and/or stage-specific expression	Phenotypically normal
CS70131	E1801	N	…	…
CS70132	E1809	N	…	…
CS70133	E1815	N	…	…
CS70134	E1817	N	…	…
CS70135	E1818	N	…	…
CS70136	E1819	N	…	…
CS70137	E1825	N	…	…
CS70138	E1828	N	…	…
CS70139	E1832	N	…	…
CS70140	E1833	N	…	…
CS70141	E1853	N	…	…
CS70142	E1868	N	…	…
CS70143	E1950	N	…	…
CS70144	E1998	N	…	…
CS70145	E2034	N	…	…
CS70146	E217	N	…	…
CS70147	E562	N	…	…
CS70148	E1001	N	…	…
CS70149	E1368	N	…	…
CS70150	E1690	N	…	…
CS70151	E1704-1	N	…	…
CS70152	E1704-3	N	…	…
CS70153	E1715	N	…	…
CS70154	E1723	N	…	…
CS70155	E1735	N	…	…
CS70156	E1935	N	…	…
CS70157	E1967	N	…	…
CS70158	E2014	N	…	…

ABRC stock no.	Donor stock no.	Expression in developing leaves	Tissue- and/or stage-specific expression	Phenotypically normal
CS70159	E2057	N	…	…
CS70160	E2207	N	…	…
CS70161	E2406	N	…	…
CS70162	E2408	Y	Y	Y
CS70163	E2410	N	…	…
CS70164	E2415	N	…	…
CS70165	E2425	N	…	…
CS70166	E2425	N	…	…
CS70167	E2441	N	…	…
CS70168	E2443	N	…	…
CS70169	E2448	N	…	…
CS70170	E2491	N	…	…
CS70171	E2502	N	…	…
CS70172	E2513	N	…	…
CS70173	E2563	N	…	…
CS70174	E2609	N	…	…
CS70175	E2633	N	…	…
CS70176	E2676	N	…	…
CS70177	E2692	Y	N	…
CS70178	E2724	N	…	…
CS70179	E2763	N	…	…
CS70180	E2764	N	…	…
CS70181	E2779	N	…	…
CS70182	E2861	N	…	…
CS70183	E2862	N	…	…
CS70184	E2897	N	…	…
CS70185	E2904	N	…	…
CS70186	E2905	N	…	…

ABRC stock no.	Donor stock no.	Expression in developing leaves	Tissue- and/or stage-specific expression	Phenotypically normal
CS70187	E2947	N	…	…
CS70188	E2993	N	…	…
CS70189	E3004	N	…	…
CS70190	E3006	N	…	…
CS70191	E3017	N	…	…
CS70192	E3065	N	…	…
CS70193	E3134	N	…	…
CS70194	E3190	N	…	…
CS70195	E3198	N	…	…
CS70196	E3258	N	…	…
CS70197	E3267	N	…	…
CS70198	E3298	N	…	…
CS70199	E3313	N	…	…
CS70200	E3317	Y	Y	N
CS70201	E3430	N	…	…
CS70202	E3459	N	…	…
CS70203	E3462	N	…	…
CS70204	E3474	N	…	…
CS70205	E3478	N	…	…
CS70206	E3501	N	…	…
CS70207	E3505	N	…	…
CS70208	E3530	N	…	…
CS70209	E3531	N	…	…
CS70210	E3598-1	N	…	…
CS70211	E3598-2	N	…	…
CS70212	E3637	N	…	…
CS70213	E3642	N	…	…
CS70214	E3655	Y	N	…

ABRC stock no.	Donor stock no.	Expression in developing leaves	Tissue- and/or stage-specific expression	Phenotypically normal
CS70215	E3683	N	…	…
CS70216	E3700	N	…	…
CS70217	E3754	N	…	…
CS70218	E3756	N	…	…
CS70219	E3783	Y	N	…
CS70220	E3806	N	…	…
CS70221	E3816	N	…	…
CS70222	E3826	N	…	…
CS70223	E3876	N	…	…
CS70224	E3879	N	…	…
CS70225	E3880	N	…	…
CS70226	E3885	Y	N	…
CS70227	E3912	Y	Y	Y
CS70228	E3927	N	…	…
CS70229	E3930	Y	N	…
CS70230	E3963	N	…	…
CS70231	E3980	N	…	…
CS70232	E4009	N	…	…
CS70233	E4028	Y	N	…
CS70234	E4058	N	…	…
CS70235	E4096	N	…	…
CS70236	E4104	N	…	…
CS70237	E4105	N	…	…
CS70238	E4110	N	…	…
CS70239	E4118	Y	N	…
CS70240	E4129	N	…	…
CS70241	E4148	N	…	…
CS70242	E4150	N	…	…

ABRC stock no.	Donor stock no.	Expression in developing leaves	Tissue- and/or stage-specific expression	Phenotypically normal
CS70243	E4151	N	…	…
CS70244	E4162	N	…	…
CS70245	E4223	N	…	…
CS70246	E4247	N	…	…
CS70247	E4256	N	…	…
CS70248	E4272	N	…	…
CS70249	E4285	N	…	…
CS70250	E4295	Y	Y	Y
CS70251	E4350	N	…	…
CS70252	E4396	N	…	…
CS70253	E4411	N	…	…
CS70254	E4423	N	…	…
CS70255	E4491	N	…	…
CS70256	E4506	Y	N	…
CS70257	E4522	Y	N	…
CS70258	E4583	N	…	…
CS70259	E4589	N	…	…
CS70260	E4633	N	…	…
CS70261	E4680	N	…	…
CS70262	E4695	N	…	…
CS70263	E4715	N	…	…
CS70264	E4716	Y	Y	Y
CS70265	E4722	Y	Y	Y
CS70266	E4751	N	…	…
CS70267	E4791	N	…	…
CS70268	E4801	N	…	…
CS70269	E4811	N	…	…
CS70270	E4812	N	…	…

ABRC stock no.	Donor stock no.	Expression in developing leaves	Tissue- and/or stage-specific expression	Phenotypically normal
CS70271	E4820	N	…	…
CS70272	E4856	Y	N	…
CS70273	E4907	N	…	…
CS70274	E4930	N	…	…
CS70275	E4940	N	…	…
CS70276	E4970	N	…	…
CS70277	E5008	N	…	…
CS70278	E5025	N	…	…
CS70279	E5026	N	…	…
CS70280	E5085	N	…	…
CS70281	E5096	Y	N	…

N, No; Y, Yes

elongated and expanded (Fig. 4.1C). By 3 DAG, the primordium has continued to expand and the first loops of veins ("first loops") have formed (Fig. 4.1D). By 4 DAG, a lamina and a petiole have become recognizable, second loops have formed and minor veins have started to form the top half of the lamina (Fig. 4.1E). By 5 DAG, lateral outgrowths (hydathodes) have become recognizable in the lower quarter of the lamina, third loops have formed and minor vein formation has spread toward the base of the lamina (Fig. 4.1F). Leaf hairs (trichomes) and pores (stomata) can be first recognized at the tip of 2.5- and 3-DAG primordia, respectively and their formation spreads toward the base of the lamina during leaf development (Fig. 4.1G–J).

Consistent with previous observations (Huang et al., 2014), E100>>erGFP was expressed at varying levels in all the cells of 2-, 2.5-, 3- and 4-DAG leaf primordia (Fig. 4.2B–E).

Consistent with previous observations (Krogan and Berleth, 2012), E861>>erGFP was expressed in all the inner cells of the 2-DAG primordium, though more strongly in its innermost cells (Fig. 4.2F). At 2.5 DAG, expression had been activated in the lowermost epidermal cells of the primordium margin and persisted in all the inner cells of the bottom half of the primordium; in the top half of the primordium, weaker expression persisted in inner cells, except near the midvein, where by then it had been terminated (Fig. 4.2G). At 3 DAG, expression continued to persist in all the inner cells of the bottom half of the primordium, though expression was stronger in the areas where second loops were forming; in the top half of the primordium, weaker expression had become restricted to the midvein, first loops and minor veins (Fig. 4.2H). At 4 DAG, expression in the top half of the leaf remained restricted to the midvein, first loops and minor veins and in the bottom half of the leaf it had declined in inner cells between the first loops and the developing second loops (Fig. 4.2I). In summary, E861>>erGFP was expressed

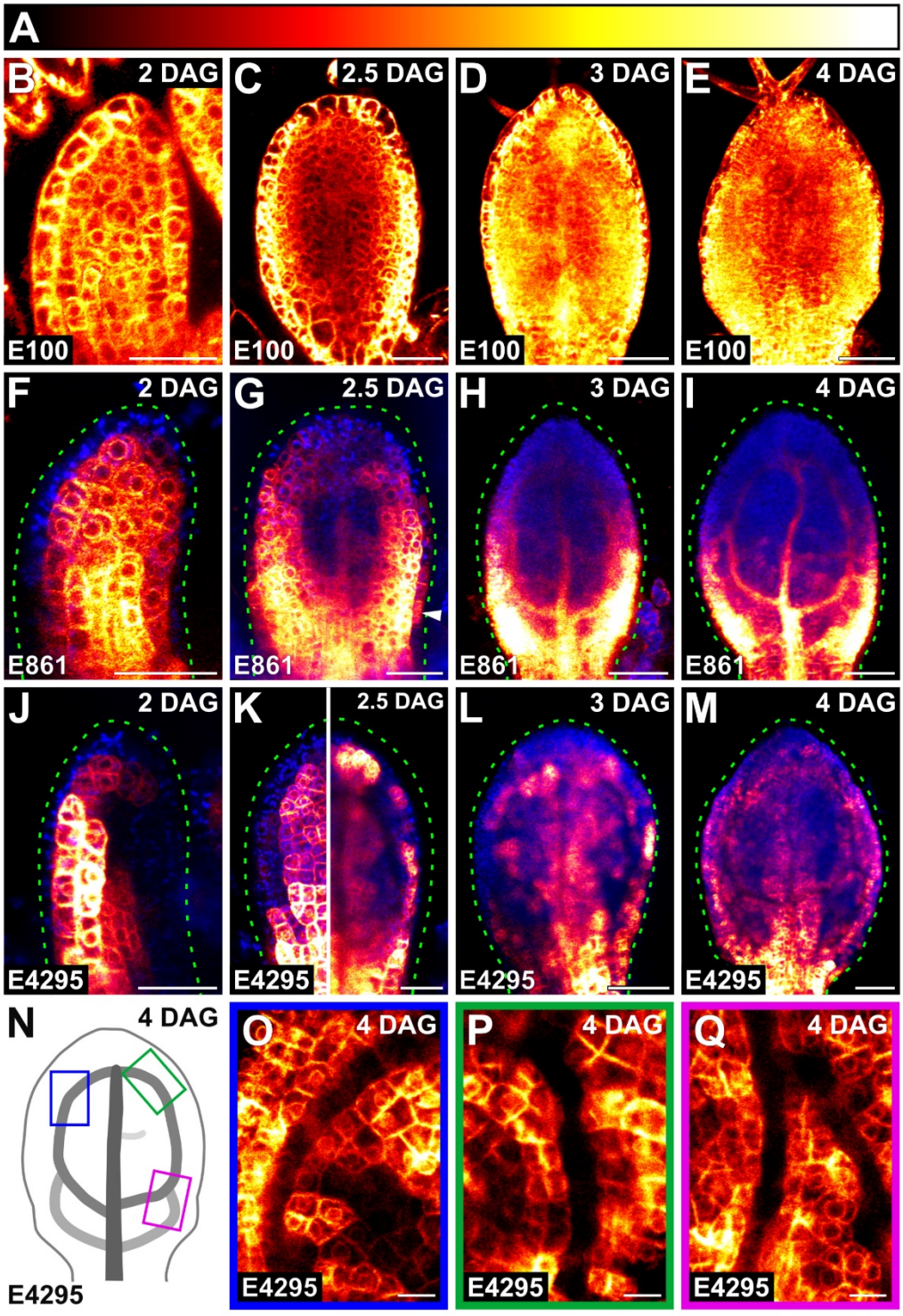

Figure 4.2. Expression of E100>>, E861>> and E4295>>erGFP in leaf development

(A) Look-up table visualizes global background (black) and erGFP expression levels (red to white through yellow). (B–Q) First leaves. Top right: leaf age in days after germination (DAG);

see Materials & methods for definition. (B–M,O–Q) Confocal laser scanning microscopy. Bottom left: genotype. Look-up table (ramp in A) visualizes erGFP expression levels (red to white through yellow). Blue: autofluorescence. Black: global background. Dashed green line delineates leaf outline. White arrowhead points to epidermal expression. (B,F,J) Side view, median plane. Abaxial (ventral) side to the left; adaxial (dorsal) side to the right. (C–E,G–I,L,M,O–Q) Front view, median plane. (K) Front ventral view, subepidermal plane (left); front view, median plane (right). (N) Increasingly darker grays depict progressively later stages of vein development. Boxes illustrate positions of closeups in O, P and Q. See Table 4.2 for reproducibility of expression features. Bars: (B,C,F,G,J,K) 30 µm; (D,E,H,I,L,M) 60 µm; (O–Q) 10 µm.

Table 4.2. Reproducibility of expression and pattern features

Figure	Panel	No. leaves with displayed features / no. analyzed leaves	Assessed expression or pattern features
4.2	B	15/18	Ubiquitous
4.2	C	15/17	Ubiquitous
4.2	D	19/19	Ubiquitous
4.2	E	33/33	Ubiquitous
4.2	F	26/29	Inner cells
4.2	G	29/29	Vascular cells in top half of primordium, inner cells in basal half of primordium
4.2	H	31/31	Vascular cells in top half of primordium, inner cells in basal half of primordium
4.2	I	19/19	Vascular cells in top half of leaf, inner cells in basal half of leaf
4.2	J	16/19	Abaxial inner cells
4.2	K	34/36	Abaxial inner cells & middle tissue layer
4.2	L	24/25	Abaxial inner cells & middle tissue layer
4.2	M	34/34	Abaxial inner cells & middle tissue layer
4.2	O	14/14	Inner, nonvascular cells
4.2	P	14/14	Inner, nonvascular cells
4.2	Q	14/14	Inner, nonvascular cells
4.3	A	26/28 (abaxial) 15/28 (adaxial)	Upper third of adaxial epidermis & whole abaxial epidermis

Figure	Panel	No. leaves with displayed features / no. analyzed leaves	Assessed expression or pattern features
4.3	B (left)	30/30	Whole epidermis
4.3	B (right)	22/23	Top three-quarters of epidermis & trichomes
4.3	C (left)	15/15	Whole epidermis
4.3	C (right)	14/14	Top three-quarters of epidermis & trichomes
4.3	D (left)	18/18	Whole epidermis
4.3	D (right)	16/16	Epidermis of whole lamina and petiole midline & trichomes
4.3	E	16/16	Trichomes
4.3	F	17/18	Top three-quarters of marginal epidermis
4.3	G	14/14	Whole marginal epidermis
4.3	H	16/16	Whole marginal epidermis
4.3	I	59/59	Whole epidermis
4.3	J (left)	45/45	Whole epidermis
4.3	J (right)	42/42	All cells of marginal epidermis, except few cells in top half of primordium
4.3	K (left)	21/21	Whole epidermis, including stomata
4.3	K (right)	33/38	Bottom quarter and few cells in top three-quarters of marginal epidermis
4.3	L (left)	21/21	Whole epidermis, including stomata
4.3	L (right)	31/31	Bottom quarter and few cells in top three-quarters of marginal epidermis
4.3	M	29/30	Absent
4.3	N	26/26	Top quarter of primordium

Figure	Panel	No. leaves with displayed features / no. analyzed leaves	Assessed expression or pattern features
4.3	P	18/18	Whole leaf
4.3	Q	31/33	Absent
4.3	R	19/21	Top quarter of primordium
4.3	S	23/28	Top half of lamina
4.3	T	16/18	Top three-quarters of lamina
4.4	A	22/22	Midvein
4.4	B	30/30	Midvein
4.4	C	16/17	Midvein & first loop
4.4	D	34/48	Midvein & first and second loop
4.4	E	25/25	Absent
4.4	F	20/20	Midvein
4.4	G	27/37	Midvein & first loop
4.4	H	24/28	Midvein & first and second loop
4.6	A	NDa	Narrow midvein & scalloped vein-network outline
4.6	B	19/20	Shapeless vascular cluster
4.6	C	32/46	Midvein & first and second loop
4.6	D	21/21	Shapeless vascular domain
4.6	E	16/23	Midvein & first and second loop
4.6	F	18/18	Broad vascular domain
4.6	G	21/21	Narrow midvein & scalloped vein-network outline

Figure	Panel	No. leaves with displayed features / no. analyzed leaves	Assessed expression or pattern features
4.6	H	19/19	Broad vascular zone

[a]Not Determined

ubiquitously at early stages of inner-cell development; over time, however, expression became restricted to developing veins. As such, expression of E861>>erGFP resembles that of *MONOPTEROS* and *PIN-FORMED1*, which marks the gradual selection of vascular cells from within the leaf inner tissue (Scarpella et al., 2006; Wenzel et al., 2007).

E4295>>erGFP expression was restricted to inner cells in 2-, 2.5-, 3- and 4-DAG leaf primordia (Fig. 4.2J–M,O–Q). At 2 DAG, E4295>>erGFP was expressed almost exclusively in the inner cells of the abaxial side of the primordium (Fig. 4.2J), but by 2.5 DAG E4295>>erGFP was additionally expressed in the middle tissue layer (Fig. 4.2K), from which veins form (Stewart 1978; Tilney-Bassett 1986). Expression persisted in the inner cells of the abaxial side and of the middle tissue layer in 3- and 4-DAG primordia (Fig. 4.2L,M). High-resolution images of the middle tissue layer showed that expression was excluded from developing veins (Fig. 4.2O–Q), suggesting that it marks inner, non-vascular cells. Therefore, expression of E4295>>erGFP resembles that of *LIGHT HARVESTING COMPLEX A6* and *SCARECROW-LIKE32* (Sawchuk et al., 2008; Gardiner et al., 2011) and that of J0571>>erGFP in the C24 background (Wenzel et al., 2012).

As described below, expression of E4259>>erGFP and E4722>>erGFP was restricted to the epidermis at all analyzed stages (Fig. 4.3A–L).

At 2 DAG, E4259>>erGFP was expressed in the upper third of the adaxial epidermis and in the whole abaxial epidermis, though expression was stronger in the top half of the primordium (Fig. 4.3A). By 2.5 DAG, E4259>>erGFP was strongly expressed in the whole abaxial epidermis and the top three-quarters of the marginal epidermis; E4259>>erGFP was also expressed in the top three-quarters of the adaxial epidermis, but expression was stronger in the top half of the primordium (Fig. 4.3B,F). At 3 DAG, E4259>>erGFP was strongly expressed in the top three-

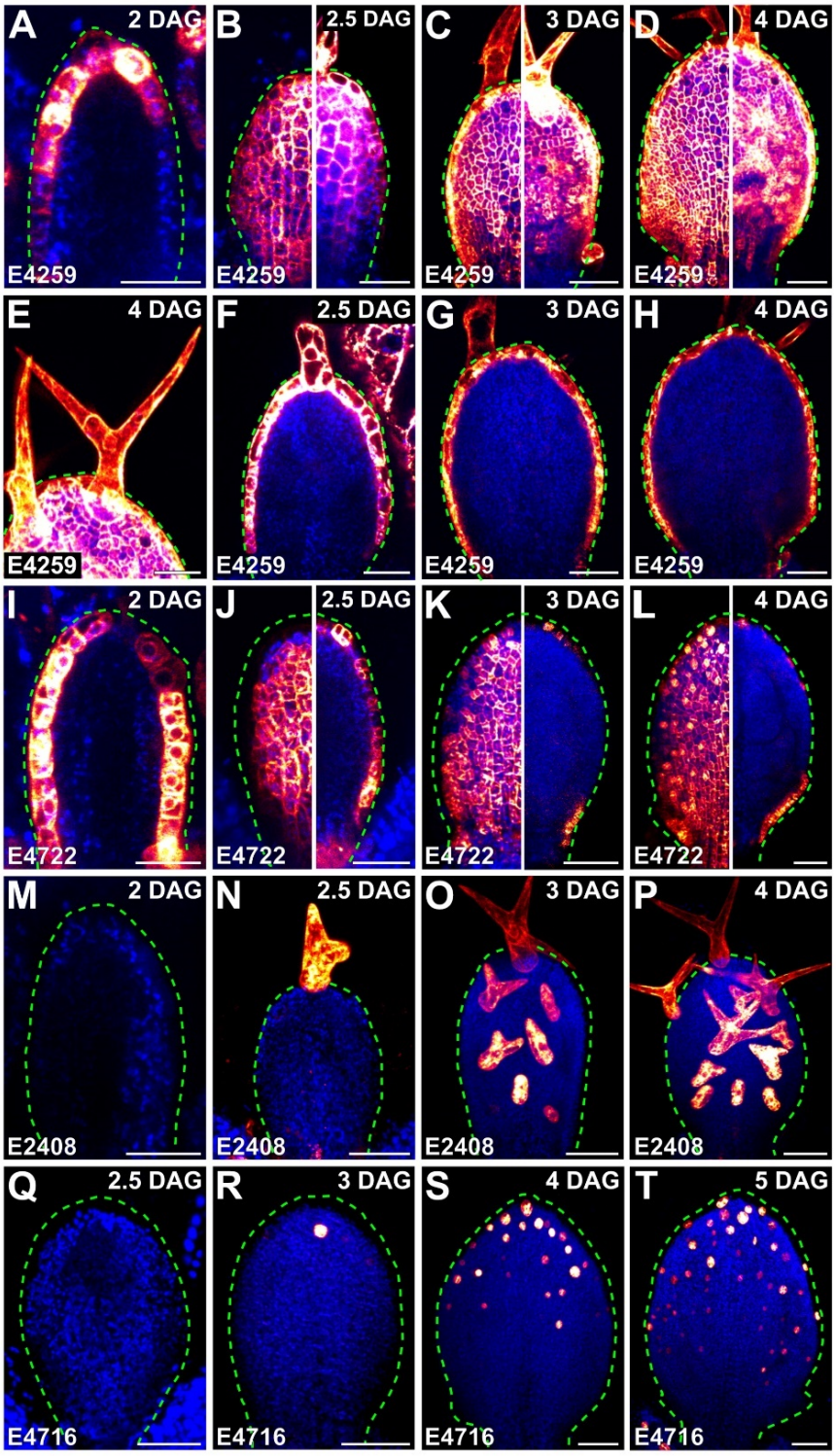

Figure 4.3. Expression of E4259>>, E4722>>, E2408>> and E4716>>erGFP in leaf development

(A–T) Confocal laser scanning microscopy. First leaves. Top right: leaf age in days after

germination (DAG); see Materials & methods for definition. Bottom left: genotype. Look-up table (ramp in Fig. 4.2A) visualizes erGFP expression levels (red to white through yellow). Blue: autofluorescence. Black: global background. Dashed green line delineates leaf outline. (A,I,M) Side view, median plane. Abaxial (ventral) side to the left; adaxial (dorsal) side to the right. (B–D) Front ventral (left) or dorsal (right) view, epidermal plane. (E) Closeup of trichome in D, right. (F–H) Front view, median plane. (J–L) Front ventral view, epidermal plane (left); front view, median plane (right). (N–P) Front dorsal view, epidermal plane. (Q–T) Front ventral view, epidermal plane. See Table 4.2 for reproducibility of expression features. Bars: (A,B,F,I,J,M,N,Q) 30 µm; (C,D,E,G,H,K,L,O,P,R,S,T) 60 µm.

quarters of the adaxial epidermis and in the whole marginal epidermis and strong expression persisted in the whole abaxial epidermis (Fig. 4.3C,G). At 4 DAG, strong expression persisted in the whole marginal epidermis, continued to persist in the whole abaxial epidermis and E4259>>erGFP was now strongly expressed also in the adaxial epidermis of the whole lamina and the petiole midline (Fig. 4.3D,H). At all analyzed stages, E4259>>erGFP was expressed in trichomes but was not expressed in mature stomata (Fig. 4.3B–H). In conclusion, expression of E4259>>erGFP resembles that of *ARABIDOPSIS THALIANA MERISTEM LAYER1* (Lu et al., 1996; Sessions et al., 1999), which marks epidermal cells and whose promoter is used to drive epidermis-specific expression (e.g., (Takada and Jürgens, 2007; Bilsborough et al., 2011; Kierzkowski et al., 2013; Govindaraju et al., 2020)).

E4722>>erGFP was expressed in all the epidermal cells of the 2-DAG primordium, though more weakly at its tip (Fig. 4.3I). E4722>>erGFP was expressed in all the epidermal cells of the 2.5-DAG primordium too, except at its margin, where expression had been terminated in a few cells of its top half (Fig. 4.3J). At 3 DAG, expression persisted in all the epidermal cells, except at the primordium margin, where expression had been terminated in most of the cells of its top three-quarters (Fig. 4.3K). At 4 DAG, expression continued to persist in all the epidermal cells, except at the leaf margin, where expression had been terminated in nearly all the cells of its top three-quarters (Fig. 4.3L). Unlike E4259>>erGFP, E4722>>erGFP was expressed in stomata but was not expressed in trichomes (Fig. 4.3J–L).

At all analyzed stages, expression of E2408>>erGFP and E4716>>erGFP was restricted to trichomes and stomata, respectively (Fig. 4.3M–T). E2408>>erGFP was first expressed in developing trichomes at the tip of the 2.5-DAG primordium (Fig. 4.3M,N). By 3 DAG, E2408>>erGFP was expressed in the developing and mature trichomes of the top three-quarters

of the primordium (Fig. 4.3O) and by 4 DAG in those of the whole lamina (Fig. 4.3P). E4716>>erGFP was first expressed in stomata at the tip of the 3-DAG primordium (Fig. 4.3Q,R). By 4 DAG, E4716>>erGFP was expressed in the stomata of the top half of the lamina (Fig. 4.3S) and by 5 DAG in those of its top three-quarters (Fig. 4.3T).

At all analyzed stages, expression of E2331>>erGFP and E3912>>erGFP was restricted to developing veins (Figure 4.4). E2331>>erGFP was expressed in both isodiametric and elongated cells of the midvein in 2- and 2.5-DAG primordia (Fig. 4.4A,B). By 3 DAG, E2331>>erGFP was expressed in first loops and by 4 DAG in second loops and minor veins (Fig. 4.4C,D). E3912>>erGFP was first expressed in the midvein of the 3-DAG primordium (Fig. 4.4E,F). By 4 DAG, E3912>>erGFP was expressed in first loops and by 5 DAG in second loops and minor veins (Fig. 4.4G,H). These observations suggest that expression of E3912>>erGFP is initiated later than that of E2331>>erGFP in vein development. Furthermore, because the expression of E2331>>erGFP resembles that of the preprocambial markers ATHB8::nYFP, J1721>>erGFP and SHR::nYFP (Sawchuk et al., 2007; Donner et al., 2009; Gardiner et al., 2011), we suggest that E2331>>erGFP expression marks preprocambial stages of vein development, a conclusion that is consistent with E2331>>erGFP expression during embryogenesis (Gillmor et al., 2010). Finally, because E3912>>erGFP expression resembles that of the procambial marker Q0990>>erGFP in the C24 background (Sawchuk et al., 2007), we suggest that E3912>>erGFP expression marks procambial stages of vein development.

In the lines characterized above, GFP was expressed in specific cells and tissues during early leaf development; however, as it is most frequently the case for other enhancer-trap lines (e.g., (Ckurshumova et al., 2009; Gardner et al., 2009; Gardiner et al., 2011; Wenzel et al., 2012;

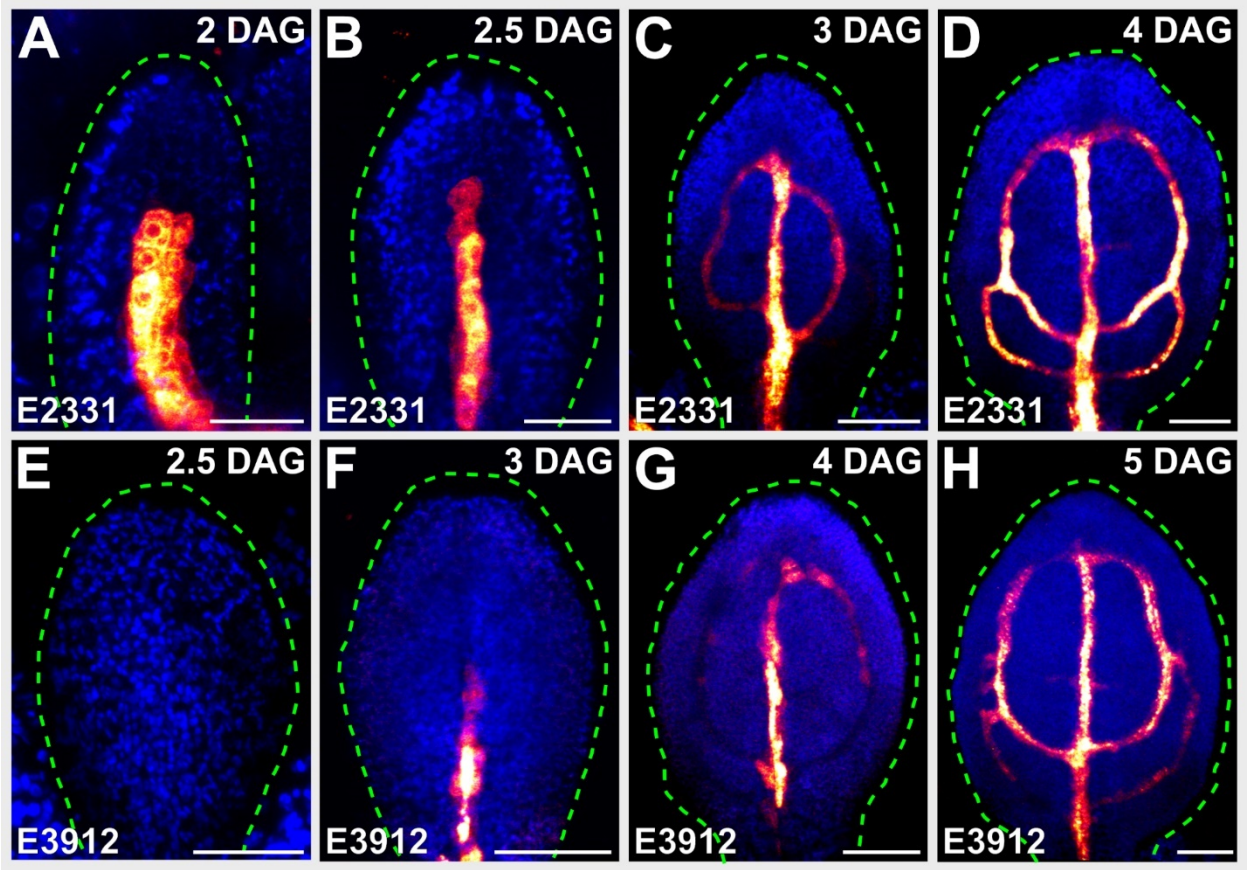

Figure 4.4. Expression of E2331>> and E3912>>erGFP in leaf development

(A–H) Confocal laser scanning microscopy. First leaves. Top right: leaf age in days after germination (DAG); see Materials & methods for definition. Bottom left: genotype. Look-up table (ramp in Fig. 3.2A) visualizes erGFP expression levels (red to white through yellow). Blue: autofluorescence. Black: global background. Dashed green line delineates leaf outline. (A) Side view, median plane. Abaxial (ventral) side to the left; adaxial (dorsal) side to the right. (B–H) Front view, median plane. See Table 4.2 for reproducibility of expression features. Bars: (A,B,E) 30 µm; (C,D,F–H) 60 µm.

Radoeva et al., 2016)), in the lines reported here GFP was additionally expressed in other organs (Figure 4.5). To show the informative power for plant developmental biology of the lines characterized above, we selected the E2331 line, which marks early stages of vein development (Fig. 4.4A–D).

In WT leaves, the elongated vascular cells are connected to one another into continuous veins (Esau 1965) (Fig. 4.6A). By contrast, in mature leaves of the *gnom* (*gn*) mutant, putative vascular cells fail to elongate and to connect to one another into continuous veins; instead, they accumulate into shapeless clusters of seemingly disconnected and randomly oriented cells (Shevell et al., 2000; Verna et al., 2019) (Fig.43.6B). Though the cells in these clusters have some features of vascular cells (e.g., distinctive patterns of secondary cell-wall thickenings), they lack others (e.g., elongated shape and end-to-end connection to form continuous veins). Therefore, it is unclear whether the clustered cells in *gn* mature leaves are abnormal vascular cells or nonvascular cells that have recruited a cellular differentiation pathway that is normally, but not always (e.g., (Solereder 1908; Kubo et al., 2005; Yamaguchi et al., 2010)), associated with vascular development. To address this question, we imaged E2331>>erGFP expression in developing leaves of WT and *gn*.

As shown above (Fig. 4.4D), E2331>>erGFP was expressed in midvein, first and second loops and minor veins in WT (Fig. 4.6C). In *gn*, the pattern of E2331>>erGFP expression in developing leaves recapitulated that of vascular differentiation in mature leaves (Fig. 4.6B,D), suggesting that the putative vascular cells in the shapeless clusters are indeed vascular cells, albeit abnormal ones.

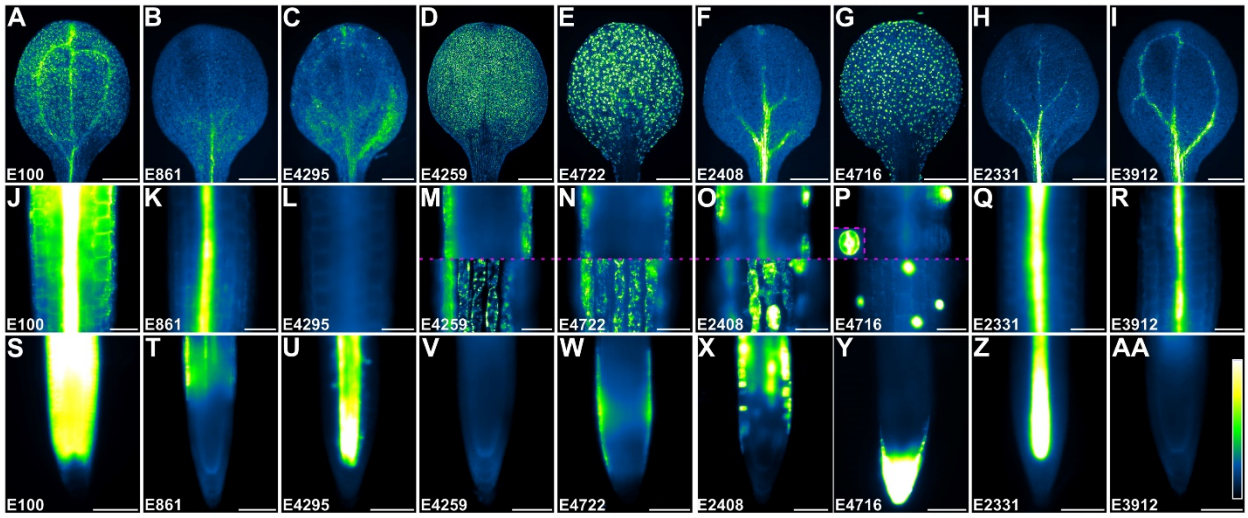

Figure 4.5. Expression of E100>>, E861>>, E4295>>, E4259>>, E4722>>, E2408>>, E4716>>, E2331>> and E3912>>erGFP in seedling organs

(A–AA) Epifluorescence microscopy. Seedlings 5 days after germination (see Materials & methods for definition). Bottom left: genotype. Look-up table (ramp in AA) visualizes global background (black) and levels of autofluorescence (blue to cyan) and erGFP expression (green to white through yellow). (A–I) Cotyledon. (J–R) Hypocotyl. (P) Inset: stoma. (S-AA) Root. (A–I) Front view, median plane. (J–L,Q–AA) Median plane. (M–P) Median (top) or tangential (bottom) plane. Bars: (A–I) 500 µm.; (J–AA) 100 µm.

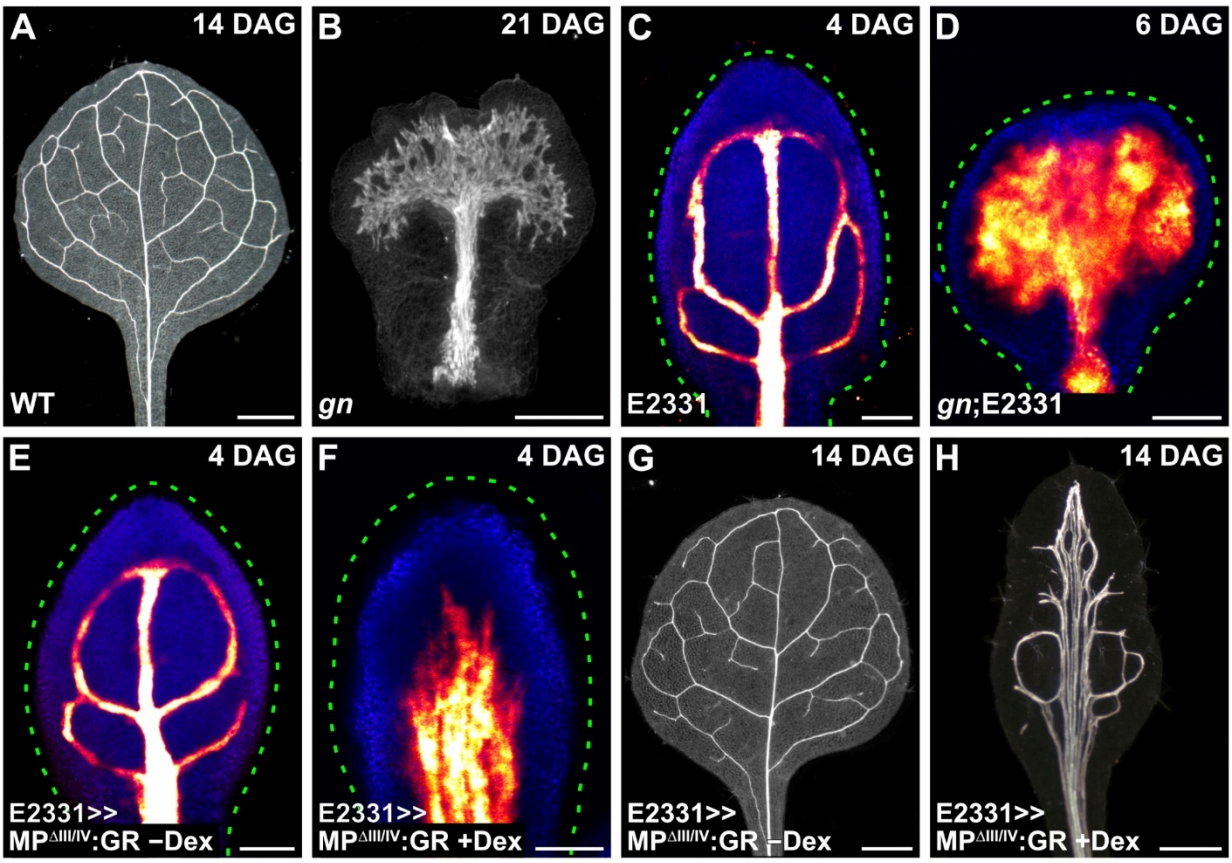

Figure 4.6. E2331-mediated visualization and manipulation of developing veins

(A–H) First leaves. Top right: leaf age in days after germination (DAG); see Materials & methods for definition. Bottom left: genotype and treatment. (A,B,G,H) Dark-field microscopy of cleared leaves. (C–F) Confocal laser scanning microscopy. Look-up table (ramp in Fig. 4.2A) visualizes erGFP expression levels (red to white through yellow). Blue: autofluorescence. Black: global background. Dashed green line delineates leaf outline. Front view, median plane. See Table 4.2 for reproducibility of expression and pattern features. Bars: (A,B,G,H) 500 µm; (C–F) 60 µm.

Auxin signals are transduced by multiple pathways (reviewed in (Leyser 2018) and (Gallei et al., 2020)); best characterized is the auxin signalling pathway that releases from repression activating transcription factors of the ARF family, thereby allowing them to induce transcription of auxin-responsive genes (reviewed in (Powers and Strader, 2019)). Auxin signalling is thought to be required for vein formation because mutations in genes involved in auxin signalling or treatment with inhibitors of auxin signalling leads to the formation of fewer, incompletely differentiated veins (Przemeck et al., 1996; Hardtke and Berleth, 1998; Mattsson et al., 2003; Verna et al., 2019). Increasing auxin signalling by means of broadly expressed mutations or transgenes leads to the formation of supernumerary veins, suggesting that auxin signalling is also sufficient for vein formation (Krogan et al., 2012; Garett et al., 2012). This interpretation assumes that it is the increased auxin signalling in the cells that normally would not differentiate into vein elements that leads those cells to differentiate in fact into such elements. However, it is also possible that it is the increased auxin signalling in the cells that normally differentiate into vein elements that leads the flanking cells, which normally would not differentiate into such elements, to do in fact so. To discriminate between these possibilities, we increased auxin signalling in developing veins by expressing by the E2331 driver a dexamethasone (dex)-inducible, constitutively active variant of the MP protein — the only activating ARF with non-redundant functions in vein formation (Stamatiou, 2007). As previously reported (Schena et al., 1991; Krogan et al., 2012; Smetana et al., 2019), we constitutively activated MP by deleting domains III and IV, which are required for ARF repression (Tiwari et al., 2003; Wang et al., 2005; Krogan et al., 2012) and fused the resulting MPΔIII/IV to a fragment of the rat glucocorticoid receptor (GR) (Picard 1998) to confer dex-inducibility. We

imaged E2331>>erGFP expression in developing leaves and vein patterns in mature leaves of E2331>>MPΔIII/IV:GR grown with or without dex.

Consistent with previous observations (Fig. 4.4D; Fig. 4.6C), in developing leaves of E2331>>MPΔIII/IV:GR grown without dex, E2331>>erGFP was expressed in narrow domains (Fig. 4.6E). By contrast, E2331>>erGFP was expressed in broad domains in developing leaves of dex-grown E2331>>MPΔIII/IV:GR (Fig. 4.6F). Whether with or without dex, the patterns of E2331>>erGFP expression in developing leaves of E2331>>MPΔIII/IV:GR presaged those of vein formation in mature leaves: narrow zones of vein formation in the absence of dex; broad areas of vascular differentiation in the presence of dex, often with multiple veins running parallel next to one another (Fig. 4.6G,H). Though the areas of vascular differentiation in dex-grown E2331>>MPΔIII/IV:GR are not as broad as those of leaves in which MPΔIII/IV is expressed in all the inner cells (Krogan et al., 2012), they are broader than those of E2331>>MPΔIII/IV:GR grown without dex. These observations suggest that, at least in part, it is the increased auxin signalling in the cells that normally differentiate into vein elements that leads the flanking cells, which normally would not differentiate into such elements, to do in fact so. Our conclusion is consistent with interpretations of similar findings in other plant organs (e.g., (Simon et al., 1996; Pautot et al., 2001; Hay et al., 2003; Fukaki et al., 2005; Nakata et al., 2018)) and, more in general, with organ-specific interpretations of genetic mosaics that span multiple organs in other organisms (e.g., (Morgan et al., 1919; Sturtevant 1920; Sturtevant 1932)). Nevertheless, we cannot rule out an effect on leaf vein patterning of increased auxin signalling in the vascular tissue of non-leaf organs, where E2331>>erGFP is also expressed (Fig. 4.5H,Q,Z); in the future, that possibility will have to be addressed by complementary approaches such as clonal analysis (e.g., (Posakony et al., 1991; Burke and Basler., 1996)).

In conclusion, we provide a set of GAL4/GFP enhancer-trap lines in the Col-0 background of Arabidopsis for the specific labeling of cells and tissues during early leaf development (Figure 4.7) and we show that these lines can be used to address key questions in plant developmental biology.

4.3. Materials & methods

4.3.1. Plants

Origin and nature of GAL4 enhancer-trap lines are in Table 4.1. *gn-13* (SALK_045424; ABRC) (Alonso et al., 2003; Verna et al., 2019) contains a T-DNA insertion after nucleotide +2835 of *GN* and was genotyped with the "SALK_045424 gn LP" (5'-TGATCCAAATCACTGGGTTTC-3') and "SALK_045424 gn RP" (5'-AGCTGAAGATAGGGAATTCGC-3') oligonucleotides (*GN*) and with the "SALK_045424 gn RP" and "LBb1.3" (5'-ATTTTGCCGATTTCGGAAC-3') oligonucleotides (*gn*). To generate the UAS::MPΔIII/IV:GR construct, the UAS promoter was amplified with the "UAS Promoter SalI Forward" (5'-ATAGTCGACCCAAGCGCGCAATTAACCCTCAC-3') and the "UAS Promoter XhoI Reverse" (5'-AGCCTCGAGCCTCTCCAAATGAAATGAACTTCC-3') oligonucleotides; MPΔIII/IV was amplified with the "MP Delta XhoI Forward" (5'-AAACTCGAGATGATGGCTTCATTGTCTTGTGTT-3') and the "MP EcoRI Reverse" (5'-ATTGAATTCGGTTCGGACGCGGGGTGTCGCAATT-3') oligonucleotides; and a fragment of the rat glucocorticoid (GR) receptor gene was amplified with the "SpeI GR Forward" (5'-GGGACTAGTGGAGAAGCTCGAAAAACAAAG-3') and the "GR ApaI Reverse" (5'-GCGGGGCCCTCATTTTTGATGAAACAG-3') oligonucleotides. Seeds were sterilized and sown as in (Sawchuk et al., 2008). Germination was synchronized as in (Scarpella et al., 2004).

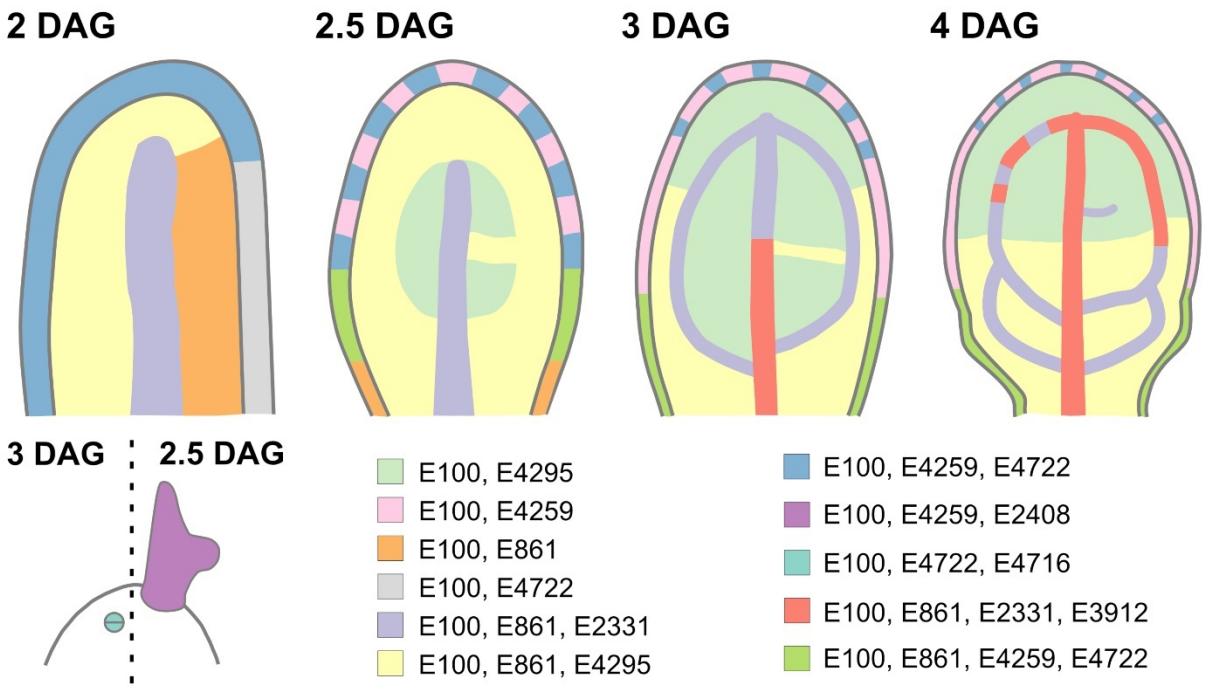

Figure 4.7. Expression Map of E100>>, E861>>, E4295>>, E4259>>, E4722>>, E2408>>, E4716>>, E2331>> and E3912>>erGFP in leaf development

First leaves. Top: leaf age in days after germination (DAG); see Materials & methods for definition. 2-DAG leaf primordium: side view, median plane; abaxial (ventral) side to the left, adaxial (dorsal) side to the right. Leaves 2.5–4 DAG: front view, median plane. 2.5-/3-DAG leaf composite: front ventral (left) or dorsal (right) view, epidermal plane. Map illustrates inferred overlap and exclusivity of expression. See text for details.

We refer to “days after germination” (DAG) as days after exposure of stratified seeds to light. Stratified seeds were germinated and seedlings were grown at 22°C under continuous fluorescent light (~80 µmol m^{-2} s^{-1}). Plants were grown at 24°C under fluorescent light (~85 µmol m^{-2} s^{-1}) in a 16-h-light/8-h-dark cycle. Plants were transformed and representative lines were selected as in (Sawchuk et al., 2008).

4.3.2. Chemicals

Dexamethasone (Sigma-Aldrich, catalogue no. D4902) was dissolved in dimethyl sulfoxide and was added to growth medium just before sowing.

4.3.3. Imaging

Seedlings were imaged with a 1.0x Planapochromat (NA, 0.041; WD, 55 mm) objective of a Leica MZ 16FA stereomicroscope equipped with an HBO103 mercury vapor short-arc lamp and an Andor iXonEM+ camera. GFP was detected with a 480/40-nm excitation filter and a 510-nm emission filter, or with a 470/40-nm excitation filter and a 525/50-nm emission filter. Seedling organs were imaged with a 5x Fluar (NA, 0.25; WD, 12.5 mm) or a 20x Planapochromat (NA, 0.8; WD, 0.55 mm) objective of an Axio Imager.M1 microscope (Carl Zeiss) equipped with an HBO103 mercury vapor short-arc lamp and a Hamamatsu ORCA-AG camera. GFP was detected with a BP 470/40 excitation filter, an FT495 beam splitter and a BP 525/50 emission filter. Developing leaves were mounted and imaged as in (Sawchuk et al., 2013), except that emission was collected from ~1.5–5-µm-thick optical slices. Fluorophores were excited with the 488-nm line of a 30-mW Ar laser; GFP emission was collected with a BP 505–530 filter and autofluorescence was collected between 550 and 754 nm. Mature leaves were fixed in 3 : 1 or 6 :

1 ethanol : acetic acid, rehydrated in 70% ethanol and in water, cleared briefly (few seconds to few minutes) — when necessary — in 0.4 M sodium hydroxide, washed in water, mounted in 80% glycerol or in 1 : 2 : 8 or 1 : 3 : 8 water : glycerol : chloral hydrate and imaged as in (Odat et al., 2014). In the Fiji distribution (Schindelin et al., 2012) of ImageJ (Schneider et al., 2012; Schindelin et al., 2015; Rueden et al., 2017), grayscaled RGB color images were turned into 8-bit images; when necessary, 8-bit images were combined into stacks and maximum-intensity projection was applied to stacks; look-up-tables (Sawchuk et al., 2007) were applied to images or stacks and brightness and contrast were adjusted by linear stretching of the histogram.

Chapter 5: General discussion

5.1. Conclusion summary

The evidence discussed in Chapter 1 suggests that the plant hormone auxin induces the polar formation of veins and that such inductive and orienting property of auxin depends on the function of *PIN-FORMED* (*PIN*) genes (reviewed in Berleth et al., 2000; Linh et al., 2018). How auxin precisely controls *PIN* gene function and derived polar formation of veins is unclear, but the prevailing hypothesis has long been that the GNOM (GN) guanine-nucleotide exchange factor for ADP-ribosylation-factor GTPases, which regulates vesicle formation in membrane trafficking, coordinates the cellular localization of PIN proteins between cells; the resulting cell-to-cell, polar transport of auxin would coordinate the polar localization of PIN proteins between auxin-transporting cells and control polar developmental processes such as vein formation (reviewed in Berleth et al., 2000; Richter et al., 2010; Nakamura et al., 2012; Linh et al., 2018). Contrary to predictions of the hypothesis, however, auxin-induced polar vein-formation occurs in the absence of PIN proteins or any known intercellular auxin transporter (Verna et al., 2019), suggesting the presence of auxin-transport-independent vein-patterning pathways. The goal of my M.Sc. research was to identify such pathways in Arabidopsis leaves.

The auxin-transport-independent vein-patterning activity relies, at least in part, on auxin signalling and *GN* turns out to be controlling both auxin transport and signalling to induce vein formation (Verna et al., 2019). Whereas mechanisms by which GN may control PIN polarity and derived polar auxin transport have been suggested (reviewed in (Richter et al., 2010; Luschnig and Vert, 2014); see also (Naramoto et al., 2014) and references therein), it is unclear how *GN* could control auxin signalling, which takes place in the nucleus and is inherently non-polar

(reviewed in Leyser, 2018). The most parsimonious account is that auxin signalling leads to the production of proteins which control vein patterning and whose localization is controlled by GN. In Chapter 2, we tested this hypothesis and identified a family of putative candidates for such proteins that includes the receptor-like kinase PHLOEM INTERCALATED WITH XYLEM (PXY) (Fischer & Turner, 2007) (Figure 5.1).

The current hypothesis of vein formation proposes that GN controls both auxin transport and auxin signalling to induce vein formation (Verna et al., 2019). However, plants in which both auxin transport and signalling are compromised phenocopy only weak alleles of *gn* (Verna et al., 2019), suggesting the presence of additional, yet-to-be-identified *GN*-dependent pathways that act redundantly to auxin signalling and transport to induce vein formation. To identify such pathways, in Chapter 4 we identified and characterized six genetic suppressors of the fragmented vein-pattern phenotype of the *fewer roots* allele of *gn* (Figure 5.2).

The identification of putative candidate proteins which are targets of auxin signalling, which control vein patterning and whose localization is controlled by GN required gene misexpression by different promoters. This imposed the burden of generating different constructs for different gene and promoter combinations. This approach could have been simplified if GAL4/GFP enhancer-trap lines existed in Columbia-0, the genotype of reference in Arabidopsis (Koornneef and Meinke, 2010), with which to drive expression of genes of interest in desired cells and tissues of developing leaves. Unfortunately, such lines were not available when I started my M.Sc.. In Chapter 4, we addressed this limitation and provided GAL4/GFP enhancer-trap lines in the Col-0 background of Arabidopsis for the identification and manipulation of cells and tissues in developing leaves (Amalraj et al., 2020).

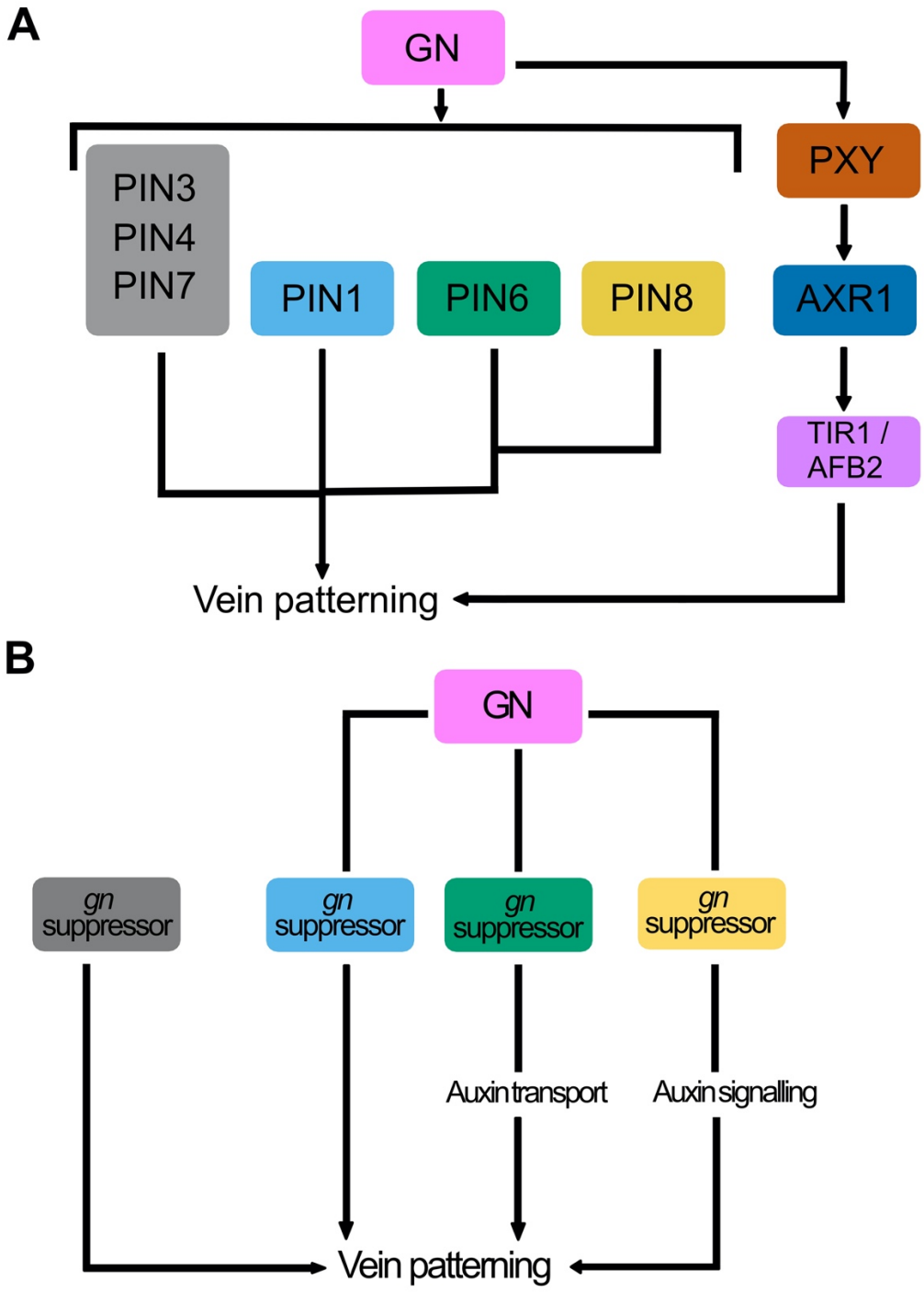

Figure 5.1. Interpretation summary

Genetic interaction networks controlling GNOM-mediated auxin-transport- and auxin-signalling-dependent vein patterning. Arrows indicate positive effects. (A) Derived from results in Chapter 2. (B) Derived from results in Chapter 3.

In the discussion section of the respective chapters, we provided an account of how we drew conclusions from results and how those conclusions could be integrated with one another and with those in studies of others to advance our understanding of vein formation. Here we instead wish to propose and discuss a hypothesis to account for how the auxin signalling target *PXY* — identified in Chapter 2 — could control vein formation redundantly with auxin transport. This hypothesis should be understood as an attempt to develop a conceptual framework to guide future experimentation and not as an exhaustive mechanistic account.

5.2. Premises

Abundant evidence — discussed in Chapter 1 — suggests that vein formation depends on the polar transport of auxin through plant tissues (reviewed in Berleth et al., 2000; Sachs, 1981; Linh 2018). In turn, polar auxin transport depends on the polar localization of auxin transporters of the PIN-FORMED (PIN) family to the basal plasma membrane of auxin-transporting cells. Therefore, if vein formation only depended on polar auxin transport and if polar auxin transport only depended on the polar localization of PIN proteins, the most severe *pin* mutants should form no veins. However, mutants in all the *PIN* genes with vein patterning function (*pin1*;*3*;*4*;*6*;*7*;*8*) form veins in a reproducible, albeit abnormal pattern, suggesting the presence of residual vein patterning activity in these mutants (Verna et al., 2019).

That auxin application to *pin1*;*3*;*4*;*6*;*7*;*8* leaves gives rise to narrow veins, as opposed to broad areas of vascular differentiation and that such veins are oriented from the auxin application site toward the base of the leaf (Verna et al., 2019) suggests that auxin-induced vein formation in *pin1*;*3*;*4*;*6*;*7*;*8* leaves is a polar response and this polar response is based on a positive feedback that laterally restricts vascular differentiation. The most parsimonious account for these observations is that auxin moves polarly in *pin1*;*3*;*4*;*6*;*7*;*8* leaves and that the movement of auxin

out of the mutant cells has a positive feedback on the cells' ability to move auxin. But how could auxin move polarly in the absence of PIN auxin transporters?

Because auxin cannot diffuse freely out of the cells (Raven, 1975; Rubery & Sheldrake, 1974), polar auxin movement in *pin1*;*3*;*4*;*6*;*7*;*8* leaves may be mediated by specialized auxin transporters with vein patterning function other than PIN proteins. Such specialized auxin transporters cannot be members of the ABCB or AUX1/LAX families of auxin transporters because *abcb* and *aux1*/*lax* mutants have no vein pattern defects and their mutation fails to enhance vein pattern defects of *pin* mutants (Verna et al., 2019). Therefore, if such specialized auxin transporters exist, they must be novel. But they also must be insensitive to the effects of auxin transport inhibitors like N-1-naphthylphthalamic acid (NPA) because WT leaves developed in the presence of NPA phenocopy *pin1*;*3*;*4*;*6*;*7*;*8* leaves and NPA fails to induce additional defects in *pin1*;*3*;*4*;*6*;*7*;*8* leaves (Verna et al., 2019). Finally, such specialized auxin transporters must be inefficient because very little — if any — auxin is transported in the presence of auxin transport inhibitors like NPA (e.g., Keitt & Baker 1966). Therefore, while possible, the existence of such specialized auxin transporters is unlikely. What is the origin then of the residual vein patterning activity in *pin1*;*3*;*4*;*6*;*7*;*8* leaves?

It turns out vein patterning in *pin1*;*3*;*4*;*6*;*7*;*8* leaves depends on auxin signalling (Verna et al., 2019). Whereas auxin signalling mutants have a normal vein pattern, albeit with fewer veins (Przemeck et al., 1996; Hardtke & Berleth, 1998; Candela et al., 1999; Alonso-Peral et al., 2006; Strader et al., 2008; Esteve-Bruna et al., 2013; Verna et al., 2019), plants in which both auxin transport and auxin signalling are inhibited have vein pattern defects that are more severe than those of plants in which only auxin transport is inhibited (Verna et al., 2019). In the most severe cases, vascular cells are no longer aligned along the length of the vein, but are arranged in

seemingly random orientations. How auxin signalling, which takes place in the nucleus and is inherently non-polar (reviewed in (Leyser, 2018)), could contribute to the polar propagation of the auxin signal is unclear. However, our results suggest that such function of auxin signalling is mediated, at least in part, by the auxin signalling target PXY and related proteins (Chapter 2). Indeed, vein pattern defects of leaves in which both auxin transport and PXY-mediated signalling are inhibited phenocopy leaves in which both auxin transport and auxin signalling are inhibited. But how could PXY-mediated signalling contribute to polar auxin movement and positive feedback of auxin movement on itself?

One possibility to account for auxin movement in the absence of PIN auxin transporters is that auxin moves through the plasmodesmata (PD) intercellular channels. We know such movement is possible (Han et al., 2014); the size of PD aperture is developmentally regulated (Kim et al., 2002); the size of PD aperture depends on auxin signalling (Han et al., 2014, Sager et al., 2020); the size of PD aperture is regulated by callose production and degradation (Vaten et al., 2011); and callose-mediated PD aperture controls vein patterning (N.M. Linh and E. Scarpella, unpublished).

5.3. Hypothesis

Based on the premises above, I hypothesize that PXY is localized to PD and is a component of a signalling pathway that controls callose-mediated regulation of PD aperture size in response to auxin movement through PD.

5.4. Experimental tests

1. The hypothesis predicts that PXY is localized to PD. To test this prediction, we propose to create a translational fusion of *PXY* to the sequence encoding YFP and express the resulting

PXY:YFP fusion by the *PXY* promoter in the *pxy* mutant background. Should the PXY:YFP fusion be functional and be expressed in PXY's native domain, we would expect the vein pattern defects of *pxy* (Chapter 2) to be rescued by PXY::PXY:YFP. We would then cross PXY::PXY:YFP;*pxy* plants with plants expressing GFP-tagged PD markers (e.g., MOVEMENT PROTEIN17, PLASMODESMATA-LOCALIZED PROTEIN and PLASMODESMATA CALLOSE-BINDING PROTEIN1 (Fitzgibbon et al., 2013, Simpson et al., 2008)). Because it is unknown whether any of the available PD markers label all the PD in all the cells at all the stages of their development, we would cross PXY::PXY:YFP;*pxy* plants to multiple PD markers. We would then image YFP and GFP in the resulting F1 plants and measure the extent of fluorescent signal colocalization. Should PXY be localized to PD, as the hypothesis proposes, we would expect YFP and GFP signals to be, at least in part, colocalized.

2. The hypothesis predicts that defects induced by inhibition of PXY-mediated signalling should enhance defects induced by inhibition of PIN-mediated auxin transport. That NPA induces more severe defects in MP::PXYΔK;*pxy* than in WT and that the defects of NPA-grown MP::PXYΔK;*pxy* match those of NPA- and PBA-grown WT and of NPA-grown *tir1*;*afb2* (Chapter 2) is consistent with that prediction. To more stringently test the prediction, we propose to create the MP::PXYΔK;*pxy*;*pin1*;*3*;*4*;*6*;*7*;*8* background and analyze the vein pattern of its mature leaves. We expect the vein pattern defects of MP::PXYΔK;*pxy*;*pin1*;*3*;*4*;*6*;*7*;*8* to match those of NPA- and PBA-grown WT and NPA-grown *tir1*;*afb2*.

3. The hypothesis predicts that defects induced by mutation in *CLE41, CLE42* and *CLE44*, which encode ligands of *PXY* (Hirakawa et al., 2008; Etchells and Turner, 2010), should enhance defects induced by inhibition of PIN-mediated auxin transport. To test this prediction, we propose to grow the *cle41*;*42*;*44* mutant in the presence of NPA, create the

cle41;*42*;*44*;*pin1*;*3*;*4*;*6*;*7*;*8* background and analyze the vein pattern of their mature leaves. We expect the vein pattern defects of NPA-grown *cle41*;*42*;*44* and *cle41*;*42*;*44*;*pin1*;*3*;*4*;*6*;*7*;*8* to match those of NPA-grown MP::PXYΔK;*pxy,* MP::PXYΔK;*pxy*;*pin1*;*3*;*4*;*6*;*7*;*8,* NPA- and PBA-grown WT and NPA-grown *tir1*;*afb2*.

4. The hypothesis predicts that auxin application to leaves in which both PXY-mediated signalling and PIN-mediated auxin transport are inhibited should lead to the formation of broad veins, the formation of broad areas of vascular differentiation, or the failure to form vascular tissue altogether. To test this prediction, we propose to apply auxin to the developing leaves of NPA-grown MP::PXYΔK;*pxy*, MP::PXYΔK;*pxy*;*pin1*;*3*;*4*;*6*;*7*;*8*, NPA-grown *cle41*;*42*;*44* and *cle41*;*42*;*44*;*pin1*;*3*;*4*;*6*;*7*;*8* and analyze the vein pattern of their mature leaves. We expect auxin application to those leaves to lead to the formation of broad veins, the formation of broad areas of vascular differentiation, or the failure to form vascular tissue altogether.

5. The hypothesis predicts that defects induced by inhibition of PXY-mediated signalling should enhance defects induced by inhibition of callose production or degradation. To test this hypothesis, we propose to combine the *gsl8* or *cals3-d* mutations — which, respectively, produce limited or excess amounts of callose (Vaten et al., 2011; Chen at al., 2009) — with MP::PXYΔK;*pxy* and *cle41*;*42*;*44* and analyze the vein pattern of their mature leaves. We expect the vein pattern defects of MP::PXYΔK;*pxy*;*gsl8*, *cle41*;*42*;*44*;*gsl8*, MP::PXYΔK;*pxy*;*cals3-d*, *cle41*;*42*;*44*;*cals3-d* to be more severe than the addition of those of MP::PXYΔK;*pxy* or *cle41*;*42*;*44*, on the one hand and *gsl8* and *cals3-d*, on the other.

6. Finally, the hypothesis predicts that the defects induced by inhibition of PXY-mediated signalling should cause defects in callose production or degradation. To test this hypothesis, we propose to visualize callose in MP::PXYΔK;*pxy* and *cle41*;*42*;*44* by histochemical stainings

(Schenk et al., 2015, Herburger et al., 2016). We expect the amount of callose in MP::PXYΔK;*pxy* and *cle41*;*42*;*44* to be different from that in WT.

5.5. Directions

The hypothesis proposed above should not be understood as an exhaustive mechanistic account but as an attempt to develop a conceptual framework to guide future experimentation. Nevertheless, and even though the hypothesis makes testable predictions, because of the complexity of vein patterning, it may be difficult to evaluate intuitively the results of experimental tests of those predictions; a more precise formulation of the hypothesis — a mathematical one, one that can be simulated computationally — may be necessary. In the most optimistic scenario, iterative cycles of computational simulations and experimentation will take us closer to understanding how plant vascular systems form and how the mechanisms by which vascular systems form in plants compare to those by which vascular systems form in animals — a key question to address if we are to understand how multicellular organisms develop and function.

Literature cited

Agusti, J., Lichtenberger, R., Schwarz, M., Nehlin, L. and Greb, T. (2011). Characterization of transcriptome remodeling during cambium formation identifies MOL1 and RUL1 as opposing regulators of secondary growth. *PLoS Genet* 7, e1001312.

Alonso-Peral, M. M., Candela, H., del Pozo, J. C., Martinez-Laborda, A., Ponce, M. R. and Micol, J. L. (2006). The HVE/CAND1 gene is required for the early patterning of leaf venation in Arabidopsis. *Development* 133, 3755-3766.

Amalraj, B., Govindaraju, P., Krishna, A., Lavania, D., Linh, N. M., Ravichandran, S. J. and Scarpella, E. (2020). GAL4/GFP enhancer-trap lines for identification and manipulation of cells and tissues in developing Arabidopsis leaves. *Developmental Dynamics*. 2020 Apr 21. doi: 10.1002/dvdy.181. Online ahead of print.

Amaya, E., Musci, T. J. and Kirschner, M. W. (1991). Expression of a dominant negative mutant of the FGF receptor disrupts mesoderm formation in Xenopus embryos. *Cell* 66, 257-270.

Avery, G. S., Jr. (1935). Differential Distribution of a Phytohormone in the Developing Leaf of Nicotiana and Its Relation to Polarized Growth. *Bulletin of the Torrey Botanical Club* 62, 313-330.

Bayer, E. M., Smith, R. S., Mandel, T., Nakayama, N., Sauer, M., Prusinkiewicz, P. and Kuhlemeier, C. (2009). Integration of transport-based models for phyllotaxis and midvein formation. *Genes Dev* 23, 373-384.

Benkova, E., Michniewicz, M., Sauer, M., Teichmann, T., Seifertova, D., Jurgens, G., & Friml, J. (2003). Local, efflux-dependent auxin gradients as a common module for plant organ formation. *Cell*, *115*(5), 591–602.

Berleth, T., & Jurgens, G. (1993). The Role of the Monopteros Gene in Organizing the Basal Body Region of the Arabidopsis Embryo. *Development*, *118*(2), 575–587.

Berleth, T., Mattsson, J. and Hardtke, C. S. (2000). Vascular continuity and auxin signals. *Trends Plant Sci* 5, 387-393.

Beuchat, J., Scacchi, E., Tarkowska, D., Ragni, L., Strnad, M. and Hardtke, C. S. (2010). BRX promotes Arabidopsis shoot growth. *New Phytol* 188, 23-29.

Bilsborough GD, Runions A, Barkoulas M et al. Model for the regulation of Arabidopsis thaliana leaf margin development. Proc Natl Acad Sci U S A. 2011; 108: 3424-3429.

Brand AH, Perrimon N. Targeted gene expression as a means of altering cell fates and generating dominant phenotypes. Development. 1993; 118: 401-415.

Burke R, Basler K. Dpp receptors are autonomously required for cell proliferation in the entire developing Drosophila wing. Development. 1996; 122: 2261-2269.

Busch, M., Mayer, U. and Jurgens, G. (1996). Molecular analysis of the Arabidopsis pattern formation of gene GNOM: gene structure and intragenic complementation. *Molecular & General Genetics* 250, 681-691.

Candela, H., Martinez-Laborda, A. and Micol, J. L. (1999). Venation pattern formation in Arabidopsis thaliana vegetative leaves. *Dev Biol* 205, 205-216.

Causier, B., Ashworth, M., Guo, W., & Davies, B. (2012). The TOPLESS interactome: A framework for gene repression in Arabidopsis. *Plant Physiology*, *158*(1), 423–438.

Ceserani, T., Trofka, A., Gandotra, N. and Nelson, T. (2009). VH1/BRL2 receptor-like kinase interacts with vascular-specific adaptor proteins VIT and VIK to influence leaf venation. *Plant J* 57, 1000-1014.

Chandler, J. W. (2016). Auxin response factors. *Plant Cell and Environment*, *39*(5), 1014–1028.

Chen, M. K., Wilson, R. L., Palme, K., Ditengou, F. A. and Shpak, E. D. (2013). ERECTA family genes regulate auxin transport in the shoot apical meristem and forming leaf primordia. *Plant Physiol* 162, 1978-1991.

Chen, X. Y., & Kim, J. Y. (2009). Callose synthesis in higher plants. *Plant signaling & behavior*, *4*(6), 489–492.

Cheung, A. Y., Chen, C. Y., Tao, L. Z. andreyeva, T., Twell, D. and Wu, H. M. (2003). Regulation of pollen tube growth by Rac-like GTPases. *J Exp Bot* 54, 73-81.

Choi, Y., Lee, Y. and Hwang, J.-U. (2014). Arabidopsis ROP9 and ROP10 GTPases differentially regulate auxin and ABA responses. *Journal of Plant Biology* 57, 245-254.

Chomczynski, P. and Sacchi, N. (1987). Single-step method of RNA isolation by acid guanidinium thiocyanate-phenol-chloroform extraction. *Anal Biochem* 162, 156-159.

Ckurshumova W, Koizumi K, Chatfield SP et al. Tissue-specific GAL4 expression patterns as a resource enabling targeted gene expression, cell type-specific transcript profiling and gene function characterization in the Arabidopsis vascular system. Plant Cell Physiol. 2009; 50: 141-150.

Ckurshumova W, Smirnova T, Marcos D, Zayed Y, Berleth T. Irrepressible MONOPTEROS/ARF5 promotes de novo shoot formation. New Phytol. 2014; 204: 556-566.

DeYoung, B. J., Bickle, K. L., Schrage, K. J., Muskett, P., Patel, K. and Clark, S. E. (2006). The CLAVATA1-related BAM1, BAM2 and BAM3 receptor kinase-like proteins are required for meristem function in Arabidopsis. *The Plant Journal* 45, 1-16.

Dharmasiri, N., Dharmasiri, S., Weijers, D., Lechner, E., Yamada, M., Hobbie, L., Ehrismann, J. S., Jurgens, G. and Estelle, M. (2005). Plant Development Is Regulated by a Family of Auxin Receptor F Box Proteins. *Developmental Cell* 9, 109-119.

Donnelly PM, Bonetta D, Tsukaya H, Dengler RE, Dengler NG. Cell cycling and cell enlargement in developing leaves of Arabidopsis. Dev Biol. 1999; 215: 407-419.

Donner TJ, Sherr I, Scarpella E. Regulation of preprocambial cell state acquisition by auxin signaling in Arabidopsis leaves. Development. 2009; 136: 3235-3246.

Enders, T. A., Frick, E. M. and Strader, L. C. (2017). An Arabidopsis kinase cascade influences auxin-responsive cell expansion. *Plant J* 92, 68-81.

Esau, K. (1965). *Plant anatomy* (2nd ed.). New York; London: John Wiley.

Esteve-Bruna, D., Perez-Perez, J. M., Ponce, M. R., & Micol, J. L. (2013). incurvata13, a novel allele of AUXIN RESISTANT6, reveals a specific role for auxin and the SCF complex in Arabidopsis embryogenesis, vascular specification and leaf flatness. *Plant Physiol*, *161*(3), 1303–1320.

Feiguelman, G., Fu, Y. and Yalovsky, S. (2018). ROP GTPases Structure-Function and Signalling Pathways. *Plant Physiol* 176, 57-79.

Fitzgibbon J, Beck M, Zhou J, Faulkner C, Robatzek S, Oparka K. (2013). A developmental framework for complex plasmodesmata formation revealed by large-scale imaging of the Arabidopsis leaf epidermis. *Plant Cell*. 25,57-70.

Fisher, K. and Turner, S. (2007). PXY, a receptor-like kinase essential for maintaining polarity during plant vascular-tissue development. *Curr Biol* 17, 1061-1066.

Franzmann, L., Patton, D. A. and Meinke, D. W. (1989). Invitro Morphogenesis of Arrested Embryos from Lethal Mutants of Arabidopsis-Thaliana. *Theoretical and Applied Genetics* 77, 609-616.

Fukaki H, Nakao Y, Okushima Y, Theologis A, Tasaka M. Tissue-specific expression of stabilized SOLITARY-ROOT/IAA14 alters lateral root development in Arabidopsis. Plant J. 2005; 44: 382-395.

Gardiner J, Donner TJ, Scarpella E. Simultaneous activation of SHR and ATHB8 expression defines switch to preprocambial cell state in Arabidopsis leaf development. Dev Dyn. 2011; 240: 261-270.

Gardiner, J., Donner, T. J. and Scarpella, E. (2011). Simultaneous activation of SHR and ATHB8 expression defines switch to preprocambial cell state in Arabidopsis leaf development. *Dev Dyn* 240, 261-270.

Gardner MJ, Baker AJ, Assie JM, Poethig RS, Haseloff JP, Webb AA. GAL4 GFP enhancer trap lines for analysis of stomatal guard cell development and gene expression. J Exp Bot. 2009; 60: 213-226.

Garrett JJ, Meents MJ, Blackshaw MT et al. A novel, semi-dominant allele of MONOPTEROS provides insight into leaf initiation and vein pattern formation. Planta. 2012; 236: 297-312.

Geldner, N., Richter, S., Vieten, A., Marquardt, S., Torres-Ruiz, R. A., Mayer, U. and Jurgens, G. (2004). Partial loss-of-function alleles reveal a role for GNOM in auxin transport-related, post-embryonic development of Arabidopsis. *Development* 131, 389-400.

Gillmor CS, Park MY, Smith MR, Pepitone R, Kerstetter RA, Poethig RS. The MED12-MED13 module of Mediator regulates the timing of embryo patterning in Arabidopsis. Development. 2010; 137: 113-122.

Govindaraju, P., Verna, C., Zhu, T., & Scarpella, E. (2020). Vein patterning by tissue-specific auxin transport. *Development*, dev.187666.

Groszmann M, Gonzalez-Bayon R, Greaves IK et al. Intraspecific Arabidopsis hybrids show different patterns of heterosis despite the close relatedness of the parental genomes. Plant Physiol. 2014; 166: 265-280.

Halder G, Callaerts P, Gehring WJ. Induction of ectopic eyes by targeted expression of the eyeless gene in Drosophila. Science. 1995; 267: 1788-1792.

Hamann, T, Mayer, U., & Jurgens, G. (1999). The auxin-insensitive bodenlos mutation affects primary root formation and apical-basal patterning in the Arabidopsis embryo. *Development*, *126*(7), 1387–1395.

Hardtke, C. S., & Berleth, T. (1998). The Arabidopsis gene MONOPTEROS encodes a transcription factor mediating embryo axis formation and vascular development. *Embo J*, *17*(5), 1405–1411

Haseloff J. GFP variants for multispectral imaging of living cells. Methods Cell Biol. 1999; 58: 139-151.

Hay, A., Barkoulas, M., & Tsiantis, M. (2006). ASYMMETRIC LEAVES1 and auxin activities converge to repress BREVIPEDICELLUS expression and promote leaf development in Arabidopsis. *Development*, *133*(20), 3955–3961.

Hazak, O., Bloch, D., Poraty, L., Sternberg, H., Zhang, J., Friml, J. and Yalovsky, S. (2010). A rho scaffold integrates the secretory system with feedback mechanisms in regulation of auxin distribution. *PLoS Biol* 8, e1000282.

He, Y., Zhou, J., Shan, L. and Meng, X. (2018). Plant cell surface receptor-mediated signalling - a common theme amid diversity. *J Cell Sci* 131,

Heisler, M. G., Ohno, C., Das, P., Sieber, P., Reddy, G. V, Long, J. A., & Meyerowitz, E. M. (2005). Patterns of Auxin Transport and Gene Expression during Primordium Development Revealed by Live Imaging of the Arabidopsis Inflorescence Meristem. *Curr Biol*, *15*(21), 1899–1911.

Hemmati-Brivanlou, A. and Melton, D. A. (1992). A truncated activin receptor inhibits mesoderm induction and formation of axial structures in Xenopus embryos. *Nature* 359, 609-614.

Hirakawa, Y., Shinohara, H., Kondo, Y., Inoue, A., Nakanomyo, I., Ogawa, M., Sawa, S., Ohashi-Ito, K., Matsubayashi, Y. and Fukuda, H. (2008). Non-cell-autonomous control of vascular stem cell fate by a CLE peptide/receptor system. *Proc Natl Acad Sci U S A* 105, 15208-15213.

Hobbie, L., McGovern, M., Hurwitz, L. R., Pierro, A., Liu, N. Y., Bandyopadhyay, A., & Estelle, M. (2000). The axr6 mutants of Arabidopsis thaliana define a gene involved in auxin response and early development. *Development*, *127*(1), 23–32.

Hooper, C. M., Castleden, I. R., Tanz, S. K., Aryamanesh, N. and Millar, A. H. (2017). SUBA4: the interactive data analysis centre for Arabidopsis subcellular protein locations. *Nucleic Acids Res* 45, D1064-D1074.

Huang T, Harrar Y, Lin C et al. Arabidopsis KANADI1 acts as a transcriptional repressor by interacting with a specific cis-element and regulates auxin biosynthesis, transport and signaling in opposition to HD-ZIPIII factors. Plant Cell. 2014; 26: 246-262.

Ito K, Awano W, Suzuki K, Hiromi Y, Yamamoto D. The Drosophila mushroom body is a quadruple structure of clonal units each of which contains a virtually identical set of neurones and glial cells. Development. 1997; 124: 761-771.

Jürgens, G., Mayer, U., Berleth, T. and Miséra, S. (1991). Genetic analysis of pattern formation in the Arabidopsis embryo. *Development* 113, 27-38.

Kang J, Dengler N. Cell cycling frequency and expression of the homeobox gene ATHB-8 during leaf vein development in Arabidopsis. Planta. 2002; 216: 212-219.

Kang J, Dengler N. Vein pattern development in adult leaves of Arabidopsis thaliana. Int J Plant Sci. 2004; 165: 231-242.

Kawanabe T, Ishikura S, Miyaji N et al. Role of DNA methylation in hybrid vigor in Arabidopsis thaliana. Proc Natl Acad Sci U S A. 2016; 113: E6704-E6711.

Keitt G, Baker R. Auxin activity of substituted benzoic acids and their effect on polar auxin transport. *Plant Physiology* 10, 1561-1569.

Kierzkowski D, Lenhard M, Smith R, Kuhlemeier C. Interaction between meristem tissue layers controls phyllotaxis. Dev Cell. 2013; 26: 616-628.

Kim, D., Langmead, B. and Salzberg, S. L. (2015). HISAT: a fast-spliced aligner with low memory requirements. *Nat Methods* 12, 357-360.

Kinsman, E. A. and Pyke, K. A. (1998). Bundle sheath cells and cell-specific plastid development in Arabidopsis leaves. *Development* 125, 1815-1822.

Koizumi, K., Sugiyama, M. and Fukuda, H. (2000). A series of novel mutants of Arabidopsis thaliana that are defective in the formation of continuous vascular network: calling the auxin signal flow canalization hypothesis into question. *Development* 127, 3197-3204.

Koornneef, M., & Meinke, D. (2010). The development of Arabidopsis as a model plant. *The Plant Journal*, *61*(6), 909–921.

Krogan NT, Berleth T. A dominant mutation reveals asymmetry in MP/ARF5 function along the adaxial- abaxial axis of shoot lateral organs. Plant Signal Behav. 2012; 7: 940-943.

Krogan NT, Ckurshumova W, Marcos D, Caragea AE, Berleth T. Deletion of MP/ARF5 domains III and IV reveals a requirement for Aux/IAA regulation in Arabidopsis leaf vascular patterning. New Phytol. 2012;

Kubo M, Udagawa M, Nishikubo N et al. Transcription switches for protoxylem and metaxylem vessel formation. Genes Dev. 2005; 19: 1855-1860.

Kwak, S.-H., Woo, S., Lee, M. M. and Schiefelbein, J. (2014). Distinct signalling mechanisms in multiple developmental pathways by the SCRAMBLED receptor of Arabidopsis. *Plant physiology* 166, 976-987.

Lamesch, P., Berardini, T. Z., Li, D., Swarbreck, D., Wilks, C., Sasidharan, R., Muller, R., Dreher, K., Alexander, D. L., Garcia-Hernandez, M. et al. (2012). The Arabidopsis Information Resource (TAIR): improved gene annotation and new tools. *Nucleic Acids Res* 40, D1202-10.

Laplaze L, Parizot B, Baker A et al. GAL4-GFP enhancer trap lines for genetic manipulation

Larkin JC, Young N, Prigge M, Marks MD. The control of trichome spacing and number in Arabidopsis Development. 1996; 122: 997-1005.

Lavy, M., Bloch, D., Hazak, O., Gutman, I., Poraty, L., Sorek, N., Sternberg, H. and Yalovsky, S. (2007). A Novel ROP/RAC effector links cell polarity, root-meristem maintenance and vesicle trafficking. *Curr Biol* 17, 947-952.

Leyser, O. (2018). Auxin Signalling. *Plant Physiol* 176, 465-479.

Li, H., Cai, Z., Wang, X., Li, M., Cui, Y., Cui, N., Yang, F., Zhu, M., Zhao, J., Du, W. et al. (2019). SERK Receptor-like Kinases Control Division Patterns of Vascular Precursors and Ground Tissue Stem Cells during Embryo Development in Arabidopsis. *Mol Plant* 12, 984-1002.

Li, H., Handsaker, B., Wysoker, A., Fennell, T., Ruan, J., Homer, N., Marth, G., Abecasis, G., Durbin, R. and 1000, G. P. D. P. S. (2009). The Sequence Alignment/Map format and SAMtools. *Bioinformatics* 25, 2078-2079.

Lightner, J. and Caspar, T. (1998). Seed mutagenesis of Arabidopsis. *Methods Mol Biol* 82, 91-103.

Lin, L., Zhong, S. H., Cui, X. F., Li, J. and He, Z. H. (2012). Characterization of temperature-sensitive mutants reveals a role for receptor-like kinase SCRAMBLED/STRUBBELIG in coordinating cell proliferation and differentiation during Arabidopsis leaf development. *Plant J* 72, 707-720.

Lindsey, B. E., Rivero, L., Calhoun, C. S., Grotewold, E. and Brkljacic, J. (2017). Standardized Method for High-throughput Sterilization of Arabidopsis Seeds. *J Vis Exp*

Linh, N. M., Verna, C. and Scarpella, E. (2018). Coordination of cell polarity and the patterning of leaf vein networks. *Curr Opin Plant Biol* 41, 116-124.

Lu P, Porat R, Nadeau JA, O'Neill SD. Identification of a meristem L1 layer-specific gene in Arabidopsis that is expressed during embryonic pattern formation and defines a new class of homeobox genes. Plant Cell. 1996; 8: 2155-2168.

Lukowitz, W., Gillmor, C. S. and Scheible, W. R. (2000). Positional cloning in Arabidopsis. Why it feels good to have a genome initiative working for you. *Plant Physiol* 123, 795-805.

Lukowitz, W., Roeder, A., Parmenter, D. and Somerville, C. (2004). A MAPKK kinase gene regulates extra-embryonic cell fate in Arabidopsis. *Cell* 116, 109-119.

Luschnig, C. and Vert, G. (2014). The dynamics of plant plasma membrane proteins: PINs and beyond. *Development* 141, 2924-2938.

Marcos, D., & Berleth, T. (2014). Dynamic auxin transport patterns preceding vein formation revealed by live-imaging of Arabidopsis leaf primordia. *Front Plant Sci*, *5*, 235.

Marquès-Bueno, M. D. M., Morao, A. K., Cayrel, A., Platre, M. P., Barberon, M., Caillieux, E., Colot, V., Jaillais, Y., Roudier, F. and Vert, G. (2016). A versatile Multisite Gateway-compatible promoter and transgenic line collection for cell type-specific functional genomics in Arabidopsis. *Plant J* 85, 320-333.

Matthes, M. and Torres-Ruiz, R. A. (2016). Boronic acids induce monopteros phenocopies by affecting PIN1 membrane stability and polar auxin transport in Arabidopsis thaliana embryos. *Development* 143, 4053-4062.

Mattsson, J., Sung, Z. R. and Berleth, T. (1999). Responses of plant vascular systems to auxin transport inhibition. *Development* 126, 2979-2991.

Mayer, U., Buttner, G. and Jurgens, G. (1993). Apical-basal pattern formation in the Arabidopsis embryo: studies on the role of the gnom gene. *Development* 117, 149-162.

Mazur, E., Benková, E., & Friml, J. (2016). Vascular cambium regeneration and vessel formation in wounded inflorescence stems of Arabidopsis. *Scientific Reports*, *6*, 1–15.

Michniewicz, M., Zago, M. K., Abas, L., Weijers, D., Schweighofer, A., Meskiene, I., … Friml, J. (2007). Antagonistic regulation of PIN phosphorylation by PP2A and PINOID directs auxin flux. *Cell*, *130*(6), 1044–1056.

Miséra, S., Müller, A. J., Weiland-Heidecker, U. and Jürgens, G. (1994). The FUSCA genes of Arabidopsis: negative regulators of light responses. *Mol Gen Genet* 244, 242-252.

Morgan TH, Bridges CB. The Origin of Gynandromorphs. Contributions to the Genetics of Drosophila melanogaster. Washington, D.C.: Carnegie Institution of Washington. Press of Gibson Bross, Inc.; 1919:1-122.

Morgan, D. G. and Söding, H. (1958). Über die Wirkungsweise von Phthalsäuremono-α-Naphthylamid (PNA) auf das Wachstum der Haferkoleoptile. *Planta* 52, 235-249.

Moriwaki, T., Miyazawa, Y., Fujii, N. and Takahashi, H. (2014). GNOM regulates root hydrotropism and phototropism independently of PIN-mediated auxin transport. *Plant Sci* 215-216, 141-149.

Mouchel, C. F., Osmont, K. S. and Hardtke, C. S. (2006). BRX mediates feedback between brassinosteroid levels and auxin signalling in root growth. *Nature* 443, 458-461.

Nakamura, M., Kiefer, C. S. and Grebe, M. (2012). Planar polarity, tissue polarity and planar morphogenesis in plants. *Curr Opin Plant Biol* 15, 593-600.

Nakata MT, Tameshige T, Takahara M, Mitsuda N, Okada K. The functional balance between the WUSCHEL- RELATED HOMEOBOX1 gene and the phytohormone auxin is a key factor for cell proliferation in Arabidopsis seedlings. Plant Biotech. 2018; 35: 141-154.

Naramoto, S., Otegui, M. S., Kutsuna, N., de Rycke, R., Dainobu, T., Karampelias, M., Fujimoto, M., Feraru, E., Miki, D., Fukuda, H. et al. (2014). Insights into the localization and function of the membrane trafficking regulator GNOM ARF-GEF at the Golgi apparatus in Arabidopsis. *Plant Cell* 26, 3062-3076.

Nelson, T. and Dengler, N. (1997). Leaf Vascular Pattern Formation. *Plant Cell* 9, 1121-1135.

Nibau, C., Tao, L., Levasseur, K., Wu, H. M. and Cheung, A. Y. (2013). The Arabidopsis small GTPase AtRAC7/ROP9 is a modulator of auxin and abscisic acid signalling. *J Exp Bot* 64, 3425-3437.

Noden, D. M. (1988). Interactions and fates of avian craniofacial mesenchyme. *Development* 103 Supplement, 121-140.

Normanly, J. (2010). Approaching cellular and molecular resolution of auxin biosynthesis and metabolism. *Cold Spring Harb Perspect Biol*, *2*(1), a001594. doi:10.1101/cshperspect.a001594.

Odat, O. (2015). Control of Arabidopsis vein-network formation by cell proliferation. *Department of Biological Sciences* Ph.D., i-xiv,1.

Odat, O., Gardiner, J., Sawchuk, M. G., Verna, C., Donner, T. J. and Scarpella, E. (2014). Characterization of an allelic series in the MONOPTEROS gene of Arabidopsis. *Genesis* 52, 127-133.

Okumura, K., Goh, T., Toyokura, K., Kasahara, H., Takebayashi, Y., Mimura, T., Kamiya, Y. and Fukaki, H. (2013). GNOM/FEWER ROOTS is required for the establishment of an auxin response maximum for arabidopsis lateral root initiation. *Plant Cell Physiol* 54, 406-417.

Pautot V, Dockx J, Hamant O et al. KNAT2: evidence for a link between knotted-like genes and carpel development. Plant Cell. 2001; 13: 1719-1734.

Pertea, M., Kim, D., Pertea, G. M., Leek, J. T. and Salzberg, S. L. (2016). Transcript-level expression analysis of RNA-seq experiments with HISAT, StringTie and Ballgown. *Nat Protoc* 11, 1650-1667.

Petrasek, J., Mravec, J., Bouchard, R., Blakeslee, J. J., Abas, M., Seifertova, D., Wisniewska, J., Tadele, Z., Kubes, M., Covanova, M. et al. (2006). PIN proteins perform a rate-limiting function in cellular auxin efflux. *Science* 312, 914-918.

Posakony LG, Raftery LA, Gelbart WM. Wing formation in Drosophila melanogaster requires decapentaplegic gene function along the anterior-posterior compartment boundary. Mech Dev. 1991; 33: 69-82.

Powers, S. K., & Strader, L. C. (2020). Regulation of auxin transcriptional responses. *Developmental Dynamics*, *249*(4), 483–495.

Przemeck, G. K., Mattsson, J., Hardtke, C. S., Sung, Z. R., & Berleth, T. (1996). Studies on the role of the Arabidopsis gene MONOPTEROS in vascular development and plant cell axialization. *Planta*, *200*(2), 229–237.

Pyke KA, Marrison JL, Leech RM. Temporal and Spatial Development of the Cells of the Expanding 1st Leaf of Arabidopsis-Thaliana (L) Heynh. J Exp Bot. 1991; 42: 1407-1416.

Radoeva T, Ten Hove CA, Saiga S, Weijers D. Molecular Characterization of Arabidopsis GAL4/UAS Enhancer Trap Lines Identifies Novel Cell-Type-Specific Promoters. Plant Physiol. 2016; 171: 1169-1181.

Raven, J. A. (1975). Transport of indole acetic acid in plant cells in relation to pH and electrical potential gradients and its significance for polar IAA transport. *New Phytologist*, *74*, 163–172.

Ravichandran, S. J., Linh, N. M. and Scarpella, E. (2020). The canalization hypothesis - challenges and alternatives. *New Phytologist* 227, 1051-1059.

Redei, G. P. and Koncz, C. (1992). Classical Mutagenesis. In *Methods in Arabidopsis research* (ed. C. Koncz, N.-H. Chua and J. Schell), pp. 16-82. Singapore: Wolrd Scientific.

Reinhardt, D., Pesce, E. R., Stieger, P., Mandel, T., Baltensperger, K., Bennett, M., … Kuhlemeier, C. (2003). Regulation of phyllotaxis by polar auxin transport. *Nature*, *426*(6964), 255–260.

Richter, S. anders, N., Wolters, H., Beckmann, H., Thomann, A., Heinrich, R., Schrader, J., Singh, M. K., Geldner, N., Mayer, U. et al. (2010). Role of the GNOM gene in Arabidopsis apical-basal patterning--From mutant phenotype to cellular mechanism of protein action. *Eur J Cell Biol* 89, 138-144.

Rubery, P. H., & Sheldrake, A. R. (1974). Carrier-Mediated Auxin Transport. *Planta*, *118*(2), 101–121.

Rueden CT, Schindelin J, Hiner MC et al. ImageJ2: ImageJ for the next generation of scientific image data. BMC Bioinformatics. 2017; 18: 529.

Rueden, C. T., Schindelin, J., Hiner, M. C., DeZonia, B. E., Walter, A. E., Arena, E. T. and Eliceiri, K. W. (2017). ImageJ2: ImageJ for the next generation of scientific image data. *BMC Bioinformatics* 18, 529.

Ruiz Sola, M. A., Coiro, M., Crivelli, S., Zeeman, S. C., Schmidt Kjølner Hansen, S. and Truernit, E. (2017). OCTOPUS-LIKE 2, a novel player in Arabidopsis root and vascular

development, reveals a key role for OCTOPUS family genes in root metaphloem sieve tube differentiation. *New Phytol* 216, 1191-1204.

Sabatini S, Beis D, Wolkenfelt H et al. An auxin-dependent distal organizer of pattern and polarity in the Arabidopsis root. Cell. 1999; 99: 463-472.

Sachs, T. (1981). The control of the patterned differentiation of vascular tissues. *Advances in Botanical Research* 9, 151-262.

Sauer, M., Balla, J., Luschnig, C., Wisniewska, J., Reinohl, V., Friml, J., & Benkova, E. (2006). Canalization of auxin flow by Aux/IAA-ARF-dependent feedback regulation of PIN polarity. *Genes Dev*, *20*(20), 2902–2911.

Sawchuk MG, Donner TJ, Head P, Scarpella E. Unique and overlapping expression patterns among members of photosynthesis-associated nuclear gene families in Arabidopsis. Plant Physiol. 2008; 148: 1908-1924.

Sawchuk MG, Head P, Donner TJ, Scarpella E. Time-lapse imaging of Arabidopsis leaf development shows dynamic patterns of procambium formation. New Phytol. 2007; 176: 560-571.

Sawchuk, M. G. and Scarpella, E. (2013). Polarity, continuity and alignment in plant vascular strands. *J Integr Plant Biol* 55, 824-834.

Sawchuk, M. G., Donner, T. J., Head, P. and Scarpella, E. (2008). Unique and overlapping expression patterns among members of photosynthesis-associated nuclear gene families in Arabidopsis. *Plant Physiol* 148, 1908-1924.

Sawchuk, M. G., Edgar, A. and Scarpella, E. (2013). Patterning of leaf vein networks by convergent auxin transport pathways. *PLoS Genet* 9, e1003294.

Scacchi, E., Osmont, K. S., Beuchat, J., Salinas, P., Navarrete-Gómez, M., Trigueros, M., Ferrándiz, C. and Hardtke, C. S. (2009). Dynamic, auxin-responsive plasma membrane-to-nucleus movement of Arabidopsis BRX. *Development* 136, 2059-2067.

Scarpella E, Francis P, Berleth T. Stage-specific markers define early steps of procambium development in Arabidopsis leaves and correlate termination of vein formation with mesophyll differentiation. Development. 2004; 131: 3445-3455.

Scarpella E, Marcos D, Friml J, Berleth T. Control of leaf vascular patterning by polar auxin transport. Genes Dev. 2006; 20: 1015-1027.

Scarpella, E., Francis, P. and Berleth, T. (2004). Stage-specific markers define early steps of procambium development in Arabidopsis leaves and correlate termination of vein formation with mesophyll differentiation. *Development* 131, 3445-3455.

Scarpella, E., Marcos, D., Friml, J., & Berleth, T. (2006). Control of leaf vascular patterning by polar auxin transport. *Genes Dev*, *20*(8), 1015–1027.

Scheres, B., Wolkenfelt, H., Willemsen, V., Terlouw, M., Lawson, E., Dean, C., & Weisbeek, P. (1994). Embryonic Origin of the Arabidopsis Primary Root and Root-Meristem Initials. *Development*, *120*(9), 2475–2487.

Schindelin J, Arganda-Carreras I, Frise E et al. Fiji: an open-source platform for biological-image analysis. Nat Methods. 2012; 9: 676-682.

Schindelin J, Rueden CT, Hiner MC, Eliceiri KW. The ImageJ ecosystem: An open platform for biomedical image analysis. Mol Reprod Dev. 2015; 82: 518-529.

Schindelin, J., Arganda-Carreras, I., Frise, E., Kaynig, V., Longair, M., Pietzsch, T., Preibisch, S., Rueden, C., Saalfeld, S., Schmid, B. et al. (2012). Fiji: an open-source platform for biological-image analysis. *Nat Methods* 9, 676-682.

Schindelin, J., Rueden, C. T., Hiner, M. C. and Eliceiri, K. W. (2015). The ImageJ ecosystem: An open platform for biomedical image analysis. *Mol Reprod Dev* 82, 518-529.

Schneider CA, Rasband WS, Eliceiri KW. NIH Image to ImageJ: 25 years of image analysis. Nat Methods. 2012; 9: 671-675.

Schneider, C. A., Rasband, W. S. and Eliceiri, K. W. (2012). NIH Image to ImageJ: 25 years of image analysis. *Nat Methods* 9, 671-675.

Schuetz, M., Berleth, T. and Mattsson, J. (2008). Multiple MONOPTEROS-dependent pathways are involved in leaf initiation. *Plant Physiol* 148, 870-880.

Sessions A, Weigel D, Yanofsky MF. The Arabidopsis thaliana MERISTEM LAYER 1 promoter specifies epidermal expression in meristems and young primordia. Plant J. 1999; 20: 259-263.

Shevell DE, Kunkel T, Chua NH. Cell wall alterations in the arabidopsis emb30 mutant. Plant Cell. 2000; 12: 2047-2060.

Shevell, D. E., Leu, W. M., Gillmor, C. S., Xia, G., Feldmann, K. A. and Chua, N. H. (1994). EMB30 is essential for normal cell division, cell expansion and cell adhesion in Arabidopsis and encodes a protein that has similarity to Sec7. *Cell* 77, 1051-1062.

Sieburth, L. E. (1999). Auxin is required for leaf vein pattern in Arabidopsis. *Plant Physiol* 121, 1179-1190.

Simon R, Igeño MI, Coupland G. Activation of floral meristem identity genes in Arabidopsis. Nature. 1996; 384: 59-62.

Smékalová, V., Luptovčiak, I., Komis, G., Šamajová, O., Ovečka, M., Doskočilová, A., Takáč, T., Vadovič, P., Novák, O., Pechan, T. et al. (2014). Involvement of YODA and

mitogen activated protein kinase 6 in Arabidopsis post-embryogenic root development through auxin up-regulation and cell division plane orientation. *New Phytol* 203, 1175-1193.

Smetana O, Mäkilä R, Lyu M et al. High levels of auxin signalling define the stem-cell organizer of the vascular cambium. Nature. 2019; 565: 485-489.

Smit, M. E., Llavata-Peris, C. I., Roosjen, M., van Beijnum, H., Novikova, D., Levitsky, V., Weijers, D. (2020). Specification and regulation of vascular tissue identity in the Arabidopsis embryo. *Development (Cambridge)*, *147*(8).

Solereder H. Systematic Anatomy of the Dicotyledons. Oxford: Clarendon Press; 1908.

Steinmann, T., Geldner, N., Grebe, M., Mangold, S., Jackson, C. L., Paris, S., Galweiler, L., Palme, K. and Jurgens, G. (1999). Coordinated polar localization of auxin efflux carrier PIN1 by GNOM ARF GEF. *Science* 286, 316-318.

Stewart RN. Ontogeny of the primary body in chimeral forms of higher plants. In: Subtelny S, Sussex IM, eds. The Clonal Basis of Development. New York: Academic Press; 1978:131-160.

Steynen, Q. J. and Schultz, E. A. (2003). The FORKED genes are essential for distal vein meeting in Arabidopsis. *Development* 130, 4695-4708.

Strader, L. C., Monroe-Augustus, M., & Bartel, B. (2008). The IBR5 phosphatase promotes Arabidopsis auxin responses through a novel mechanism distinct from TIR1-mediated repressor degradation. *Bmc Plant Biology*, *8*

Sturtevant AH. The use of mosaics in the study of the developmental effects of genes. Proc 6

Sturtevant AH. The Vermilion Gene and Gynandromorphism. Proc Soc Exp Biol Med. 1920; 17: 70-71.

Taiz, L. Zeiger, E., Moller, I.M. and Murphy, A. (2015) *Plant Physiology and Development*. 6th Edition, Sinauer Associates, Sunderland, CT

Takada S, Jürgens G. Transcriptional regulation of epidermal cell fate in the Arabidopsis embryo. Development. 2007; 134: 1141-1150.

Telfer A, Poethig RS. Leaf development in Arabidopsis. In: Meyerowitz EM, Somerville CR, eds. Arabidopsis. New York: Cold Spring Harbor Press; 1994:379-401.

Telfer, A. and Poethig, R. S. (1994). Leaf development in Arabidopsis. In *Arabidopsis* (ed. E. M. Meyerowitz and C. R. Somerville), pp. 379-401. New York: Cold Spring Harbor Press.

Th Int Congr Genet. 1932; 1: 304-307.

Thimann, K. V. and Skoog, F. (1934). On the Inhibition of Bud Development and other Functions of Growth Substance in Vicia Faba. *Proceedings of the Royal Society of London. Series B, Containing Papers of a Biological Character* 114, 317-339.

Thompson, N. P. (1966). Vascular Regeneration and Long Distance Transport of Indole-3-acetic Acid in Coleus Stems. *Plant Physiol* 41, 1106-1112.

Tilney-Bassett RAE. Plant Chimeras. London: Edward Arnold; 1986.

Trapnell, C., Roberts, A., Goff, L., Pertea, G., Kim, D., Kelley, D. R., Pimentel, H., Salzberg, S. L., Rinn, J. L. and Pachter, L. (2012). Differential gene and transcript expression analysis of RNA-seq experiments with TopHat and Cufflinks. *Nat Protoc* 7, 562-578.

Uchida, N. and Tasaka, M. (2013). Regulation of plant vascular stem cells by endodermis-derived EPFL-family peptide hormones and phloem-expressed ERECTA-family receptor kinases. *J Exp Bot* 64, 5335-5343.

Ueno, H., Colbert, H., Escobedo, J. A. and Williams, L. T. (1991). Inhibition of PDGF beta receptor signal transduction by coexpression of a truncated receptor. *Science* 252, 844-848.

Vatén, A., Dettmer, J., Wu, S., Stierhof, Y.D., Miyashima, S., Yadav, S.R., Roberts, C.J., Campilho, A., Bulone, V., Lichtenberger, R., Lehesranta, S., Mähönen, A.P., Kim, J.Y., Jokitalo, E., Sauer, N., Scheres, B., Nakajima, K., Carlsbecker, A., Gallagher, K.L., Helariutta, Y. Callose biosynthesis regulates symplastic trafficking during root development. (2011). *Dev Cell* 21,1144-1155.

Verna, C., Ravichandran, S. J., Sawchuk, M. G., Linh, N. M. and Scarpella, E. (2019). Coordination of Tissue Cell Polarity by Auxin Transport and Signalling. *eLife* 8, e51061.

Verna, C., Sawchuk, M. G., Linh, N. M. and Scarpella, E. (2015). Control of vein network topology by auxin transport. *BMC Biol* 13, 94.

Wang, J., Kucukoglu, M., Zhang, L., Chen, P., Decker, D., Nilsson, O., Jones, B., Sandberg, G. and Zheng, B. (2013). The Arabidopsis LRR-RLK, PXC1, is a regulator of secondary wall formation correlated with the TDIF-PXY/TDR-WOX4 signalling pathway. *BMC Plant Biol* 13, 94.

Wang, N., Bagdassarian, K. S., Doherty, R. E., Kroon, J. T., Connor, K. A., Wang, X. Y., Wang, W., Jermyn, I. H., Turner, S. R. and Etchells, J. P. (2019). Organ-specific genetic interactions between paralogues of the PXY and ER receptor kinases enforce radial patterning in Arabidopsis vascular tissue. *Development* 146, dev177105.

Wangermann, E. (1974). The pathway of transport of applied indolyl-acetic acid through internode segments. *New Phytologist* 73, 623-636.

Weijers D, Van Hamburg JP, Van Rijn E, Hooykaas PJ, Offringa R. Diphtheria toxin-mediated cell ablation reveals interregional communication during Arabidopsis seed development. Plant Physiol. 2003; 133: 1882- 1892.

Weijers, D., Franke-van Dijk, M., Vencken, R. J., Quint, A., Hooykaas, P. and Offringa, R. (2001). An Arabidopsis Minute-like phenotype caused by a semi-dominant mutation in a RIBOSOMAL PROTEIN S5 gene. *Development* 128, 4289-4299.

Went, F. W. (1928). Wuchsstoff und Wachstum. *Recueil des travaux botaniques néerlandais* 25, I-IV,1.

Wenzel CL, Marrison J, Mattsson J, Haseloff J, Bougourd SM. Ectopic divisions in vascular and ground tissues of Arabidopsis thaliana result in distinct leaf venation defects. J Exp Bot. 2012; 63: 5351-5364.

Wenzel, C. L., Schuetz, M., Yu, Q., & Mattsson, J. (2007). Dynamics of MONOPTEROS and PIN-FORMED1 expression during leaf vein pattern formation in Arabidopsis thaliana. *Plant J*, *49*(3), 387–398.

Wisniewska, J., Xu, J., Seifertova, D., Brewer, P. B., Ruzicka, K., Blilou, I., Rouquie, D., Benkova, E., Scheres, B. and Friml, J. (2006). Polar PIN localization directs auxin flow in plants. *Science* 312, 883.

Wu, G., Gu, Y., Li, S. and Yang, Z. (2001). A genome-wide analysis of Arabidopsis Rop-interactive CRIB motif-containing proteins that act as Rop GTPase targets. *Plant Cell* 13, 2841-2856.

Xue, Y., Gao, X., Lindsell, C. E., Norton, C. R., Chang, B., Hicks, C., Gendron-Maguire, M., Rand, E. B., Weinmaster, G. and Gridley, T. (1999). Embryonic lethality and vascular defects in mice lacking the Notch ligand Jagged1. *Hum Mol Genet* 8, 723-730.

Yamaguchi M, Goué N, Igarashi H et al. VASCULAR-RELATED NAC-DOMAIN6 and VASCULAR- RELATED NAC-DOMAIN7 effectively induce transdifferentiation into xylem vessel elements under control of an induction system. Plant Physiol. 2010; 153: 906-914.

Yoshida, S., Barbier de Reuille, P., Lane, B., Bassel, G. W., Prusinkiewicz, P., Smith, R. S., & Weijers, D. (2014). Genetic control of plant development by overriding a geometric division rule. *Dev Cell*, *29*(1), 75–87.

Zhang Q, Wang D, Lang Z et al. Methylation interactions in Arabidopsis hybrids require RNA-directed DNA methylation and are influenced by genetic variation. Proc Natl Acad Sci U S A. 2016; 113: E4248-56.

Zhang, M., Su, J., Zhang, Y., Xu, J. and Zhang, S. (2018). Conveying endogenous and exogenous signals: MAPK cascades in plant growth and defense. *Curr Opin Plant Biol* 45, 1-10.

Zhao, Y. (2010). Auxin biosynthesis and its role in plant development. *Annu Rev Plant Biol*, *61*, 49–64.